

# Simple Bosonization Solution of the 2-channel Kondo Model: I. Analytical Calculation of Finite-Size Crossover Spectrum

<sup>1,2</sup>Gergely Zarand and <sup>3</sup>Jan von Delft

<sup>1</sup>*Institute of Physics, Technical University of Budapest, H 1521 Budafoki ut 8., Budapest, Hungary*

<sup>2</sup>*International School for Advanced Studies, I-34014, Trieste, Italy*

<sup>3</sup>*Institut fur Theoretische Festkrperphysik, Universitat Karlsruhe, 76128 Karlsruhe, Germany*

(Submitted to Phys. Rev. B on December 10, 1998)

We present in detail a simple, exact solution of the anisotropic 2-channel Kondo (2CK) model at its Toulouse point. We reduce the model to a quadratic resonant-level model by generalizing the bosonization-refermionization approach of Emery and Kivelson to finite system size, but improve their method in two ways: firstly, we construct all boson fields and Klein factors explicitly in terms of the model's original fermion operators  $c_{k\sigma j}$ , and secondly we clarify explicitly how the Klein factors needed when refermionizing act on the original Fock space. This enables us to explicitly follow the adiabatic evolution of the 2CK model's free-fermion states to its exact eigenstates, found by simply diagonalizing the resonant-level model for arbitrary magnetic fields and spin-flip coupling strengths. In this way we obtain an *analytic* description of the cross-over from the free to the non-Fermi-liquid fixed point. At the latter, it is remarkably simple to recover the conformal field theory results for the finite-size spectrum (implying a direct proof of Affleck and Ludwig's fusion hypothesis). By analyzing the finite-size spectrum, we directly obtain the operator content of the 2CK fixed point and the dimension of various relevant and irrelevant perturbations. Our method goes beyond previous conformal field theory results, since it works for arbitrary magnetic fields and can easily be generalized to include various symmetry-breaking perturbations, and to study the crossover to other fixed points produced by these. Furthermore it establishes instructive connections between different renormalization group schemes such as poor man's scaling, Anderson-Yuval type scaling, the numerical renormalization group and finite-size scaling.

## I. INTRODUCTION

Quantum impurity models displaying non-Fermi-liquid (NFL) behavior have attracted substantial interest during the past few years. These models have the common property that their exact elementary excitations are not free-electron like and cannot be described using Fermi-liquid theory. Such single-impurity models have been proposed as relevant for certain properties of heavy-fermion alloys<sup>1–3</sup> and high- $T_c$  superconductors.<sup>4,5</sup> They also emerge in the tunneling-impurity Kondo problem,<sup>6–10</sup> and infinite-dimensional strongly-correlated lattice models can be mapped onto such models as well.<sup>11</sup> All these models possess regimes in which the physical quantities are non-analytic (logarithmic or power-law) functions of parameters such as temperature or magnetic field.

The two-channel Kondo (2CK) model, introduced in 1980 by Nozieres and Blandin,<sup>12</sup> is one of the simplest and most-studied quantum impurity models with NFL behavior. In this model two channels of spinful conduction electrons interact with a single spin 1/2 impurity via a local antiferromagnetic exchange interaction. In contrast to the single-channel Kondo (1CK) model, which has a stable infinite-coupling fixed point at which the conduction electrons screen the impurity spin completely by forming a spin 0 complex, in the two-channel case they *overscreen* the impurity spin at infinite coupling, leaving a non-trivial residual spin object, so that

the 2CK model's infinite-coupling fixed point becomes unstable. A stable fixed point exists at intermediate coupling strength, which leads to the appearance of a non-zero residual entropy and to non-analytical behavior for various physical quantities. Such non-analytical behavior was directly observed, for example, in anomalous conductance signals of metallic nanoconstrictions containing 2-state tunneling systems,<sup>13–17</sup> which are perhaps the most convincing realizations of 2CK physics found experimentally.

The two-channel Kondo model has been studied theoretically by an impressive number of different methods, which are comprehensively reviewed in Ref. 18. These include approximate methods such as the multiplicative<sup>7,12,19</sup> and the path-integral<sup>20,21</sup> renormalization group approaches and slave-boson methods,<sup>22–24</sup> effective models such as the so-called compactified model<sup>25–27</sup> which is partially equivalent to the 2CK model; the numerical renormalization group (NRG);<sup>28–30</sup> and exact methods, such as the Bethe Ansatz,<sup>31–33</sup> conformal field theory (CFT)<sup>30,34–39</sup> and abelian bosonization.<sup>4,40–43</sup> Excepting abelian bosonization, however, the price for using powerful numerical or exact methods has hitherto always been a very high degree of technical sophistication and a lack of physical transparency. The Bethe Ansatz provides an analytical solution of the model, allowing for the calculation of the cross-over from Fermi-liquid to non-Fermi-liquid behavior of the thermodynamical quantities. It is, however,

rather involved, and is unable to calculate dynamical correlation functions. With the numerical renormalization group technique, which likewise is able to describe cross-over behavior, one can obtain thermodynamical properties, carry out a finite-size analysis of the model, investigate the effect of various perturbations such as different electronic and impurity magnetic fields and channel anisotropy, and in principle also calculate dynamical local correlation functions of the impurity. However, this method, though powerful, is approximate by construction, requires considerable numerical prowess, is physically not very transparent and is not well-suited to calculate dynamical properties of the conduction electrons. Finally, the elegant conformal field theory solution of Affleck and Ludwig (AL) focuses exclusively on the NFL regime in the vicinity of  $T = 0$  fixed point. By exploiting its symmetry properties to the full, it provides the finite-size spectrum of the model, all thermodynamical quantities and furthermore all dynamical correlation functions. However, the CFT solution relies crucially on the so-called fusion hypothesis that can only be verified *a posteriori* by comparing the CFT results with other exact methods. Moreover, it cannot be used to calculate the cross-over behavior, and requires, of course, extensive knowledge of the technical subject of boundary conformal field theory.

A major advance towards finding a *simple and transparent* exact solution of the 2CK model was achieved by Emery and Kivelson (EK)<sup>4</sup> with the rather simple technique of 1-dimensional abelian bosonization (pedagogically reviewed in Ref. 44). Using bosonization and refermionization, EK showed that along a certain line in parameter space, known as the Toulouse “point” or Emery-Kivelson line, the anisotropic 2CK model can be mapped exactly onto a *quadratic* resonant-level model, which can be solved straightforwardly by diagonalization. Since spin anisotropy is known to be irrelevant for the multichannel Kondo model, this yielded new insight also about the generic behavior of the isotropic 2CK model. Though their approach works only in the vicinity of the EK line, the latter connects the Fermi-liquid and non-Fermi-liquid regimes, so that EK’s method captures both the model’s NFL behavior and the cross-over from the free to the NFL fixed point. EK calculated a number of thermodynamic and impurity properties and some electron correlation functions, and related the NFL behavior to the fact that, remarkably, only “one half” of the impurity’s degrees of freedom (a Majorana fermion instead of a proper complex fermion) couple to the electrons.

In the present work, which is an extended version of a previous publication,<sup>45</sup> we generalize EK’s bosonization technique to *finite system sizes*. For this purpose two important modifications are needed:

(i) While EK use the field-theoretical approach to bosonization in which the bosonization relation  $\psi_{\alpha j} \simeq F_{\alpha j} e^{-i\phi_{\alpha j}}$  is used merely as a formal correspondence, we use the more careful and explicit *constructive* bosonization procedure of Haldane<sup>46</sup>. In the latter approach both

the boson fields  $\phi_{\alpha j}$  and Klein factors  $F_{\alpha j}$  are constructed *explicitly* from the original  $\psi_{\alpha j}$  operators, so that the bosonization formula becomes an operator identity in Fock space.

(ii) Since EK were interested mainly in impurity properties, they did not need to discuss at all the Klein factors  $F_{\alpha j}$  [which lower the number of  $\alpha j$ -electrons by one and ensure proper anticommutation relations for the  $\psi_{\alpha j}$ ’s]. These Klein factors, however, are essential for quantities like the finite-size spectrum or various electron correlation functions. Therefore it is crucial to specify how the Klein factors for the refermionized operators act on the Fock space. As we shall see, these new Klein factors are only well defined on a suitably *enlarged* Fock space that also contains unphysical states, which must be discarded at the end using certain *gluing conditions*.

With these modifications, EK’s bosonization approach enables us by straightforward diagonalization of the quadratic resonant-level model (i) for the first time to analytically trace the cross-over of the 2CK model’s finite-size spectrum from the FL to the NFL fixed point, at which we reproduce the fixed-point spectrum previously found by CFT using a certain fusion hypothesis; (ii) to construct the eigenstates of the 2CK model corresponding to this crossover spectrum explicitly; (iii) and to extract the operator content of the NFL fixed point and determine the dimensions of different relevant and irrelevant operators. Since our method works also in the presence of an arbitrary magnetic field (unlike CFT), we can also (iv) investigate how a finite magnetic field destroys the NFL spectrum for the low-energy excitations of the model and restores the FL properties. (v) Furthermore, our finite-size bosonization approach can easily be related to various popular renormalization group methods; it therefore not only provides a useful bridge between them, but can potentially be used as a pedagogical tool for *analytically* illustrating their main ideas.

In a future publication<sup>47</sup> we shall show that this method furthermore allows one (vi) to construct very easily the scattering states of the model; (vii) to prove explicitly the validity of the bosonic description of the NFL fixed point Maldacena and Ludwig,<sup>42</sup> (viii) to determine the fixed point boundary conditions at the impurity site for the different currents and fields in a very straightforward way; and (ix) to calculate with ease all correlation functions at and around the NFL fixed point. This implies that all CFT results can be derived from first principles using the bosonization approach.

The paper is organized as follows. In Section II we define the 2CK model to be studied. For completeness, and since the proper use of Klein factors is essential, Section III briefly reviews the “constructive” (operator identity-based) approach to finite-size bosonization used throughout this paper. The Emery-Kivelson mapping onto a resonant-level model is discussed in Section IV, using our novel, more explicit formulation of refermionization within a suitably extended Fock space. The solution of the resonant level model and the construction of

the non-Fermi liquid spectrum using generalized gluing conditions is presented in Section V. In Section VI the results of our finite-size calculations are compared with and interpreted in terms of various RG procedures. Finally, in Section VII we summarize our conclusions and compare our method to a few others.

The centerpiece of our work, and indeed the prerequisite for all of our results, is the uncommonly careful and detailed finite-size formulation of the Emery-Kivelson mapping in the main text. Technicalities not related to this mapping are relegated to the Appendices: Appendix A discusses in some detail matters related to the choice of an ultraviolet cutoff, and also gives the often-used position-space definition of the 2CK model, to facilitate comparison with our momentum-space version. The construction of the extended Fock space needed for refermionization is discussed in Appendix B, and the technical details used to diagonalize the resonant-level model and to calculate several of its properties are given in Appendix C. Finally, for pedagogical reasons and for the sake of completeness, in Appendix D we use our finite-size bosonization method to solve the 1-channel Kondo model as well.

## II. DEFINITION OF THE MODEL

### A. Hamiltonian in Momentum Space

Throughout the main part of this paper we shall use the standard 2CK Hamiltonian in momentum space (its position-space representation is given in Appendix A). We consider a magnetic impurity with spin 1/2 placed at the origin of a sphere of radius  $R = L/2$ , filled with two species of free, spinful conduction electrons, labeled by a spin index  $\alpha = (\uparrow, \downarrow) = (+, -)$  and a channel or flavor index  $j = (1, 2) = (+, -)$ . We assume that the interaction between the impurity and the conduction electron is sufficiently short-ranged that it involves only  $s$ -wave conduction electrons, whose kinetic energy can be written as ( $v_F = \hbar = 1$ )

$$H_0 = \sum_{k\alpha j} k :c_{k\alpha j}^\dagger c_{k\alpha j}: , \quad (1)$$

The operator  $c_{k\alpha j}^\dagger$  creates an  $s$ -wave conduction electron of species  $(\alpha j)$  with radial momentum  $k \equiv p - p_F$  relative to the Fermi momentum  $p_F$ , and the dispersion has been linearized around the Fermi energy  $\varepsilon_F$ :  $\varepsilon_k - \varepsilon_F \approx k$ . The symbol  $: \cdot :$  in Eq. (1) denotes normal ordering with respect to the free Fermi sea or “vacuum state”  $|\vec{0}\rangle_0$  (the reason for this notation will become clear in the next section), defined by

$$c_{k\alpha j} |\vec{0}\rangle_0 \equiv 0 \quad \text{for } k > 0, \quad (2a)$$

$$c_{k\alpha j}^\dagger |\vec{0}\rangle_0 \equiv 0 \quad \text{for } k \leq 0. \quad (2b)$$

The  $c_{k\alpha j}$ ’s obey standard anticommutation relations,

$$\{c_{k\alpha j}, c_{k'\alpha' j'}^\dagger\} = \delta_{kk'} \delta_{\alpha\alpha'} \delta_{jj'} , \quad (3)$$

where due to radial momentum quantization in the spherical box, the values taken on by  $k$  are quantized:

$$k = \frac{2\pi}{L} (n_k - P_0/2) , \quad n_k \in \mathbb{Z} . \quad (4)$$

Here  $P_0 = 0$  or  $1$ , since at zero temperature the chemical potential (and hence  $p_F$ ) must either coincide with a degenerate level ( $P_0 = 0$ ) or lie midway between two of them, respectively ( $P_0 = 1$ ). Evidently the level spacing in both cases is

$$\Delta_L = \frac{2\pi}{L} . \quad (5)$$

Since the  $s$ -wave conduction electrons form an effectively one-dimensional system they can also be described by a one dimensional chiral field, defined as<sup>36</sup>

$$\psi_{\alpha j}(x) \equiv \sqrt{\frac{2\pi}{L}} \sum_{n_k \in \mathbb{Z}} e^{-ikx} c_{k\alpha j} , \quad (x \in [-\frac{L}{2}, \frac{L}{2}]) , \quad (6)$$

$$\{\psi_{\alpha j}(x), \psi_{\alpha' j'}^\dagger(x')\} = \delta_{\alpha\alpha'} \delta_{jj'} 2\pi \delta(x - x') . \quad (7)$$

In the continuum limit  $L \rightarrow \infty$ , the  $x > 0$  and  $x < 0$  portions of  $\psi_{\alpha j}(x)$  can be associated with the incoming and outgoing scattering states, respectively. Note that for  $P_0 = 0$  or  $1$  the fields  $\psi_{\alpha j}(x)$  have periodic or antiperiodic boundary conditions at  $x = \pm L/2$ , respectively, hence  $P_0$  will be called the “periodicity parameter”.

We assume a short-ranged anisotropic exchange interaction between the impurity spin and the  $s$ -wave conduction electron spin density at the origin, i.e. a Kondo interaction of the form

$$H_{\text{int}} = \Delta_L \sum_{\mu, k, k' \atop \alpha, \alpha', j} \lambda_\mu S_\mu :c_{k\alpha j}^\dagger (\frac{1}{2} \sigma_{\alpha\alpha'}^\mu) c_{k'\alpha' j}: . \quad (8)$$

Here the  $S_\mu$  ( $\mu = x, y, z$ ) are the impurity spin operators, with  $S_z$  eigenvalues  $(\uparrow, \downarrow) = (\frac{1}{2}, -\frac{1}{2})$ , and the  $\lambda_\mu$ ’s denote dimensionless couplings:  $\lambda_z$  generates different phase shifts for spin-up and spin-down conduction electrons, while  $\lambda_x \equiv \lambda_y \equiv \lambda_\perp$  describe spin-flip scattering off the impurity. Finally, the effect of a finite magnetic field is described by

$$H_h = h_i S_z + h_e \hat{\mathcal{N}}_s , \quad (9)$$

where  $h_i$  and  $h_e$  denote the magnetic fields acting on the impurity and conduction electron spins, respectively, and  $\hat{\mathcal{N}}_s$  (to be defined slightly below) denotes the total spin of the conduction electrons.

Finally, note that we have taken all sums  $\sum_k$  over fermion momenta above to be unbounded, since the constructive bosonization scheme we intend to use requires an unbounded fermion momentum spectrum. We thus have effectively taken the fermion bandwidth, say  $D$ , to be infinite, but will reintroduce an ultraviolet cutoff when defining the boson fields in Eq. (14) below.

### III. BOSONIZATION BASICS

The key to diagonalizing the Hamiltonian is to find the relevant quantum numbers of the problem and to bosonize the Hamiltonian carefully. While the technique of bosonization is widely used in the literature, the so-called Klein factors mentioned in the introduction are often neglected or not treated with sufficient care. However, it has recently been emphasized by several authors<sup>41,44,48,49</sup> that these Klein factors are very important in some situations, one of which is the calculation of the finite-size spectrum. In the present Section we therefore discuss our bosonization approach in somewhat more detail than usual, formulating it as a set of *operator identities in Fock space*, and emphasizing in particular the proper use of Klein factors to ladder between states with different particle numbers in Fock space. (An elementary, pedagogical and detailed introduction to the bosonization scheme used here, which is based on that of Haldane,<sup>46</sup> may be found in Ref. 44.)

#### A. Bosonization Ingredients

To characterize the electronic states, we start by introducing the number operators

$$\hat{N}_{\alpha j} \equiv \sum_k :c_{k\alpha j}^\dagger c_{k\alpha j}: , \quad (10)$$

which count the number of electrons in channel  $(\alpha j)$  with respect to the free electron reference ground state  $|\vec{0}\rangle_0$ . The non-unique eigenstates of  $\hat{N}_{\alpha j}$  will generically be denoted by  $|\vec{N}\rangle \equiv |N_{\uparrow 1}\rangle \otimes |N_{\downarrow 1}\rangle \otimes |N_{\uparrow 2}\rangle \otimes |N_{\downarrow 2}\rangle$ , where the  $N_{\alpha j}$ 's can be arbitrary integers, i.e.  $\vec{N} \in \mathbb{Z}^4$ .

Next, we define bosonic electron-hole creators by

$$b_{q\alpha j}^\dagger \equiv \frac{i}{\sqrt{n_q}} \sum_{n_k \in \mathbb{Z}} c_{k+q\alpha j}^\dagger c_{k\alpha j} , \quad (q = 2\pi n_q/L > 0) , \quad (11)$$

where the  $n_q$  are positive integers. The operators  $b_{q\alpha j}^\dagger$  create “density excitations” with momentum  $q$  in channel  $\alpha j$ , satisfy standard bosonic commutation relations, and commute with the  $\hat{N}_{\alpha j}$ 's:

$$\begin{aligned} [b_{q\alpha j}, b_{q'\alpha' j'}^\dagger] &= \delta_{qq'} \delta_{\alpha\alpha'} \delta_{jj'} , \\ [b_{q\alpha j}, \hat{N}_{\alpha' j'}] &= 0 . \end{aligned} \quad (12)$$

Among all states  $|\vec{N}\rangle$  with given  $\vec{N}$ , there is a unique state, to be denoted by  $|\vec{N}\rangle_0$ , that contains *no holes* and thus has the defining property

$$b_{q\alpha j} |\vec{N}\rangle_0 = 0 \quad (\text{for any } q > 0, \alpha, j) . \quad (13)$$

We shall call it the “ $\vec{N}$ -particle ground state”, since in the absence of the interaction term (8), no  $|\vec{N}\rangle$  has a lower

energy than  $|\vec{N}\rangle_0$ ; likewise, no  $|\vec{N}\rangle_0$  has a lower energy than the “vacuum state”  $|\vec{0}\rangle_0$  defined in Eq. (2). Note, though, that if  $P_0 = 0$ , the states  $c_{0\alpha j} |\vec{0}\rangle_0$  are degenerate with  $|\vec{0}\rangle_0$ , because then  $c_{0\alpha j}$  removes a zero-energy electron. [In the conformal field theory literature the states  $|\vec{N}\rangle_0$  are sometimes referred to as  $[U(1)]^4$  primary states, since the quantum numbers  $\hat{N}_{\alpha j}$  are just the charges associated with the  $U(1)$  gauge transformations of the fields  $\psi_{\alpha j} \rightarrow \psi_{\alpha j} e^{i\delta_{\alpha j}}$ .] It can be proven<sup>46,44</sup> that any  $\vec{N}$ -electron state  $|\vec{N}\rangle$  can be written as  $|\vec{N}\rangle = f(b^\dagger) |\vec{N}\rangle_0$ , i.e. by acting on the  $\vec{N}$ -electron ground state with an appropriate function of electron-hole operators.

Next, we define bosonic fields by

$$\phi_{\alpha j}(x) \equiv \sum_{q>0} \frac{-1}{\sqrt{n_q}} \left( e^{-iqx} b_{q\alpha j} + e^{iqx} b_{q\alpha j}^\dagger \right) e^{-aq/2} . \quad (14)$$

Here  $a \sim 1/p_F$  is a short-distance cutoff; it is introduced to cure any ultraviolet divergences the theory may have acquired by taking the fermion bandwidth  $D$  to be infinite. It is well-known, however, that within this *bosonization cutoff scheme* the coupling constants have different meanings than for other standard regularization schemes using a finite fermion bandwidth, and that the relations between coupling constants in different regularization schemes can be found by requiring that they yield the same phase shifts. For the sake of completeness, we discuss this and other cutoff related matters in some detail in Appendix A.

It is easy to prove that the fields  $\partial_x \phi_{\alpha j}(x)$  are canonically conjugate to the  $\phi_{\alpha j}(x)$ 's, in that

$$[\phi_{\alpha j}(x), \partial_{x'} \phi_{\alpha' j'}(x')] = 2\pi i (\delta_a(x - x') - 1/L) \delta_{\alpha\alpha'} \delta_{jj'} , \quad (15)$$

where  $\delta_a(x - x')$  is a smeared delta function:

$$\delta_a(x - x') = \frac{a/\pi}{(x - x')^2 + a^2} . \quad (16)$$

As final bosonization ingredient, we need the so-called Klein factors  $F_{\alpha j}$ , which ladder between states with different  $N_{\alpha j}$ 's (which no function containing only  $b_{q\alpha j}^\dagger$  can accomplish, since these conserve  $N_{\alpha j}$ ). By definition, the  $F_{\alpha j}$ 's are required to satisfy the following relations:

$$[F_{\alpha j}, \hat{N}_{\alpha' j'}] = \delta_{\alpha\alpha'} \delta_{jj'} F_{\alpha j} , \quad (17a)$$

$$[F_{\alpha j}, b_{q\alpha' j'}] = [F_{\alpha j}, b_{q\alpha' j'}^\dagger] = 0 , \quad (17b)$$

$$F_{\alpha j} F_{\alpha j}^\dagger = F_{\alpha j}^\dagger F_{\alpha j} = 1 , \quad (17c)$$

$$\{F_{\alpha j}, F_{\alpha' j'}^\dagger\} = 2 \delta_{\alpha\alpha'} \delta_{jj'} \quad (17d)$$

$$\{F_{\alpha j}, F_{\alpha' j'}\} = 0 \quad \text{for } (\alpha j) \neq (\alpha' j') . \quad (17e)$$

These relations imply that when  $F_{\alpha j}$  is applied to a state  $|\vec{N}\rangle = f(b^\dagger) |\vec{N}\rangle_0$ , it commutes past  $f(b^\dagger)$  [by (17b)], and

then removes [by (17a)] an  $(\alpha j)$  electron from the top-most filled level of  $|\vec{N}\rangle_0$ , namely  $n_{k,\alpha j} = N_{\alpha j}$ ; to be explicit,  $F_{\alpha j}|\vec{N}\rangle = f(b^\dagger)c_{N_{\alpha j}\alpha j}|\vec{N}\rangle_0$ . Thus  $F_{\alpha j}$  decreases the electron number in channel  $\{\alpha j\}$  by one,  $N_{\alpha j} \rightarrow N_{\alpha j} - 1$ , without creating particle-hole excitations. Similarly,  $F_{\alpha j}^\dagger$  adds a single  $(\alpha j)$  electron. As shown in Refs. 46 or 44, the construction  $F_{\alpha j} = a^{1/2}\psi_{\alpha j}(0)e^{i\phi_{\alpha j}(0)}$ , which explicitly expresses  $F_{\alpha j}$  in terms of the fermion operators  $c_{k\alpha j}$ , has all the desired properties.

## B. Bosonization Identities

Having introduced the Klein factors  $F_{\alpha j}$  and the boson fields  $\phi_{\alpha j}$ , we are ready to bosonize, i.e. to rewrite expressions involving the fermion operators  $c_{k\alpha j}$  in terms of the bosonization ingredients defined above. In our notation, the standard bosonization identities<sup>46</sup> for the fermion field, density and kinetic energy take the following forms:<sup>44</sup>

$$\psi_{\alpha j}(x) = F_{\alpha j}a^{-1/2}e^{-i(\hat{N}_{\alpha j}-P_0/2)2\pi x/L}e^{-i\phi_{\alpha j}(x)}, \quad (18)$$

$$\frac{1}{2\pi}:\psi_{\alpha j}^\dagger(x)\psi_{\alpha j}(x):= \frac{1}{2\pi}\partial_x\phi_{\alpha j}(x) + \hat{N}_{\alpha j}/L, \quad (19)$$

$$H_0 = \sum_{\alpha j} \frac{\Delta_L}{2} \hat{N}_{\alpha j} (\hat{N}_{\alpha j} + 1 - P_0) + \sum_{\substack{\alpha j \\ q > 0}} q b_{q\alpha j}^\dagger b_{q\alpha j}. \quad (20)$$

Several comments are in order: Firstly, in the limit  $a \rightarrow 0$  Eqs. (18) to (20) are not mere formal correspondences between the fermionic and bosonic expressions, but hold as rigorous *operator identities in Fock space*. For  $a \neq 0$ , (18) and (19) are not rigorously exact, but instead should be viewed as conveniently regularized redefinitions of the fermion fields and densities (as discussed in Appendix A 2). Next, in Eq. (18) for  $\psi_{\alpha j}$ , the Klein factors  $F_{\alpha j}$  play a twofold role: firstly, by Eq. (17a) they ensure that the right-hand side of Eq. (18) acting on any state indeed does lower the number of  $\alpha j$ -electrons by one, just as  $\psi_{\alpha j}$  does; and secondly, by Eqs. (17d) and (17e) they ensure that fields with different  $(\alpha j)$ 's do have the proper anticommutation relations (7). In contrast, Eq. (19) for the density operator contains no Klein factors [because of (17c)]. Finally, in Eqs. (20) for the kinetic energy, the first  $\Delta_L$  term is just  $0\langle\vec{N}|H_0|\vec{N}\rangle_0$ , the energy of the  $\vec{N}$ -particle ground state  $|\vec{N}\rangle_0$  relative to  $|\vec{0}\rangle_0$ . Since the Klein factors do not commute with this term, they evidently cannot be neglected when calculating the full model's finite-size spectrum, for which all terms of order  $\Delta_L$  must be retained. The second term of (20) describes the energy of electron-hole excitations relative to  $|\vec{0}\rangle_0$ . [Its form can be obtained by observing that the commutator  $[b_{q\alpha j}, H_0]$  is the same when calculated in terms of  $c_{k\alpha j}$ 's using (1) and (11), or in terms of  $b_{q\alpha j}$ 's using (12) and (20).]

## IV. MAPPING ONTO RESONANT-LEVEL MODEL

In this section we map the 2CK model onto a resonant level model, using a finite-size version of the strategy invented by Emery and Kivelson: using bosonization and refermionization, we make a unitary transformation to a more convenient basis, in which the Hamiltonian is quadratic for a certain choice of parameters.

### A. Conserved Quantum Numbers

The quantum numbers  $N_{\alpha j}$  of Eq. (10) are conserved under the action of  $H_0$ ,  $H_h$  and  $H_z$  (the  $\lambda_z$  term of  $H_{\text{int}} \equiv H_z + H_\perp$ ), but fluctuate under the action of the spin-flip interaction  $H_\perp$  (the  $\lambda_\perp$  term). On the other hand, the total charge and flavor of the conduction electrons is obviously conserved by all terms in the Hamiltonian, including  $H_\perp$ . Therefore it is natural to introduce the following new quantum numbers:

$$\begin{pmatrix} \hat{\mathcal{N}}_c \\ \hat{\mathcal{N}}_s \\ \hat{\mathcal{N}}_f \\ \hat{\mathcal{N}}_x \end{pmatrix} \equiv \frac{1}{2} \begin{pmatrix} 1 & 1 & 1 & 1 \\ 1 & -1 & 1 & -1 \\ 1 & 1 & -1 & -1 \\ 1 & -1 & -1 & 1 \end{pmatrix} \begin{pmatrix} \hat{N}_{\uparrow 1} \\ \hat{N}_{\downarrow 1} \\ \hat{N}_{\uparrow 2} \\ \hat{N}_{\downarrow 2} \end{pmatrix}, \quad (21)$$

where  $2\hat{\mathcal{N}}_c$ ,  $\hat{\mathcal{N}}_s$ , and  $\hat{\mathcal{N}}_f$  denote the total charge, spin, and flavor of the conduction electrons, and  $\hat{\mathcal{N}}_x$  measures the spin difference between channels 1 and 2. Clearly, any conduction electron state  $|\vec{N}\rangle$  can equally well be labeled by the corresponding quantum numbers  $\vec{\mathcal{N}} \equiv (\mathcal{N}_c, \mathcal{N}_s, \mathcal{N}_f, \mathcal{N}_x)$ . However, whereas the  $N_{\alpha j}$ 's take arbitrary independent integer values, the  $\vec{\mathcal{N}}$ 's generated by Eq. (21) (with  $\vec{N} \in \mathbb{Z}^4$ ) can easily be shown to satisfy the following two constraints, to be called the *free gluing conditions*:

$$\vec{N} \in (\mathbb{Z} + P/2)^4, \quad (22a)$$

$$\mathcal{N}_c \pm \mathcal{N}_f = (\mathcal{N}_s \pm \mathcal{N}_x) \bmod 2, \quad (22b)$$

where the *parity index*  $P$  equals 0 or 1 if the total number of electrons is even or odd, respectively. Eq. (22a) formalizes the obvious fact that the addition or removal of one  $\alpha j$  electron to or from the system necessarily changes *each* of the  $\mathcal{N}_y$ 's by  $\pm 1/2$ , so that they are either all integers or all half-integers. Eq. (22b) selects out from the set of  $\vec{\mathcal{N}}$  of the form (22a) those that correspond in the old basis to  $\vec{N} \in \mathbb{Z}^4$ , i.e. to physical states (an  $\vec{\mathcal{N}}$  of the form (22a) that violates (22b) would correspond to  $\vec{N} \in (\mathbb{Z} + 1/2)^4$ , which does not exist in the physical Fock space).

The new basis has two major advantages: firstly,  $\mathcal{N}_c$  and  $\mathcal{N}_f$  are conserved quantum numbers; and secondly, the quantum number  $\mathcal{N}_s$  fluctuates only "mildly" between the values  $S_T \mp 1/2$ , since the total spin,

$$S_T \equiv \mathcal{N}_s + S_z , \quad (23)$$

is conserved. In contrast, *the quantum number  $\mathcal{N}_x$  fluctuates “wildly”,* because an appropriate succession of spin-flips can produce *any*  $\mathcal{N}_x$  that satisfies (22b), as illustrated in Fig. 1. *This wildly fluctuating quantum number will be seen below to be at the heart of the 2CK model’s NFL behavior.* In revealing contrast, the 1CK model, which shows no NFL behavior, lacks such a wildly fluctuating quantum number (see Appendix D).

Since  $S_T$ ,  $\mathcal{N}_c$  and  $\mathcal{N}_f$  are conserved, the Fock space  $\mathcal{F}_{\text{phys}}$  of all physical states can evidently be divided as follows into subspaces invariant under the action of  $H$ :

$$\mathcal{F}_{\text{phys}} = \sum_{\oplus' S_T, \mathcal{N}_c, \mathcal{N}_f} \mathcal{S}_{\text{phys}}(S_T, \mathcal{N}_c, \mathcal{N}_f) , \quad (24)$$

$$\begin{aligned} \mathcal{S}_{\text{phys}}(S_T, \mathcal{N}_c, \mathcal{N}_f) = \sum_{\oplus' \mathcal{N}_x} \Big\{ & |\mathcal{N}_c, S_T - 1/2, \mathcal{N}_f, \mathcal{N}_x; \uparrow\rangle \\ & \oplus |\mathcal{N}_c, S_T + 1/2, \mathcal{N}_f, \mathcal{N}_x + 1; \downarrow\rangle \Big\} . \end{aligned} \quad (25)$$

In both equations the prime on the sum indicates a restriction to those  $\mathcal{N}_y$ ’s that satisfy the free gluing conditions (22). To diagonalize the Hamiltonian for given  $S_T$ ,  $\mathcal{N}_c$  and  $\mathcal{N}_f$ , it evidently suffices to restrict one’s attention to the corresponding subspace  $\mathcal{S}_{\text{phys}}(S_T, \mathcal{N}_c, \mathcal{N}_f)$ .

## B. Emery-Kivelson transformation

Following Emery and Kivelson, we now introduce, in analogy to Eq. (21), new electron-hole operators and boson fields via the transformations,

$$\begin{aligned} b_{qy} & \equiv \sum_{\alpha j} R_{y,\alpha j} b_{q\alpha j} \\ \varphi_y & \equiv \sum_{\alpha j} R_{y,\alpha j} \phi_{\alpha j} \end{aligned} \quad \left\{ \begin{aligned} (y &= c, s, f, x) , \end{aligned} \right. \quad (26)$$

where  $R_{y,\alpha j}$  is the unitary matrix in (21). These obey relations analogous to (12) and (15), with  $\alpha j \rightarrow y$ . Moreover, we define  $|\vec{\mathcal{N}}\rangle_0$ , the  $\vec{\mathcal{N}}$ -particle vacuum state, to satisfy  $b_{qy}|\vec{\mathcal{N}}\rangle_0 = 0$ , as in (13). If  $\vec{\mathcal{N}}$  and  $\vec{N}$  are related by (21), then the states  $|\vec{\mathcal{N}}\rangle_0$  and  $|\vec{N}\rangle_0$  are equal up to an unimportant phase (see Appendix B), because both have the same  $\hat{N}_{\alpha j}$  and  $\hat{\mathcal{N}}_y$  eigenvalues and both are annihilated by all  $b_{q\alpha j}$ ’s and  $b_{qy}$ ’s.

Using the quantum numbers  $\hat{\mathcal{N}}_y$  and the bosonic fields  $\varphi_y(x)$ , the Hamiltonian takes a transparent form. The free electron part  $H_0$  of (20) can be written as

$$H_0 = \Delta_L \left[ \hat{\mathcal{N}}_c (1 - P_0) + \sum_y \hat{\mathcal{N}}_y^2 / 2 \right] + \sum_{y, q > 0} q b_{qy}^\dagger b_{qy} , \quad (27)$$

while Eqs. (19) and (18) are used to obtain, respectively,

$$H_z = \lambda_z \left[ \partial_x \varphi_s(0) + \Delta_L \hat{\mathcal{N}}_s \right] S_z , \quad (28)$$

$$\begin{aligned} H_\perp = \frac{\lambda_\perp}{2a} \Big[ & e^{-i\varphi_s(0)} S_+ (F_{\downarrow 1}^\dagger F_{\uparrow 1} e^{-i\varphi_x(0)} \\ & + F_{\downarrow 2}^\dagger F_{\uparrow 2} e^{i\varphi_x(0)}) + \text{h.c.} \Big] . \end{aligned} \quad (29)$$

Eqs. (27) to (29) and (9) constitute the bosonized form of the Hamiltonian for the anisotropic 2CK model, *up to and including terms of order  $\Delta_L$ .*

Next we simplify  $H_z$ , which, being diagonal in spin indices, merely causes a phase shift in the spin sector. This phase shift can be obtained explicitly using a unitary transformation (due to EK) parameterized by a real number  $\gamma$ , whose value will be determined below:

$$H \rightarrow H' = U H U^\dagger , \quad (30)$$

$$U \equiv e^{i\gamma S_z \varphi_s(0)} . \quad (31)$$

Under this transformation the impurity spin, the spin-diagonal part of the Hamiltonian, the spin boson field and the fermion fields transform as follows (using e.g. the operator identities of Appendix C of Ref. 44):

$$S_\pm \rightarrow U S_\pm U^\dagger = e^{\pm i\gamma \varphi_s(0)} S_\pm , \quad (32)$$

$$\begin{aligned} H_0 + H_z \rightarrow H_0 + (\lambda_z - \gamma) \partial_x \varphi_s(0) S_z \\ + \lambda_z \Delta_L \hat{\mathcal{N}}_s S_z + \gamma^2 [1/(4a) - \pi/(4L)] , \end{aligned} \quad (33)$$

$$\varphi_s(x) \rightarrow \varphi_s(x) - 2\gamma S_z \arctan(x/a) , \quad (|x| \ll L) . \quad (34)$$

$$\psi_{\alpha j}(x) \rightarrow \psi_{\alpha j}(x) e^{i\alpha \gamma S_z \arctan(x/a)} , \quad (|x| \ll L) . \quad (35)$$

Eq. (33) is most easily derived in the momentum-space representation [using (12), (14) and (20), see Section 7 of Ref. 44]; on the other hand, since in Eq. (34) we only give the  $|x| \ll L$  limit in which order  $1/L$  terms can be neglected, this equation is easier to derive in the position-space representation (by first evaluating  $U \partial_x \varphi_s(x) U^{-1}$  using (15) and (16), then integrating). Eq. (35) follows from (34), since  $\psi_{\alpha j} \propto e^{-i\alpha \varphi_s/2}$  [by (18) and (26)].

Recalling [from (19)] that  $\partial_x \varphi_s(x)/2\pi$  contributes to the conduction electron spin density, we note by differentiating (34) that the EK transformation produces a change in the spin density of  $-2\gamma S_z \pi \delta_a(x)/2\pi$ ; intuitively speaking, it ties a spin of  $-\gamma S_z$  from the conduction band to the impurity spin  $S_z$  at the origin.

To eliminate the  $S_z \partial_x \varphi_s$  term in (33), we now choose  $\gamma \equiv \lambda_z$ ; then the spin-flip-independent part of the Hamiltonian takes the form

$$\begin{aligned} H'(\lambda_\perp = 0) = \lambda_z \Delta_L \hat{\mathcal{N}}_s S_z + \sum_y \Delta_L \hat{\mathcal{N}}_y^2 / 2 \\ + \sum_{y, q > 0} q b_{qy}^\dagger b_{qy} + H_h + \text{const} , \end{aligned} \quad (36)$$

and  $H'_\perp$  contains the factors  $e^{\pm i(1-\lambda_z)\varphi_s(0)}$ . These factors are simply equal to 1 at the special line  $\lambda_z = 1$ , the so-called *Emery-Kivelson line*, at which  $H'_\perp$  simplifies to

$$H'_\perp = \frac{\lambda_\perp}{2a} \left[ S_+ (F_{\downarrow 1}^\dagger F_{\uparrow 1} e^{-i\varphi_x(0)} + F_{\downarrow 2}^\dagger F_{\uparrow 2} e^{i\varphi_x(0)}) + \text{h.c.} \right]. \quad (37)$$

We shall henceforth focus on the case  $\lambda_z = 1$ , which will enable us to diagonalize the model exactly by repermionization. Deviations from the EK line will be shown in Section VI C to be irrelevant, by taking  $\gamma = 1$  but  $\lambda_z = 1 + \delta\lambda_z$ , and doing perturbation theory in

$$\delta H'_z = \delta\lambda_z [\partial_x \varphi_s(0) + \Delta_L \hat{\mathcal{N}}_s] S_z. \quad (38)$$

Before proceeding, it is instructive to interpret the significance of the EK line using the standard heuristic language of Nozières and Blandin. They argued that in the *strong-coupling limit*, an anti-ferromagnetically-coupled impurity will “capture” one spin 1/2 from *both* the  $j = 1$  and 2 channels (capturing a spin from just one channel would break channel symmetry), i.e. it will tie a spin of  $-2S_z$  from the conduction band to its own  $S_z$ , which yields an “overscreened effective spin of  $-S_z$ ”. However, since the latter is again anti-ferromagnetically coupled to the remaining conduction electrons, this strong-coupling fixed point is unstable in the RG sense, just as the weak-coupling fixed point. Thus, they argued that there must be a NFL fixed point at intermediate coupling which is stable (for  $h_e = h_i = 0$ ).

Now, a crucial property of the EK line is that it contains this NFL intermediate-coupling fixed point. A heuristic way to see this is to note that on the EK line, the impurity spin *is* in fact “perfectly screened”: the spin  $-\gamma S_z$  from the conduction band [mentioned after (34)], that is tied to the impurity by the EK transformation, is equal to  $-S_z$  if  $\gamma = \lambda_z = 1$ , thus precisely “canceling” the impurity’s spin  $S_z$ . Thus, on the EK line the impurity “captures” exactly one spin 1/2 from the conduction band to form a “perfectly screened singlet” with *zero* total spin (which is the heuristic reason why the EK line is stable), but it does so *without* breaking channel symmetry, since  $\partial_x \varphi_s$  is constructed in equal amounts from all four species of  $\phi_{\alpha j}$  fields.

Of course, there are also more rigorous ways of seeing that the NFL fixed point lies on the EK line: Firstly, for  $\lambda_z = 1$  it follows from (35) that the phase shift  $\delta$  of the outgoing relative to the incoming fields, defined by  $\psi_{\alpha j}(0^-) \equiv e^{i2\delta} \psi_{\alpha j}(0^+)$  (with  $|0^\pm| \gg a$ ), is  $|\delta| = \pi/4$ , which is just the value known for the NFL fixed point from other approaches.<sup>20,30</sup> Secondly, we shall deduce in Section VI C from an analysis of the finite-size spectrum that the leading irrelevant operators (with dimensions 1/2) vanish exclusively *along* this line, but not away from it. Since the presence or absence of the leading irrelevant operators strongly influences the low-temperature properties of the model (such as its critical exponents)<sup>4,40</sup>, and since these must stay invariant under any RG transformation, one concludes that the Emery-Kivelson line must be stable under RG transformations.

## C. Repermionization

### 1. Definition of New Klein Factors

The most nontrivial step in the solution of the model is the proper treatment of Klein factors when repermionizing the transformed Hamiltonian. In their original treatment Emery and Kivelson did not discuss Klein factors at all and simply identified  $e^{-i\varphi_x(x)}/\sqrt{a}$  as a new pseudofermion field  $\psi_x(x)$ . Although this procedure happened to be adequate for their purposes, the proper consideration of the Klein factors and gluing conditions is essential, as already emphasized in the introduction, for giving a rigorous solution of the problem and obtaining the finite-size spectrum. Some other authors tried to improve the Emery-Kivelson procedure by representing the Klein factors by  $F_{\alpha j} \sim e^{-i\Theta_{\alpha j}}$ , where  $\Theta_{\alpha j}$  is a “phase operator conjugate to  $\hat{N}_{\alpha j}$ ”, and added these to the bosonic fields  $\phi_{\alpha j}$  before making the linear transformation (26). This procedure is problematic, however, since then the  $e^{-i\varphi_y(0)}$ ’s contain factors such as  $e^{-i\Theta_{\alpha j}/2}$ , which are ill-defined (for a more detailed discussion of this point, see Appendix D.2 of Ref. 44).

A novel, rigorous way of dealing with Klein factors when repermionizing was presented in Ref. 45 (and adapted in Ref. 44 to treat an impurity in a Luttinger liquid): We introduce a new set of ladder operators  $\mathcal{F}_y^\dagger$  and  $\mathcal{F}_y$  ( $y = c, s, f, x$ ) to raise or lower the new quantum numbers  $\mathcal{N}_y$  by  $\pm 1$ , with, by definition, the following properties [in analogy to Eqs. (17)]:

$$[\mathcal{F}_y, \hat{\mathcal{N}}_{y'}] = \delta_{yy'} \mathcal{F}_y, \quad (39a)$$

$$[\mathcal{F}_y, b_{qy'}] = [\mathcal{F}_y, b_{qy'}^\dagger] = 0, \quad (39b)$$

$$\mathcal{F}_y \mathcal{F}_y^\dagger = \mathcal{F}_y^\dagger \mathcal{F}_y = 1, \quad (39c)$$

$$\{\mathcal{F}_y, \mathcal{F}_{y'}^\dagger\} = 2 \delta_{yy'}, \quad (39d)$$

$$\{\mathcal{F}_y, \mathcal{F}_{y'}\} = 0 \quad \text{for } y \neq y'. \quad (39e)$$

Now, note that the action of any one of the new Klein factors  $\mathcal{F}_y$  or  $\mathcal{F}_y^\dagger$  respects the first of the free gluing conditions, (22a), but not the second, (22b). More generally, (22b) is respected only by products of an *even* number of new Klein factors, but violated by products of an *odd* number of them. This implies that the physical Fock space  $\mathcal{F}_{\text{phys}}$  of all  $|\vec{\mathcal{N}}\rangle$  satisfying both (22a) and (22b) is closed under the action of even but not of odd products of new Klein factors. For example, let  $|\psi\rangle_{\text{phys}}$  be in  $\mathcal{F}_{\text{phys}}$ , then  $\mathcal{F}_y^\dagger \mathcal{F}_{y'} |\psi\rangle_{\text{phys}}$  is too, but  $\mathcal{F}_y |\psi\rangle_{\text{phys}}$  violates (22b) and hence is an unphysical state. *The action of arbitrary combinations of new Klein factors thus generates an extended Fock space  $\mathcal{F}_{\text{ext}}$ , which contains  $\mathcal{F}_{\text{phys}}$  as a subspace and is spanned by the set of all  $|\vec{\mathcal{N}}\rangle$  satisfying (22a), including unphysical states violating (22b).* To demonstrate that  $\mathcal{F}_{\text{phys}}$  can indeed be so embedded in  $\mathcal{F}_{\text{ext}}$ , we explicitly construct a set of basis states for the latter in Appendix B.

Since *odd* products of  $\mathcal{F}_y$ 's lead out of  $\mathcal{F}_{\text{phys}}$ , they *cannot* be expressed in terms of the original Klein factors  $F_{\alpha j}$ , which leave  $\mathcal{F}_{\text{phys}}$  invariant. However, and this is crucial, the Hamiltonian contains only *even* products of old Klein factors. Now, any “diagonal” combination  $F_{\alpha j}^\dagger F_{\alpha j} = 1$ ; and any “off-diagonal” combination  $F_{\alpha j}^\dagger F_{\alpha' j'}$  or  $F_{\alpha j}^\dagger F_{\alpha' j'}$ , acting on any state  $|\vec{N}\rangle$  *just changes two of its  $N_{\alpha j}$  quantum numbers*. Using (21) to read off the corresponding changes in  $\mathcal{N}_s$ ,  $\mathcal{N}_f$  and  $\mathcal{N}_x$ , we can thus make the following identifications between *pairs* of the old and new Klein factors:

$$\mathcal{F}_x^\dagger \mathcal{F}_s^\dagger \equiv F_{\uparrow 1}^\dagger F_{\downarrow 1} , \quad \mathcal{F}_x \mathcal{F}_s^\dagger \equiv F_{\uparrow 2}^\dagger F_{\downarrow 2} , \quad (40a)$$

$$\mathcal{F}_x^\dagger \mathcal{F}_f^\dagger \equiv F_{\uparrow 1}^\dagger F_{\uparrow 2} , \quad \mathcal{F}_c^\dagger \mathcal{F}_s^\dagger = F_{\uparrow 1}^\dagger F_{\uparrow 2}^\dagger . \quad (40b)$$

Each of these relations involves an arbitrary choice of phase, whose consequences for the basis states  $|\vec{N}\rangle$  are discussed in Appendix B. These choices uniquely fix the phases of all other similar bilinear relations between old and new Klein factors, which can be found from composing (and conjugating) the above four, e.g.  $\mathcal{F}_s^\dagger \mathcal{F}_f^\dagger = -(\mathcal{F}_x \mathcal{F}_s^\dagger)(\mathcal{F}_x^\dagger \mathcal{F}_f^\dagger) = F_{\uparrow 1}^\dagger F_{\downarrow 2}$ . Since the relations (40) by construction respect (21) (as can be verified by acting on any  $|\vec{N}\rangle$ ), they, and all similar bilinear relations derived from them, also respect both of the free gluing conditions (22). The relations involving  $\mathcal{F}_c$  and  $\mathcal{F}_f$  are not needed for the present 2CK model, but are included for completeness; for example,  $\mathcal{F}_f$  would be needed for models involving “flavor-flip” processes.

We can thus replace the Klein factor pairs occurring in Eq. (37) by the ones in Eq. (40a):

$$H'_\perp = \frac{\lambda_\perp}{2a} \left[ S_+ F_s (F_x e^{-i\varphi_x(0)} + F_x^\dagger e^{i\varphi_x(0)}) + \text{h.c.} \right] \quad (41)$$

The only consequence of this change is that we now work in the extended Fock space  $\mathcal{F}_{\text{ext}}$ , and will diagonalize  $H'$  not in the physical invariant subspace  $\mathcal{S}_{\text{phys}}(S_T, \mathcal{N}_c, \mathcal{N}_f)$  of (25), but in the corresponding extended subspace  $\mathcal{S}_{\text{ext}}(S_T, \mathcal{N}_c, \mathcal{N}_f)$ , given by an equation similar to (25), but where the  $\oplus' \mathcal{N}_x$  sum now is restricted only to satisfy (22a), not also (22b). At the end of the calculation we shall then use the gluing condition (22b), satisfied only by the physical states in  $\mathcal{S}_{\text{ext}}$  but not by its additional unphysical states, to identify and discard the latter (see Section V C). This approach is completely analogous to the use of gluing conditions in AL's CFT solution of the 2CK model. It is also in some sense analogous to Abrikosov's pseudofermion technique<sup>50</sup>; there an impurity-spin operator is represented in terms of pseudofermion operators acting in an enlarged Hilbert space, which contains not only the physical one-pseudofermion states, but also unphysical many- or no-pseudofermion states that are projected away at the end of the calculation.

## 2. Pseudofermions and Refermionized Hamiltonian

We now note that  $H'_\perp$  of (41) can be written in a form *quadratic* in fermionic variables,

$$H'_\perp = \frac{\lambda_\perp}{2\sqrt{a}} (\psi_x(0) + \psi_x^\dagger(0)) (c_d - c_d^\dagger) , \quad (42)$$

by defining a local pseudofermion  $c_d$  and a pseudofermion field  $\psi_x(x)$  by the following refermionization relations:

$$c_d \equiv F_s^\dagger S_- , \quad c_d^\dagger c_d = S_z + 1/2 , \quad (43)$$

$$\psi_x(x) \equiv F_x a^{-1/2} e^{-i(\hat{\mathcal{N}}_x - 1/2)2\pi x/L} e^{-i\varphi_x(x)} \quad (44a)$$

$$\equiv \sqrt{\frac{2\pi}{L}} \sum_{\bar{k}} e^{-i\bar{k}x} c_{\bar{k}x} . \quad (44b)$$

where Eq. (44b) defines the  $c_{\bar{k}x}$  as Fourier coefficients of the field  $\psi_x(x)$ . For reasons discussed below, the field  $\psi_x$  in Eq. (44a) has been defined in such a way that its boundary condition at  $\pm L/2$  is  $P$ -dependent, since  $\mathcal{N}_x \in \mathbb{Z} + P/2$  and  $\varphi_x(x)$  is a periodic function. Thus the quantized  $\bar{k}$  momenta in the Fourier expansion (44b) must have the form

$$\bar{k} = \Delta_L [n_{\bar{k}} - (1 - P)/2] , \quad (n_{\bar{k}} \in \mathbb{Z}) \quad (45)$$

(i.e. the periodicity parameter  $P_0$  of (4) here equals  $1 - P$ ).

The new pseudofermions were constructed in such a way that they satisfy the following commutation/anticommutation relations

$$\{c_{\bar{k}x}, c_{\bar{k}'x}^\dagger\} = \delta_{\bar{k}\bar{k}'} , \quad (46)$$

$$\{c_d, c_d^\dagger\} = 1 , \quad (47)$$

$$\{c_d, c_{\bar{k}x}^\dagger\} = \{c_d, c_{\bar{k}x}\} = 0 , \quad (48)$$

$$[c_d, \hat{\mathcal{N}}_s] = c_d , \quad (49)$$

which follow directly from the properties of  $\varphi_x$  [by analogy to the relations of Section III] and Eqs. (39). Note that  $c_d$  lowers the impurity spin, raises the total electron spin  $\hat{\mathcal{N}}_s$  and hence conserves the total spin  $S_T$ , whereas  $\psi_x$  conserves each of the impurity, electron and total spins.

Next we have to relate the number operator for the new  $x$ -pseudofermions to the quantum number  $\mathcal{N}_x$ . This requires defining a free reference ground state, say  $|0\rangle_{\mathcal{S}_{\text{ext}}}$ , in the extended subspace  $\mathcal{S}_{\text{ext}}$ , with respect to which the number of pseudofermions are counted. In analogy to (2), we define  $|0\rangle_{\mathcal{S}_{\text{ext}}}$  by

$$c_{\bar{k}x} |0\rangle_{\mathcal{S}_{\text{ext}}} \equiv 0 \quad \text{for } \bar{k} > 0 , \quad (50a)$$

$$c_{\bar{k}x}^\dagger |0\rangle_{\mathcal{S}_{\text{ext}}} \equiv 0 \quad \text{for } \bar{k} \leq 0 , \quad (50b)$$

$$c_d |0\rangle_{\mathcal{S}_{\text{ext}}} \equiv 0 \quad \text{for } \varepsilon_d > 0 , \quad \text{i.e. } n_d^{(0)} \equiv 0 , \quad (50c)$$

$$c_d^\dagger |0\rangle_{\mathcal{S}_{\text{ext}}} \equiv 0 \quad \text{for } \varepsilon_d \leq 0 , \quad \text{i.e. } n_d^{(0)} \equiv 1 . \quad (50d)$$

Here  $\varepsilon_d$ , whose value will be derived below [see (56)], is the energy associated with the  $c_d$  pseudofermion, and  $n_d^{(0)}$  denotes its occupation number in the reference ground state  $|0\rangle_{\mathcal{S}_{\text{ext}}}$ . Using the symbol  $:\cdot:$  to henceforth denote normal ordering of the pseudofermions w.r.t.  $|0\rangle_{\mathcal{S}_{\text{ext}}}$ , we have  $:c_d^\dagger c_d := c_d^\dagger c_d - n_d^{(0)}$ . Furthermore, we define the number operator for the  $x$ -pseudofermions by  $\hat{N}_x \equiv \sum_{\bar{k}} :c_{\bar{k}x}^\dagger c_{\bar{k}x}:$ . Then equations (44), (45) and (50) together imply that

$$\hat{N}_x = \hat{\mathcal{N}}_x - P/2 \quad (51)$$

holds as an operator identity. This can be seen intuitively by noting that  $\psi_x \sim \mathcal{F}_x \sim c_{\bar{k}x}$  [by (44)], hence the application of  $\psi_x$  (or  $\psi_x^\dagger$ ) to a state decreases (or increases) both  $\mathcal{N}_x$  and  $\bar{N}_x$  by one. These two numbers can thus differ only by a constant, which must ensure that  $\bar{N}_x$  is an integer. Our definition of  $|0\rangle_{\mathcal{S}_{\text{ext}}}$  effectively fixes this constant to be  $P/2$ , by setting  $\bar{N}_x = 0$  for  $\mathcal{N}_x = P/2$ . (This can be verified rigorously by checking<sup>69</sup> that  $\lim_{x_0 \rightarrow 0} \lim_{a \rightarrow 0} \int_{-L/2}^{L/2} \frac{dx}{2\pi} [\psi_x^\dagger(x + x_0) \psi_x(x) - \frac{1}{x_0}]$ , when evaluated using either (44a) or (44b), yields the right- or left-hand sides of (51), respectively. Similarly, Eq. (52) below can be proven by evaluating  $\lim_{x_0 \rightarrow 0} \lim_{a \rightarrow 0} \int_{-L/2}^{L/2} \frac{dx}{2\pi} [\psi_x^\dagger(x + x_0) i\partial_x \psi_x(x) - \frac{1}{x_0^2}]$ .)

We are now ready to repermionize the Hamiltonian  $H'$ . The kinetic energy of the  $\bar{k}$  pseudofermions obeys the following operator identity:

$$\sum_{\bar{k}} \bar{k} :c_{\bar{k}x}^\dagger c_{\bar{k}x} := \frac{\Delta_L}{2} \hat{N}_x (\hat{N}_x + P) + \sum_q q b_{qx}^\dagger b_{qx} . \quad (52)$$

This follows by analogy with (1) and (20), with  $\hat{N}_x$  and  $1 - P$  instead of  $\hat{N}_{\alpha j}$  and  $P_0$ . Now note that  $\hat{N}_x (\hat{N}_x + P) = \hat{\mathcal{N}}_x^2 - P/4$ , i.e. (52) does *not* contain a term linear in  $\hat{N}_x$ . Actually, the choice of the phase  $e^{-i(\hat{N}_x-1/2)2\pi x/L}$  in our repermionization Ansatz (44a) for  $\psi_x(x)$  was made specifically to achieve this. Hence (52) can be directly used to represent the kinetic energy of the  $x$ -sector in Eq. (27) in terms of  $c_{\bar{k}x}$  fermions:

$$H_{x0} = \Delta_L \hat{\mathcal{N}}_x^2 / 2 + \sum_{q>0} q b_{qx}^\dagger b_{qx} \quad (53a)$$

$$= \sum_{\bar{k}} \bar{k} :c_{\bar{k}x}^\dagger c_{\bar{k}x} : + \Delta_L P/8 . \quad (53b)$$

As a check, note that this equation also follows from the following observations: firstly, the equation of motion for the field  $\psi_x(x)$ , expressed as (44a) or (44b), is the same when calculated using (53a) or (53b), respectively, and therefore the latter two expressions can differ only by a constant; and secondly, this constant can be determined to be  $\Delta_L P/8$ , by requiring the free ground state energies for  $|0\rangle_{\mathcal{S}_{\text{ext}}}$  given by the two expressions to be the same.

Finally, in the subspace  $\mathcal{S}_{\text{phys}}$  [of (25)] and hence also in  $\mathcal{S}_{\text{ext}}$ , we can use (23) and (43) to express  $\hat{\mathcal{N}}_s S_z$  and

$\hat{\mathcal{N}}_s^2$  in terms of  $c_d^\dagger c_d$ . Thus, the EK-transformed 2CK Hamiltonian of Eqs. (36) and (37) takes the form

$$H' = H_{\text{csf}} + H_x + E_G + \text{const.} , \quad (54)$$

$$H_{\text{csf}} = \sum_{c,s,f} \sum_{q>0} q b_{qy}^\dagger b_{qy} , \quad (55)$$

$$H_x = \varepsilon_d :c_d^\dagger c_d: + \sum_{\bar{k}} \bar{k} :c_{\bar{k}x}^\dagger c_{\bar{k}x}: + \sqrt{\Delta_L \Gamma} \sum_{\bar{k}} (c_{\bar{k}x}^\dagger + c_{\bar{k}x})(c_d - c_d^\dagger) , \quad (56)$$

$$E_G = \Delta_L \left[ \mathcal{N}_c (1 - P_0) + (\mathcal{N}_c^2 + \mathcal{N}_f^2 + S_T^2 - 1/4)/2 + P/8 \right] + \varepsilon_d (n_d^{(0)} - 1/2) + S_T h_e . \quad (57)$$

The charge, spin and flavor degrees of freedom in  $H_{\text{csf}}$  evidently decouple completely.  $H_x$  in (56) has the form of a quadratic resonant level model whose “resonant level” has energy  $\varepsilon_d$  and width  $\Gamma$ , where  $\varepsilon_d \equiv h_i - h_e$  is the energy cost for an impurity spin-flip, and  $\Gamma = \lambda_\perp^2/4a$ , which will be identified below as the Kondo temperature.

$E_G$  is the “free ground state energy” of the subspace  $\mathcal{S}_{\text{ext}}$  in the presence of magnetic fields. Its  $S_T h_e$  term implies that the magnetic fields do *not* enter only in the combination  $h_i - h_e$  of  $\varepsilon_d$ , thus the role of the magnetic field  $h_e$  applied to the conduction electrons is somewhat different from that of the local field  $h_i$ . Note though, that for  $h_e = 2n\Delta_L$  (with  $n \in \mathbb{Z}$ ) the  $S_T h_e$  term can formally be absorbed (up to a total energy shift) by introducing a “new total spin”  $S'_T = S_T + 2n$ , since then  $\Delta_L S_T^2 / 2 + S_T h_e = \Delta_L S'_T^2 / 2 - 2n^2 \Delta_L$ . Now, since the construction of the complete finite-size spectrum involves enumerating all possible values of  $S_T$ , and since the generalized gluing condition (75) to be derived below is invariant under  $S_T \rightarrow S_T + 2n$ , the finite-size spectrum for  $h_e = 2n\Delta_L$  and a local field  $h_i$  (so that  $\varepsilon_d = h_i - 2n\Delta_L$ ) will be identical to that for  $h_e = 0$  and a local field of  $h_i - 2n\Delta_L$  (so that  $\varepsilon_d$  is unchanged). The physical origin of this “periodicity” is that as  $h_e$  increases, at each value  $2n\Delta_L$  a “level crossing” occurs in which the free-electron ground state changes from, say,  $|\mathcal{N}_c, \mathcal{N}_s, \mathcal{N}_f, \mathcal{N}_x\rangle_0$  to a new one differing from it *only* in the spin quantum number, namely  $|\mathcal{N}_c, \mathcal{N}_s - 2, \mathcal{N}_f, \mathcal{N}_x\rangle_0$ , by flipping the top-most spin-up electrons in both channels  $j = 1$  and  $2$  to spin down.

For general values  $h_e \neq 2n\Delta_L$ , there is no such symmetry (essentially since electron-hole symmetry in the spin sector is lost), and the corresponding finite-size spectrum differs from that at the periodicity points in that some additional splitting of states occurs.<sup>51</sup> For simplicity we henceforth set  $h_e = 0$  and consider only a local magnetic field, with  $\varepsilon_d \equiv h_i$ , but the more general case  $h_e \neq 0$  can be treated completely analogously.

## V. FINITE-SIZE SPECTRUM OF 2CK MODEL

EK studied the resonant level model  $H_x$  of (56) in the continuum limit  $L \rightarrow \infty$ . They mainly analyzed its *impurity* properties, showing that these have NFL behavior because “half of the impurity”, namely  $c_d + c_d^\dagger$ , decouples. By keeping  $L$  finite, one can extend their analysis to include also the NFL behavior of electron properties. In this section, we illustrate this by diagonalizing  $H_x$  at finite  $L$  and constructing its finite-size spectrum in terms of its exact eigenexcitations.

### A. Diagonalization of $H_x$

Since  $H_{csf}$  is trivial, we just have to diagonalize the resonant level part  $H_x$  in the extended subspace  $\mathcal{S}_{\text{ext}}(S_T, \mathcal{N}_c, \mathcal{N}_f)$ , which is straightforward in principle, since  $H_x$  is quadratic. However, care has to be exercised, in particular regarding normal ordering: the change in ground state energy due to the interaction turns out to be of order  $-\Gamma$ , and the sub-leading (state-dependent) contributions of order  $\Delta_L$  relative to this energy have to be extracted carefully when constructing the finite-size spectrum.

As first step, we define new fermionic excitations, illustrated in Fig. 2, whose energies are strictly non-negative,

$$\left. \begin{aligned} \alpha_{\bar{k}} &\equiv (c_{\bar{k}x} + c_{-\bar{k}x}^\dagger)/\sqrt{2} \\ \beta_{\bar{k}} &\equiv -i(c_{\bar{k}x} - c_{-\bar{k}x}^\dagger)/\sqrt{2} \end{aligned} \right\} \quad \text{for } \bar{k} > 0, \quad (58a)$$

$$\alpha_0 \equiv c_{0x}^\dagger \quad \text{for } \bar{k} = 0 \text{ if } P = 1, \quad (58b)$$

$$\alpha_d \equiv \begin{cases} c_d & \text{for } \varepsilon_d > 0 \\ c_d^\dagger & \text{for } \varepsilon_d \leq 0 \end{cases}, \quad (58c)$$

and which have the virtue that the  $\beta_{\bar{k}}$  excitations decouple completely from the impurity:

$$\begin{aligned} H_x &= \sum_{\bar{k} \geq 0} \bar{k} \alpha_{\bar{k}}^\dagger \alpha_{\bar{k}} + \sum_{\bar{k} > 0} \bar{k} \beta_{\bar{k}}^\dagger \beta_{\bar{k}} + |\varepsilon_d| \alpha_d^\dagger \alpha_d \\ &+ \sum_{\bar{k} \geq 0} V_{\bar{k}} (\alpha_{\bar{k}}^\dagger + \alpha_{\bar{k}}) (\alpha_d - \alpha_d^\dagger). \end{aligned} \quad (59)$$

Here the possible  $\bar{k}$ -values are given by Eq. (45), and the hybridization amplitudes  $V_{\bar{k}}$  by

$$V_0 \equiv V_{\bar{k} \neq 0}/\sqrt{2} \equiv e^{i\pi n_d^{(0)}} \sqrt{\Gamma \Delta_L}. \quad (60)$$

Note that in (58) we purposefully defined  $\alpha_n^\dagger$  and  $\beta_{\bar{k}}^\dagger$  such that the free reference ground state  $|0\rangle_{\mathcal{S}_{\text{ext}}}$ , by (50), contains *no*  $\alpha_n^\dagger$  or  $\beta_{\bar{k}}^\dagger$  excitations, i.e.

$$\alpha_d |0\rangle_{\mathcal{S}_{\text{ext}}} = \alpha_{\bar{k}} |0\rangle_{\mathcal{S}_{\text{ext}}} = \beta_{\bar{k}} |0\rangle_{\mathcal{S}_{\text{ext}}} = 0, \quad (61)$$

as illustrated in the middle entries of the first rows of Figs. 2(a), 2(b) and 2(c). Note too that  $\alpha_d^\dagger |0\rangle_{\mathcal{S}_{\text{ext}}}$  is degenerate with  $|0\rangle_{\mathcal{S}_{\text{ext}}}$  if  $\varepsilon_d = 0$ , as is  $\alpha_0^\dagger |0\rangle_{\mathcal{S}_{\text{ext}}}$  in the odd electron sector,  $P = 1$ .

Since the Hamiltonian Eq. (59) is quadratic, it can be brought into the diagonal form

$$H_x = \sum_{\bar{k} > 0} \bar{k} \beta_{\bar{k}}^\dagger \beta_{\bar{k}} + \sum_{\varepsilon \geq 0} \varepsilon \tilde{\alpha}_\varepsilon^\dagger \tilde{\alpha}_\varepsilon + \delta E_G, \quad (62)$$

describing a ground state energy shift  $\delta E_G$  and non-negative-energy excitations relative to a reference state  $|\tilde{0}\rangle_{\mathcal{S}_{\text{ext}}}$ , an exact ground state of  $H'$  in  $\mathcal{S}_{\text{ext}}$ , defined by

$$\tilde{\alpha}_\varepsilon |\tilde{0}\rangle_{\mathcal{S}_{\text{ext}}} = \beta_{\bar{k}} |\tilde{0}\rangle_{\mathcal{S}_{\text{ext}}} \equiv 0. \quad (63)$$

This diagonalization can be accomplished by a Bogoliubov transformation of the form

$$\tilde{\alpha}_\varepsilon^\dagger = \sum_{n \in \{\bar{k}, d\}} \sum_{\nu=\pm} B_{\varepsilon n \nu} (\alpha_n^\dagger + \nu \alpha_n)/2, \quad (64)$$

where the new operators  $\tilde{\alpha}_\varepsilon$  are required to satisfy:

$$[H_x, \tilde{\alpha}_\varepsilon^\dagger] = \varepsilon \tilde{\alpha}_\varepsilon^\dagger, \quad (65)$$

$$\{\tilde{\alpha}_\varepsilon^\dagger, \tilde{\alpha}_{\varepsilon'}\} = \delta_{\varepsilon \varepsilon'}. \quad (66)$$

Eqs. (65) and (66) yield a closed system of equations for the eigenenergies  $\varepsilon$  and the coefficients  $B_{\varepsilon n \nu}$ . In Appendix C, we solve them explicitly (by transforming to conveniently chosen Majorana fermions), with the following results.

The excitation energies  $\varepsilon$  are the non-negative roots of the transcendental equation

$$\frac{\varepsilon 4\pi \Gamma}{\varepsilon^2 - \varepsilon_d^2} = -\cot \pi (\varepsilon/\Delta_L - P/2), \quad (67)$$

and the ground state energy shift is

$$\delta E_G = \frac{|\varepsilon_d|}{2} + \sum_{\bar{k} \geq 0} \frac{\bar{k}}{2} - \sum_{\varepsilon \geq 0} \frac{\varepsilon}{2}. \quad (68)$$

For  $\varepsilon > 0$ , the coefficients  $B_{\varepsilon n \nu}$  are given by

$$B_{\varepsilon d+} = \varrho(\varepsilon) |\varepsilon_d|, \quad B_{\varepsilon d-} = \varrho(\varepsilon) \varepsilon, \quad (69a)$$

$$B_{\varepsilon \bar{k}+} = \varrho(\varepsilon) \frac{2V_{\bar{k}} \varepsilon^2}{\varepsilon^2 - \bar{k}^2}, \quad B_{\varepsilon \bar{k}-} = \varrho(\varepsilon) \frac{2V_{\bar{k}} \varepsilon \bar{k}}{\varepsilon^2 - \bar{k}^2}, \quad (69b)$$

where the normalization factor  $\varrho(\varepsilon)$  is

$$\varrho(\varepsilon) = \left[ \frac{2\Delta_L \Gamma}{\frac{1}{4}(\varepsilon^2 - \varepsilon_d^2)^2 + \Delta_L \Gamma (\varepsilon^2 + \varepsilon_d^2) + 4\pi^2 \Gamma^2 \varepsilon^2} \right]^{1/2}. \quad (70)$$

For  $\varepsilon = 0$ , the coefficients  $B_{0 n \nu}$  must be considered separately and are given in Appendix C 2 b.

Eqs. (55), (57), (62) and (67) to (70), together with the gluing conditions (75) discussed in the next subsection, constitute a complete, analytic solution of the 2CK model along the EK line.

## B. Evolution of Excitation Energies

The eigenvalue equation (67) is a central ingredient of our analytical solution, since it yields the exact excitation energies  $\varepsilon$  of  $H_x$ , and also allows one to explicitly identify the various crossover scales of the problem. Let the label  $j = 0, 1, 2, \dots$  enumerate, in increasing order, the solutions  $\varepsilon_{j,P}$  of (67) in a sector with parity  $P$ . Their smooth evolution as functions of  $\Gamma$  and  $|\varepsilon_d|$  can readily be understood by a graphical analysis of Eq. (67), see Fig. 3, and is shown in Figs. 4(a) and 4(b) for  $P = 0$  and 1, respectively. All but the lowest-lying ( $j = 0$ ) solutions can be parameterized as

$$\varepsilon_{j,P} = \Delta_L \left[ j - \frac{1}{2} - \frac{P}{2} + \delta_{j,P} \right], \quad j = 1, 2, 3, \dots, \quad (71a)$$

where  $\delta_{j,P} \in [0, 1]$  is the shift of  $\varepsilon_{j,P}/\Delta_L$  from its  $\Gamma = \varepsilon_d = 0$  value and is determined selfconsistently [from (67)] by

$$\delta_{j,P} = \frac{1}{2} + \frac{1}{\pi} \arctan \frac{1}{4\pi} \left[ \frac{T_h}{\varepsilon_{j,P}} - \frac{\varepsilon_{j,P}}{\Gamma} \right], \quad (71b)$$

with  $T_h \equiv \varepsilon_d^2/\Gamma$ . The lowest-lying modes are given by

$$\frac{\varepsilon_{0,0}}{\Delta_L} = \begin{cases} 0 & \text{for } \varepsilon_d = 0, \\ (-1/2 + \delta_{0,0}) \in (0, 1/2] & \text{for } \varepsilon_d \neq 0, \end{cases} \quad (72a)$$

$$\varepsilon_{0,1} = 0 \quad \text{for all } \Gamma, \varepsilon_d \quad (72b)$$

(see also Appendix C 2 b).

Eq. (71b) shows very nicely that  $\Gamma$  and  $T_h$  are crossover scales: Firstly, in the absence of magnetic fields, i.e. for  $|\varepsilon_d| = |h_i| = T_h = 0$ , the spectral regime *below*  $\Gamma$  is *strongly perturbed* [ $\delta_{j,P} \simeq 1/2$  for  $\varepsilon_{j,P} \ll \Gamma$ ], whereas *above*  $\Gamma$  it is *only weakly perturbed* [ $\delta_{j,P} \simeq 0$  for  $\varepsilon_{j,P} \gg \Gamma$ ]. This also follows directly from a graphical analysis of the eigenvalue equation (67). It is thus natural to identify the crossover scale  $\Gamma$  with the Kondo temperature,  $T_K \simeq \Gamma$ .

Secondly, in the presence of a local magnetic field,  $T_h = h_i^2/\Gamma > 0$  furnishes another crossover scale. When considering the  $T_h$ -induced shifts in  $\delta_{j,P}$  relative to their values for  $T_h = 0$ , several cases can be distinguished [by direct inspection of (71b)]:

(i) For  $T_h \ll \Delta_L$ , i.e. for  $|h_i|$  much smaller than a crossover field  $h_c \sim \sqrt{\Gamma\Delta_L}$ , none of the  $T_h$ -induced shifts are strong.

(ii) For  $T_h \gg \Delta_L, \Gamma$ , the crossover scale  $T_h$  divides the spectrum into two parts: the  $T_h$ -induced shifts are weak for all levels with  $\varepsilon \gg T_h$ , but strong for all those with  $\varepsilon \ll T_h$ .

(iii) For  $\Gamma \gg T_h \gg \Delta_L$  [a special case of (ii)] one can distinguish three physically different regimes: the spectrum is NFL-like (non-uniform level spacings) in the intermediate regime  $T_h \ll \varepsilon \ll \Gamma$ , and Fermi-liquid like (with uniform level spacing) in the extreme regimes  $\varepsilon \gg \Gamma$  and  $\varepsilon \ll T_h$ . In the last of these regimes (rightmost part of Fig. 4), the set of lowest-lying  $\varepsilon$ 's is in fact

identical to that for the *free* case  $T_h = 0, \Gamma = 0$  (leftmost part of Fig. 4), except that the free case has one more  $\varepsilon = 0$  mode, associated with the impurity level's two-fold degeneracy due to spin reversal symmetry for  $|h_i| = 0$  (which is broken if  $T_h \gg \Delta_L$ , implying  $|h_i| \gg \Delta_L$ ). This shows quite beautifully that a magnetic field very literally suppresses the effect of spin-flip scattering for the low-energy part of the spectrum; heuristically, this happens, of course, since low-energy electrons do not have enough energy to overcome the Zeeman energy necessary for a spin flip in a magnetic field.

Since at a finite temperature physical quantities are governed mostly by excitations of energy  $\varepsilon \sim T$ , they will show NFL behavior for  $\Gamma \gg T \gg T_h$  and Fermi liquid behavior for  $T \gg \Gamma$  or  $T \ll T_h$ <sup>31,52,4,40</sup>, as sketched in Fig 5.

## C. Generalized Gluing Conditions

A general eigenstate of  $H_x$  in  $\mathcal{S}_{\text{ext}}$  has the form

$$|\tilde{E}\rangle \propto \prod_{i=1}^{\mathcal{N}_{\alpha}} \tilde{\alpha}_{\varepsilon_i}^{\dagger} \prod_{j=1}^{\mathcal{N}_{\beta}} \tilde{\beta}_{\bar{k}_j}^{\dagger} |\tilde{0}\rangle_{\mathcal{S}_{\text{ext}}}. \quad (73)$$

However, as emphasized earlier, of all such states only those in the physical subspace  $\mathcal{S}_{\text{phys}}$  must be retained, and all others discarded as being unphysical. (Recall that we had to extend  $\mathcal{S}_{\text{phys}}$  to  $\mathcal{S}_{\text{ext}}$  to define the operators  $\psi_x$  and  $c_d$ .) To identify which  $|\tilde{E}\rangle$  are physical, we shall now derive a *generalized gluing condition* satisfied by them, by noting that  $|\tilde{E}\rangle$  can be physical only if the state  $|E\rangle \equiv \lim_{\Gamma \rightarrow 0} |\tilde{E}\rangle$ , to which it reduces when  $\Gamma$  is adiabatically switched off, satisfies the free gluing conditions (22). Key to the derivation is the fact that although the hybridization interaction  $H'_\perp$  of (42) does not conserve the number of  $\alpha_n^{\dagger}$  excitations, it *does conserve the parity* of their number.

To be explicit, let  $\mathcal{P}_{\tilde{E}}$  be the the parity of the number of excitations of  $|\tilde{E}\rangle$  relative to  $|\tilde{0}\rangle_{\mathcal{S}_{\text{ext}}}$ :

$$\mathcal{P}_{\tilde{E}} \equiv \langle \tilde{E} | \left[ \sum_{\varepsilon \geq 0} \tilde{\alpha}_{\varepsilon}^{\dagger} \tilde{\alpha}_{\varepsilon} + \sum_{\bar{k} > 0} \tilde{\beta}_{\bar{k}}^{\dagger} \tilde{\beta}_{\bar{k}} \right] \bmod 2 | \tilde{E} \rangle. \quad (74)$$

During the adiabatic switch-off of  $\Gamma$ , this quantity of course remains *fixed*, and hence equals  $\mathcal{P}_{\tilde{E}}(\Gamma \rightarrow 0)$ . This in turn can be written as

$$\begin{aligned} \mathcal{P}_{\tilde{E}}(\Gamma \rightarrow 0) &= \langle E | \left[ \sum_{n=d, \bar{k} \geq 0} \alpha_n^{\dagger} \alpha_n + \sum_{\bar{k} > 0} \beta_{\bar{k}}^{\dagger} \beta_{\bar{k}} \right] \bmod 2 | E \rangle \\ &= \langle E | \left[ \hat{N}_x + \alpha_d^{\dagger} \alpha_d \right] \bmod 2 | E \rangle \\ &= \langle E | \left[ \hat{N}_x - \frac{P}{2} + \hat{N}_s - S_T - \frac{1}{2} + n_d^{(0)} \right] \bmod 2 | E \rangle. \end{aligned}$$

The first equation follows because the hybridization interaction preserves the parity of the excitation numbers

(in other words, since  $\tilde{\alpha}_\varepsilon^\dagger$  is a linear combination of  $\alpha_n^\dagger$  and  $\alpha_n$ ); the second follows because the  $c_{\bar{k}x}^\dagger$  excitations counted by  $\hat{\mathcal{N}}_x$  are linear combinations of  $\alpha_{\bar{k}}$ ,  $\alpha_{\bar{k}}^\dagger$ ,  $\beta_{\bar{k}}$  and  $\beta_{\bar{k}}^\dagger$  [this is illustrated by Fig. 2, which depicts how states in the  $c_{\bar{k}x}$  and  $\alpha_{\bar{k}}, \beta_{\bar{k}}$  representations are related to each other]; and the third follows from (51) for  $\hat{\mathcal{N}}_x$  and (58c), (43) and (23) for  $\alpha_d$ . Imposing now the condition that  $|E\rangle$  must be in the physical subspace  $\mathcal{S}_{\text{phys}}$  and hence must satisfy the free gluing condition (22b), we obtain

$$\mathcal{P}_{\tilde{E}} = \begin{cases} [\mathcal{N}_c + \mathcal{N}_f - S_T - (P+1)/2] \bmod 2 & (\varepsilon_d > 0), \\ [\mathcal{N}_c + \mathcal{N}_f - S_T - (P-1)/2] \bmod 2 & (\varepsilon_d \leq 0). \end{cases} \quad (75)$$

This *generalized gluing condition* specifies which of all the possible states in  $\mathcal{S}_{\text{ext}}$  are physical, i.e. are in  $\mathcal{S}_{\text{phys}}$ ; it supplements the free gluing condition (22a), which stipulates that  $S_T \pm 1/2$  must be integer (half-integer) if  $\mathcal{N}_c$  and  $\mathcal{N}_f$  are integer (half-integer). The unphysical states in  $\mathcal{S}_{\text{ext}}$  that do not satisfy (75) must be discarded when constructing the finite-size spectrum (and thus no such states occur in Table I below).

#### D. Ground State Energy Shift

The form of Eq. (68) for the change in ground state energy  $\delta E_G$  suggests that it can be interpreted as *the dynamical binding energy of the impurity spin*, which results from the impurity-induced energy shifts of all the states in the filled Fermi sea. (The factor 1/2 in (68) reflects the fact<sup>4,53</sup> that only “half” of the  $x$ -pseudofermion field, namely  $\psi_x + \psi_x^\dagger$ , couples to the impurity [in (42)].) For  $\varepsilon_d = 0$ , the number of levels strongly shifted by the interaction is [by (71b)] of order  $\Gamma/\Delta_L$ , and each of these gets shifted roughly by  $\Delta_L/2$ ; we can thus estimate that  $|\delta E_G|$  will be of order  $\Gamma$ , which supports the heuristic statement that “the impurity’s binding energy is of order  $T_K$ ”.

However, since the level shifts  $\Delta_L \delta_{j,P}$  also have a  $P$ -dependence of order  $\sim \Delta_L^2/\Gamma$  [from (71b)], the total ground state energy shift  $\delta E_G$  will have a  $P$ -dependence too, of order  $\sim \Delta_L$ . We therefore write

$$\delta E_G \equiv \delta E_G^0 + P \delta \mathcal{E}_G^P, \quad (76)$$

where the first term is  $P$ -independent and hence gives only an overall energy shift. In contrast,  $\delta \mathcal{E}_G^P$  affects the finite-size spectrum since it shifts the odd electron states,  $P = 1$ , relative to even electron states,  $P = 0$ , and hence must be evaluated with particular care. This is done in Appendix C 4, where we find, for  $\Gamma/\Delta_L \gg 1$ ,

$$\delta E_G^P = \begin{cases} -\Delta_L/8 & (T_h = 0), \\ 0 & (T_h \gg \Delta_L), \end{cases} \quad (77)$$

$$\delta E_G^0 \approx \begin{cases} -2\Gamma[\ln(D/4\pi\Gamma) + 1], & (T_h = 0), \\ -2\Gamma[\ln(D/|\varepsilon_d|) + 1], & (T_h \gg \Delta_L, \Gamma). \end{cases} \quad (78)$$

Here  $D \gg \Gamma, T_h$  is a cutoff needed to regularize the sums in (68). Note that for  $T_h = 0$ , (78) is consistent with the estimate for  $\delta E_G$  above if we take  $D \simeq 1/a$  and recall that  $\Gamma = \lambda_\perp^2/4a$ . For  $T_h \gg \Gamma$ , the magnetic field  $|\varepsilon_d|$  takes over as lower energy scale in the logarithm instead of  $\Gamma$ .

#### E. Construction of the Finite-Size Spectrum

Now we are finally ready to construct the finite-size many-body excitation spectrum of the 2CK model. In doing so, we shall generally use calligraphic  $\mathcal{E}$ ’s to denote dimensionless energies measured in units of  $\Delta_L$ . Specifically, we shall construct the dimensionless energies

$$\tilde{\mathcal{E}}(L) = [\tilde{E}(L) - \tilde{E}_{\min}(L)]/\Delta_L, \quad (79)$$

associated with the lowest few exact many-body eigenstates  $|\tilde{E}\rangle$  of the full Hamiltonian  $H'$  of (54), measured relative to its ground state energy,  $\tilde{E}_{\min}$ . For the sake of simplicity we only consider the case with periodicity index  $P_0 = 1$  [see (4)], for which the  $\psi_{\alpha j}$ ’s have anti-periodic boundary conditions. In this case the free ground state in the electronic sector is unique, namely  $|\tilde{0}\rangle_0$ , which somewhat simplifies the counting of states. (Of course, one can use the same procedure for  $P_0 = 0$ , with similar results.)

The construction proceeds in three steps: we first evolve toward the EK line, second evolve along the EK line, and third turn on a local magnetic field. The results are summarized in Fig. 6 and Tables I and II. The caption of Table I also summarizes the technical details of the construction. Here we just state the main ideas:

(i) *Phase-shifted Spectrum*:— First we study the evolution of the spectrum *toward* the EK line for  $\lambda_z \in [0, 1]$  at  $\lambda_\perp = \varepsilon_d = 0$ . Since the impurity has no dynamics for  $\lambda_\perp = 0$ , the spectrum is that of a *free-electron Fermi liquid with a  $S_z$ -dependent phase shift in the spin sector*, given by  $H'(\lambda_\perp = 0)$  of (36); it evolves linearly with increasing  $\lambda_z$ , from  $\mathcal{E}_{\text{free}}$  at  $\lambda_z = 0$  to  $\mathcal{E}_{\text{phase}}$  at  $\lambda_z = 1$ , see Fig. 6(a).

(ii) *Crossover Spectrum*:— Next we study the spectrum’s further evolution *along* the EK line for  $\Gamma/\Delta_L \in [0, \infty)$  at  $\lambda_z = 1, \varepsilon_d = 0$ . To this end we enumerate in Table I the lowest-lying physical eigenstates  $|\tilde{E}\rangle$  of the full Hamiltonian  $H'$  in terms of the excitations  $\tilde{\alpha}_{\varepsilon_{j,P}}^\dagger, \beta_{\bar{k}}^\dagger$  and  $b_{qy}^\dagger$  which diagonalize it, and *follow the evolution with increasing  $\Gamma/\Delta_L$  of the excitation energies  $\varepsilon_{j,P}$*  (shown in Fig. 4), and of the ground state energy shift  $\delta E_G^P$  [see (77)]. This yields the crossover shown in Fig. 6(b) from the phase-shifted to the NFL fixed point spectrum, consisting of a set of universal, dimensionless energies defined by

$$\mathcal{E}_{\text{NFL}} \equiv \lim_{L \rightarrow \infty} \frac{\tilde{E}(L; \varepsilon_d = 0, \Gamma) - \tilde{E}_{\min}(L; \varepsilon_d = 0, \Gamma)}{\Delta_L}. \quad (80)$$

Satisfyingly, the spectrum of  $\mathcal{E}_{\text{NFL}}$  energies found in Fig. 6(b) and Table II (degeneracies are given in brackets) coincides with the ones obtained in NRG and CFT calculations.<sup>28,34–36,30</sup> This constitutes a direct and straightforward analytical proof of the soundness of the latter approaches. In particular, it proves the so-called fusion hypothesis employed by Affleck and Ludwig in their CFT calculation of this spectrum.<sup>34–36</sup> As is well-known from CFT,<sup>54</sup> each of the fixed-point values  $\mathcal{E}_{\text{NFL}}$  can be associated with the scaling dimension of one of the operators characterizing the fixed point. The occurrence of  $\mathcal{E}_{\text{NFL}}$ 's that are not simply integers or half-integers is thus a very direct sign of NFL physics, since these correspond to non-fermionic operators.

Our NFL spectrum demonstrates explicitly the well-known fact that the spin anisotropy is irrelevant at the NFL fixed point, since if we take the continuum limit  $\Delta_L \rightarrow 0$  at fixed  $\Gamma$ , the fixed point spectrum is evidently reached *independently* of the specific value of  $\Gamma$ . Said more formally: the symmetry of our anisotropic starting Hamiltonian with respect to transformations in the charge, spin and flavor sectors is  $U(1)_c \times U(1)_s \times SU(2)_f$ , i.e. in the spin sector it is only invariant under spin rotations around the  $z$  axis; in contrast, Affleck and Ludwig derived the NFL fixed point spectrum by assuming it to have the complete  $U(1)_c \times SU(2)_s \times SU(2)_f$  symmetry of the free model. The fact that the low-energy part ( $\varepsilon \ll T_K$ ) of our NFL fixed point spectrum coincides with theirs beautifully illustrates how the broken symmetry of the original model is restored in the vicinity of the NFL fixed point, and thus proves another central assumption of the CFT solution of the 2CK model, in agreement with the NRG study of Pang and Cox.<sup>29</sup>

The fact that the exact eigenenergies of  $H'$  interpolate smoothly between their values for  $\lambda_{\perp} = 0$  and  $\lambda_{\perp} \neq 0$  [Fig. 6(b)] may at first seem somewhat surprising, because a common way of heuristically characterizing a NFL is that its quasiparticles are orthogonal to the bare ones of the corresponding free Fermi liquid. This is referred to as the “breakdown of Landau's quasiparticle construction”, since in Landau's picture of a Fermi liquid, the dressed quasiparticles and the corresponding bare ones have finite overlap. Here, in fact, one can readily check that  $s_{\text{ext}} \langle \tilde{0} | \alpha_{\bar{k}} \tilde{\alpha}_{\varepsilon(\bar{k})}^{\dagger} | \tilde{0} \rangle_{\text{ext}}$  is non-zero (where  $\varepsilon(\bar{k})$  is the excitation energy that reduces to  $\bar{k}$  as  $\Gamma/\Delta_L \rightarrow 0$ ), implying that in the  $\alpha$ -basis the system is a Fermi liquid (in accord with the fact that  $H_x$  is quadratic, i.e. “simple”). However, this does not contradict the fact that in the *original*  $c_{k\alpha j}$  basis the system nevertheless behaves like a NFL, since the bosonization-refermionization relation between states in the  $\alpha$  and  $c_{k\alpha j}$  bases is very highly non-linear.

(iii) *Crossover due to local magnetic field*:— Finally, we

turn on a local magnetic field,  $\varepsilon_d = h_i \neq 0$  at fixed  $\lambda_z = 1$  and  $\Gamma/\Delta_L \gg 1$ , thus breaking spin reversal symmetry. The further evolution of the excitation energies  $\varepsilon_{j,P}$  as functions of increasing  $T_h/\Delta_L$ , shown in Fig. 4(b), yields the magnetic-field-induced crossover, shown in Fig. 6(c), from the NFL fixed point energies  $\mathcal{E}_{\text{NFL}}$  to a set of energies  $\mathcal{E}_{\text{ph}}$  corresponding to a phase-shifted Fermi liquid fixed point. For  $T_h/\Delta_L \gg 1$ , the impurity level evidently becomes empty for all low-lying states,  $\langle c_d^{\dagger} c_d \rangle = 0$ , i.e. the impurity spin is frozen in the state  $S_z = \downarrow$ . Indeed, the spectrum  $\mathcal{E}_{\text{ph}}$  which one recovers is precisely the same phase-shifted spectrum as  $\mathcal{E}_{\text{phase}}$  at the point  $\lambda_z = 1$  and  $\lambda_{\perp} = 0$ , apart from a degeneracy factor of two, due to the lack of spin reversal symmetry, compare Table II. This shows very nicely that the magnetic field “erases” all traces of NFL physics for the lowest-lying part of the spectrum, because it effectively switches off spin-flip scattering.

## F. Finite-Size Behavior of Physical Quantities

Let us now briefly discuss the finite-size,  $T = 0$  behavior of three physical quantities at the NFL fixed point, namely the entropy, susceptibility and the fluctuations in  $\mathcal{N}_x$ .

The *entropy* of the ground state at  $T = 0$ ,  $\varepsilon_d = 0$  is evidently simply  $\ln 2$  for any  $L$ , since the ground state is two-fold degenerate (see Fig. 6). This should be contrasted<sup>55</sup> with the celebrated result  $\frac{1}{2} \ln 2$  that one obtains<sup>56</sup> when taking the limit  $L \rightarrow \infty$  before  $T \rightarrow 0$ . The difference simply illustrates the triviality that the order of limits does not commute, since for finite  $L$  the system is always gapped.

The *susceptibility* at  $T = 0$  due to a local field  $h_i$  is defined by  $\chi = -\frac{\partial^2 \tilde{E}_G}{\partial h_i^2}$ . Since  $\tilde{E}_G = E_G + \delta E_G$ , we simply have to evaluate [by (57), (68)] the sum  $\chi = \frac{1}{2} \sum_{\varepsilon} \frac{\partial^2 \varepsilon}{\partial h_i^2}$ . For  $h_i = 0$ , the summands can be determined by differentiating (67), giving

$$\chi(h_i = 0) = \sum_{\varepsilon > 0} \frac{1}{\varepsilon} \frac{4\pi\Gamma\Delta_L}{(\Delta_L 4\pi\Gamma + \pi[(4\pi\Gamma)^2 + \varepsilon^2])} \quad (81)$$

$$\approx \frac{1}{4\pi^2\Gamma} \ln(4\pi\Gamma/\Delta_L) \quad (\text{for } \Gamma \gg \Delta_L). \quad (82)$$

The fact that  $\chi(h_i = 0) \rightarrow \infty$  as  $L \rightarrow \infty$  is of course a characteristic sign of 2CK NFL physics: it illustrates the instability of the NFL phase with respect to a local symmetry breaking.<sup>52</sup> At finite temperatures  $T$  takes over the role of the infrared cutoff  $\Delta_L$ , so that the susceptibility diverges logarithmically with  $T$ .<sup>31,4</sup>

The *fluctuations* in  $\hat{\mathcal{N}}_x$  can be quantified by calculating  $\langle \hat{\mathcal{N}}_x^2 \rangle - \langle \hat{\mathcal{N}}_x \rangle^2$ . In Appendix C 5 this is done at  $\varepsilon_d = 0$  for the physical ground state of  $\mathcal{S}_{\text{phys}}$  for both  $P = 0$  and 1. We find that  $\langle \hat{\mathcal{N}}_x \rangle = 0$  for arbitrary ratios of  $\Gamma/\Delta_L$ , showing that the ground state contains equal amounts of spin from both flavors  $j = 1, 2$ , as expected

from the 2CK model's flavor symmetry. Furthermore, we find that  $\langle \hat{N}_x^2 \rangle = P/4$  for  $\Gamma/\Delta \rightarrow 0$ , as expected intuitively, since in this limit the considered ground states are linear combinations of states with  $\mathcal{N}_x = \pm P/2$  [compare Fig. 2]. In contrast, in the limit  $\Gamma/\Delta_L \gg 1$  we find that the fluctuations diverge logarithmically with system size,  $\langle \hat{N}_x^2 \rangle \approx \frac{1}{\pi^2} \ln \Gamma L$ . This illustrates very vividly how severely the dynamical impurity stirs up the original Fermi sea at the NFL fixed point.

## VI. CONNECTION TO DIFFERENT RENORMALIZATION GROUP METHODS

In the literature several renormalization group (RG) methods have been applied to the multichannel Kondo model. In this section we relate these RG methods to our finite-size bosonization technique, by showing how the strategies employed by the former can be implemented, in an *exact way*, within the latter.

### A. High-energy cutoff scaling techniques

The most common types of RGs are the ones used in particle physics and in the standard treatment of critical phenomena. In these RG procedures, one reduces a high-energy cutoff, say  $\tilde{D}$ , in order to gradually eliminate some high-energy degrees of freedom, arguing that they only slightly influence the low-energy physics of the system. The change in the cutoff must be compensated by rescaling the model's dimensionless coupling constants and masses in order to keep the physical properties (different inherent energy scales and dressed masses) invariant. These kinds of scaling procedures, which include Anderson's poor man's scaling,<sup>57</sup> the multiplicative RG,<sup>19</sup> and the Yuval-Anderson real time RG,<sup>58</sup> have been widely used in the continuum limit,  $L \rightarrow \infty$ , to study the multichannel Kondo model.<sup>12,6,59,10,20</sup>

In our case the high-energy cutoff  $\tilde{D}$  can be identified with the ultraviolet cutoff  $1/a$  introduced when defining the boson fields  $\phi_{\alpha j}$  [in (14)], i.e.  $\tilde{D} \sim 1/a$ . Thus, if a dimensionless coupling constant, say  $\lambda$ , has the scaling equation

$$\frac{d \ln \lambda}{d \ln \tilde{D}} = -\frac{d \ln \lambda}{d \ln a} = \gamma(\lambda), \quad (83)$$

then in the weak-coupling regime  $\lambda \ll 1$ , its scaling dimension is  $\gamma(0)$ , and it is relevant, marginal or irrelevant for  $\gamma(0) < 0, = 0$  or  $> 0$ , respectively.

Now, along the EK line one immediately obtains the scaling equations<sup>43</sup>

$$\frac{d \lambda_{\perp}}{d \ln a} = \frac{1}{2} \lambda_{\perp}, \quad \lambda_z \equiv 1. \quad (84)$$

The first, which follows from the requirement of the invariance of the Kondo scale  $\Gamma = \lambda_{\perp}^2/4a$ , shows that  $\lambda_{\perp}$  is

relevant and grows under bandwidth rescaling, with dimension  $-1/2$ . As explained at the end of Section IV B, the second equation follows from the fact, (proven in Subsection VI C), that the leading irrelevant operator is absent only at the EK line, where  $\lambda_z = 1$ . Eqs. (84) exactly coincide with the ones obtained with the Yuval-Anderson technique,<sup>20</sup>

$$\frac{d \lambda_{\perp}}{d \ln a} = \left( 4 \frac{\delta}{\pi} - 8 \frac{\delta^2}{\pi^2} \right) \lambda_{\perp}, \quad (85a)$$

$$\frac{4}{\pi} \frac{d \delta}{d \ln a} = \left( 1 - \frac{4\delta}{\pi} \right) \lambda_{\perp}^2, \quad (85b)$$

if in these the phase shift  $\delta = \lambda_z \pi/4$  is replaced by  $\pi/4$  at the EK line,<sup>29</sup> as discussed at the end of Section IV B. Remarkably, while these latter equations result from rather non-trivial calculations in terms of the original Hamiltonian, they can trivially be derived after the EK transformation, which in effect resums all appropriate diagrams into a quadratic form.

As discussed Subsection V B, in a finite local magnetic field  $\varepsilon_d = h_i$ , a further natural energy scale appears:  $T_h = h_i^2/\Gamma$ . For energies below this scale the magnetic field destroys the non-Fermi liquid behavior and a Fermi-liquid is recovered. By requiring the invariance of  $T_h$  one immediately derives that, as long as the high-energy cutoff  $1/a$  is much larger than the Kondo scale  $\Gamma$ , the field  $h_i$  must be invariant under the RG transformation:

$$\frac{dh_i}{d \ln a} = 0 \quad (1/a \gg \Gamma). \quad (86)$$

However, once the cutoff is reduced sufficiently so that  $1/a \ll \Gamma$ , the role of  $\Gamma$  is taken over by  $1/a$ , i.e.  $T_h$  is now given by  $h_i^2 a$ , and therefore the scaling equation (86) must be replaced by

$$\frac{dh_i}{d \ln a} = -\frac{1}{2} h_i \quad (1/a \ll \Gamma). \quad (87)$$

Since  $h_i$  is dimensionfull, the scaling dimension of the local field can not be read off directly from this equation; instead one must consider the corresponding equation for the *dimensionless* field measured in units of the effective bandwidth,  $\tilde{h} \equiv h_i a$ , namely

$$\frac{d \tilde{h}}{d \ln a} = \frac{1}{2} \tilde{h} \quad (1/a \ll \Gamma). \quad (88)$$

Close to the NFL fixed point the local field thus [by (83)] has dimension  $-1/2$  and is relevant: when measured in units of the effective bandwidth, it grows when the latter is decreased. (By a similar argument, the dimension of the local field in the regime  $1/a \gg \Gamma$  of (86) is  $-1$ .)

Equations (86) and (87) are in complete agreement with those obtained by the Yuval-Anderson technique.<sup>20</sup> We remark at this point that perpendicular local magnetic fields  $h_{x,y}$  (i.e. perturbations of the form  $h_x S_x$  or  $h_y S_y$ ) are known<sup>20</sup> to scale differently from  $h_i = h_z$ , and at the EK line their scaling dimension is known to be  $-1/2$  even in the region  $1/a \gg \Gamma$ .

## B. Connection to Numerical Renormalization Group

In this subsection we show that an analysis of our finite-size spectrum as function of  $L$  in fact represents an analytical version of Wilson's numerical renormalization group<sup>60</sup> (NRG), which can simply be viewed as a special type of finite-size scaling.

In Wilson's procedure one divides the Fermi sea into energy shells using a logarithmic mesh characterized by a parameter  $\Lambda > 1$ , and then maps the model onto an equivalent one in which the impurity is coupled to the end of an infinite conducting chain, where the hopping between the sites  $n$  and  $n + 1$  scales as  $\Lambda^{-n}$ . The  $n$ 'th site in this chain represents an “onion-skin” shell of conduction electrons, characterized by spatial extension  $\sim \Lambda^{n/2}$  around the impurity site and energy  $\sim \Lambda^{-n}$ . The NRG transformation is then defined by considering truncated chains of length  $N$  with Hamiltonian  $H_N$ , and consists of (i) adding a new site to the end of the chain,  $H_N \rightarrow H_{N+1}$ , and (ii) rescaling the new Hamiltonian by  $\Lambda$ :  $H_{N+1} \rightarrow \Lambda H_{N+1}$ . Trivially, step (i) reduces the mean level spacing by a factor of  $1/\Lambda$ , while step (ii) is needed to measure all energies in units of the new mean level spacing. This strategy is implemented by numerically diagonalizing  $H_{N+1}$  and retaining only the lowest few hundred levels. One finds that after a number of iterations the spectrum of  $H_N$  converges to a fixed, universal set of energies, characteristic of some fixed point Hamiltonian.<sup>29</sup> For the 2CK model this spectrum has been shown to be identical to the one obtained by boundary CFT.<sup>30</sup>

The NRG procedure outlined above can easily be interpreted in terms of our finite-size calculations. Step (i) corresponds to increasing the system size,  $L \rightarrow \Lambda L$ , (i.e., reducing the level spacing,  $\Delta_L \rightarrow \Delta_{\Lambda L} = \Delta_L/\Lambda$ ), while step (ii) is equivalent to measuring all energies in units of  $\Delta_{\Lambda L}$ . Combining both steps, an “analytical RG step” thus has the form:

$$\frac{H_x(L, \Gamma, \varepsilon_d)}{\Delta_L} \rightarrow \frac{H_x(\Lambda L, \Gamma, \varepsilon_d)}{\Delta_{\Lambda L}} = \frac{H_x(L, \Lambda \Gamma, \Lambda \varepsilon_d)}{\Delta_L}, \quad (89)$$

where the last equality follows identically from Eq. (56). For  $\varepsilon_d = 0$  this means that increasing the system size at fixed  $\Gamma$  is equivalent to increasing  $\Gamma$  at fixed  $L$ , emphasizing once more that in this case the spectrum depends only on  $\Gamma/\Delta_L$ . Therefore the “spectral flow” as function of  $\Gamma/\Delta_L$  in Fig. 6 can be viewed as the analytical version of an NRG spectrum as a function of iteration number.

## C. Finite-Size Scaling

It is also straightforward to implement Wilson's prescription for extracting the exact scaling exponent of a perturbation around the fixed point, say  $\delta\lambda \hat{O}$ , from its effect on the finite-size spectrum: In general, it causes the dimensionless energy  $\tilde{\mathcal{E}}(L)$  [of (79)] (calculated at a finite,

non-zero  $\Delta_L \ll \Gamma$ ) to differ from its universal fixed point value  $\mathcal{E}_{\text{NFL}}$  [of (80)] by an amount  $\delta\tilde{\mathcal{E}}(L)$ , whose leading asymptotic behavior for  $L \rightarrow \infty$  is

$$\delta\tilde{\mathcal{E}}(L) \equiv \tilde{\mathcal{E}}(L) - \mathcal{E}_{\text{NFL}} \sim (\delta\lambda/L^\gamma)^n, \quad (90)$$

where  $n \geq 1$  is some integer. By definition,  $\gamma$  is the scaling dimension of the operator  $\hat{O}$ , which is relevant for  $\gamma < 0$ , marginal for  $\gamma = 0$  and irrelevant for  $\gamma > 0$ . Thus deviations from the universal spectrum are characteristic of the operator content of the fixed point.

We first consider the situation *on* the EK line (i.e. for  $\lambda_z = 1$ ), and close to the NFL fixed point, where  $\Delta_L/\Gamma$  and  $T_h/\Delta_L$  are both  $\ll 1$  (at NFL fixed point they are both 0). The leading deviations  $\varepsilon_{j,P}/\Delta_L - (\varepsilon_{j,P}/\Delta_L)_{\text{NFL}}$  of the dimensionless single-particle excitation eigenenergies from their NFL fixed point values are then given [from (71)] by

$$\delta_{j,P} - (\delta_{j,P})_{\text{NFL}} = \frac{1}{4\pi^2} \left[ \frac{T_h}{\Delta_L(j - P/2)} - \frac{\Delta_L(j - P/2)}{\Gamma} \right] \quad (91)$$

(for  $j \geq 1$ ; for  $j = 0$ , Eq. (C18) yields the same conclusions). The leading dependence on the local magnetic field via  $T_h/\Delta_L$  is evidently  $[h_i L^{1/2}]^2$ , which grows as  $L \rightarrow \infty$ . This shows that a local magnetic field has dimension  $\gamma_{h_i} = -1/2$  and is relevant: for an arbitrarily small  $h_i$ , there exists a system size  $L$  above which the lowest part of the spectrum and the ground state properties of the model are drastically affected, namely when  $\Delta_L \lesssim T_h$ ; in the language of section V B, this occurs as soon as the crossover field below which the spectrum is unaffected, namely  $h_c = \sqrt{\Gamma \Delta_L}$ , becomes smaller than  $|h_i|$  as  $L$  is increased. The dimension  $\gamma_{h_i} = -1/2$  also follows from the  $L$ -dependence of  $h_c$ , and agrees with the conclusions of our bandwidth rescaling arguments [see (88)].

In the absence of magnetic fields, the leading term in (91) vanishes with increasing  $L$  as  $(\Gamma L)^{-1}$ , implying that the least irrelevant operator *on* the EK line has dimension  $\gamma_{EK} = 1$ . Thus, we conclude that the leading irrelevant operators with dimension  $\gamma = 1/2$  that were found in the CFT treatment<sup>37</sup> are absent *on* the EK line, in agreement with Refs. 4,40.

Now let us move away from the EK line by taking  $\lambda_z = 1 + \delta\lambda_z$ , and do perturbation theory in  $\delta\lambda_z$ , i.e. in  $\delta H'_z$  of (38). Then the operators with dimension  $\gamma = 1/2$  just mentioned immediately show up: As shown in detail in Appendix C 6, we find that the “zero mode” term  $\delta\lambda_z \Delta_L \tilde{\mathcal{N}}_s S_z$  of (38) (which does not occur in the continuum limit considered in Ref. 4), affects the spectrum already in first order in  $\delta\lambda_z$ : in the absence of magnetic fields, the first excited states (with  $\mathcal{E}_{\text{NFL}} = 1/8$ ) are shifted relative to the doubly degenerate ground states (with  $\mathcal{E}_{\text{NFL}} = 0$ ) by an amount

$$\delta\tilde{\mathcal{E}}(L) \simeq -\frac{1}{4}\delta\lambda_z(1 + 4\pi^2\Gamma/\Delta_L)^{-1/2} \sim L^{-1/2}. \quad (92)$$

This implies that the leading irrelevant operator away from the EK line has dimension 1/2.

In the presence of a local magnetic field  $\varepsilon_d = h_i$ , one finds in the continuum limit  $\Delta_L \ll \Gamma, h_i$  that the ground state degeneracy is split by an amount

$$\delta\tilde{\mathcal{E}}(L) = \begin{cases} \frac{\delta\lambda_z}{2\pi^2} \frac{|h_i|}{\Gamma} \ln \frac{|h_i|}{4\pi\Gamma} & (\Delta_L \ll h_i \ll \Gamma), \\ \frac{\delta\lambda_z}{2} \left(1 - \frac{4\Gamma}{|h_i|}\right) & (\Delta_L \ll \Gamma \ll h_i). \end{cases} \quad (93)$$

This shows that the magnetic-field behavior *along* the EK line is not completely generic, since it misses this part of the  $h_i$ -dependence of the magnetic-field-induced crossover. Note that the  $|h_i|/\Gamma \ln |h_i|/\Gamma$  behavior that occurs for a local magnetic field of intermediate strength is consistent with the conclusions of the NRG studies of Ref. 30 for the  $h_i$ -dependence of a certain phase shift that can be used to characterize the NRG spectra.

Finally, we would like to comment here on the identification of the Kondo scale  $T_K$ . In Section VB we showed that the crossover scale below which the finite-size spectrum takes its fixed-point form (at  $h_i = 0$ ) was  $\Gamma$ , and hence concluded that  $T_K \simeq \Gamma$ . This differs from the suggestion of Sengupta and Georges<sup>40</sup> that the Kondo scale in the anisotropic 2CK model close to the EK line is not  $\Gamma$  but rather  $\Gamma/(\delta\lambda_z)^2$ . This scale emerged naturally in their calculation of the total susceptibility enhancement due to the impurity, which yielded  $\chi_{\text{imp}} \sim (\delta\lambda_z)^2/\Gamma \ln(\Gamma/T)$  (at  $h_i = 0$ ). However, the factor  $(\delta\lambda_z)^2$  only expresses the fact that the amplitudes of the leading irrelevant operators vanish *on* the EK line, so that the characteristic logarithmic features appear only in second order in  $\delta\lambda_z$ . The fact that the scale above which these logarithmic features vanish is  $T \simeq \Gamma$ , not  $T \simeq \Gamma/(\delta\lambda_z)^2$ , supports our above conclusion that it is rather  $\Gamma$  that should be identified as the Kondo scale.

## VII. DISCUSSION AND CONCLUSIONS

The main general conclusion of our work is that constructive finite-size bosonization is an unexpectedly powerful tool for investigating quantum impurity problems. Firstly, for the 2CK model, it enables one to *analytically calculate by elementary means the crossover along the EK-line of the finite-size spectrum (and the corresponding eigenstates)* between the free Fermi liquid and the NFL fixed point. This crossover had hitherto been tractable only with the numerical renormalization group, and has been beyond the reach of all analytical approaches used to study this model.

Secondly, finite-size bosonization *can deal without much additional effort with symmetry-breaking perturbations*, such as a finite magnetic field (or channel symmetry breaking<sup>26</sup>, which was not discussed here, but can be included by a straightforward extension of our methods). Indeed, it is to be expected that the methods de-

veloped here can fruitfully be applied to a number of related quantum impurity problems. For example, an adaption of our finite-size refermionization approach was very recently used to rigorously resolve a recent controversy regarding the tunneling density of states at the site of an impurity in a Luttinger liquid.<sup>44</sup> Other potential applications would be to the generalized Kondo models studied by Ye<sup>43</sup>, or by Moustakas and Fisher<sup>9,61</sup>, or by Kotliar and Si<sup>41</sup>.

Thirdly, finite-size bosonization allows one *to mimic in an exact way the strategy of standard RG approaches* such as poor man's bandwidth rescaling and finite-size scaling; thus it should be useful also as a pedagogical tool for teaching and analytically illustrating standard RG ideas.

Crucial to the success of our method is that we do not use field-theoretical bosonization, in which the bosonization relation just has the status of a formal correspondence, but Haldane's *constructive* formulation of bosonization, in which all operators and fields needed are constructed explicitly in terms of the initial set of electron operators  $c_{k\alpha j}$  in terms of which the model is defined. This has the great advantage that Emery and Kivelson's bosonization-refermionization mapping of the model onto a quadratic resonant level model can be implemented rigorously, not merely as a formal correspondence, but as a set of operator identities in Fock space. To achieve this, however, the Klein factors have to be treated with due care. Our main technical innovation was to demonstrate how refermionization can be performed at the same level of rigor as bosonization, by extending the Fock space to include unphysical states, and identifying and discarding these at the end of the calculation using a generalized gluing condition. However, we wish to emphasize that our method is truly elementary: in principle it requires nothing more than a knowledge of standard second quantization, since that is all one needs to derive the constructive bosonization formalism.<sup>44</sup>

Our rigorous implementation of EK's mapping of the 2CK model onto the resonant level model ensures that the latter is not merely an "effective model that captures the essential physics", but truly *identical to the original model* one starts out with (after the standard reinterpretation of the meaning of the coupling constants discussed in Appendix A, to compensate for differences that can arise relative to other methods due to the use of different regularization schemes). The fact that we are thus able to solve the *original* model exactly, constitutes a significant advance relative to a number of alternative approaches that have tried to analytically access the NFL fixed point, but end up doing so using either an "effectively equivalent" model or some assumptions that are not proven from first principles. Let us briefly mention three of these:

(i) Coleman and coworkers<sup>25,26</sup> have proposed a "pedestrian solution" of the 2CK model, in which it is argued that many of its properties can be calculated using a so-called "compactified model" involving only a single

channel of spinful conduction electrons. This model was argued to represent that part of the 2CK model that is left over when one “factorizes out” the charge and flavor degrees of freedom. Indeed, using field-theoretic bosonization, Schofield showed that there is a formal correspondence between the compactified model and our  $H_\perp$  of Eq. (29) (which involves only  $\varphi_s$  and  $\varphi_x$ ), and that it yields the same results as the 2CK model for the *impurity contribution* to thermodynamical properties. In this sense, the compactified model can be viewed as an effective model for calculating impurity properties. However, as first emphasized by Ye,<sup>43</sup> it is *not* equivalent to the original 2CK model, since Schofield’s arguments ignored the fact that there are gluing conditions such as (22) between the  $c,f$  sectors and the  $s,x$  sectors. As long as these are ignored, the compactified model can *not* be used to calculate conduction electron properties, since that requires adding back the contributions from the charge and flavor channels. This was attempted by Zhang, Hewson and Bulla,<sup>27</sup> who calculated the fixed-point spectrum of the compactified model using the NRG, from which they tried to reconstruct that of the 2CK. However, their construction has an ad hoc character (it requires knowledge of the answer) and succeeded only partially (it did not correctly reproduce all degeneracies of the 2CK fixed point spectrum).

Our constructive bosonization approach allowed us to clarify this issue completely: it makes precise in what sense the  $c$  and  $f$  sectors can be “factorized out”, rigorously yields an appropriate model for the remaining  $s$  and  $x$  sectors, emphasizes the gluing conditions between the  $c,f$  and  $s,x$  sectors, and shows how they can be used at the NFL fixed point to combine the contributions from all four sectors to obtain the NFL fixed point spectrum.

(ii) Affleck and Ludwig’s path-breaking conformal field theory solution of the model in the NFL regime, though very elegant and highly successful, rests on two assumptions that can not be proven from within their theory, but have to be confirmed by comparison with other exact methods: firstly, they assume that the NFL fixed point has the same  $U(1)_c \times U(2)_s \times SU(2)_f$  symmetry as the free model; and secondly, they need to use a certain conformal fusion hypothesis to obtain the operator

content of the NFL fixed point. In Section V, we analytically proved these assumptions in a simple, natural, direct manner. (The second assumption has also been proven by Sengupta and George using bosonization, but their proof requires extensive knowledge of CFT, and the assumption that the fixed point is invariant under modular transformations).

(iii) Maldacena and Ludwig<sup>42</sup> have used CFT to show that Affleck and Ludwig’s CFT solution can be reformulated in terms of free boson fields  $\varphi_y(x)$  satisfying certain asymptotic boundary conditions. Ye<sup>43</sup> reproduced this result using field-theoretic bosonization (in the continuum limit) and scaling arguments, which, however, have the standard weakness of scaling arguments in strong-coupling problems: they give the initial flow of the coupling constants, but become non-rigorous once the weak-coupling regime is left.

We have shown in Ref. 45 (and will elaborate this in a future publication<sup>47</sup>) that these results can be reproduced with great ease and much more rigor by simply taking the continuum limit  $L \rightarrow \infty$  of our above finite-size calculation. In fact, this allows us to fully reproduce all Affleck and Ludwig’s results for electronic correlations functions.

In summary, we believe that our finite-size bosonization approach is the first straightforward analytical calculation which, starting from first principles and without any assumptions, yields the crossover of the finite-size spectrum of the 2CK model from the free to the NFL fixed point and allows a detailed finite-size scaling analysis of the fixed points.

*Acknowledgments:*— We are deeply indebted to Michele Fabrizio for carefully reading the manuscript and for invaluable help in the early stages of this work. We are also grateful to Andreas Ludwig and Abraham Schiller for illuminating discussions and generous help, Gabriel Kotliar and Anirvan Sengupta for useful suggestions, and Volker Meden for a discussion on cutoff-related matters. This research has been supported by SFB195 of the Deutsche Forschungsgesellschaft and by the Hungarian Grants OTKA T026327 and OTKA F016604. G. Z. has been supported by the Magyary Zoltán Scholarship.

## APPENDIX A: CUTOFF-RELATED MATTERS

In this appendix we discuss in some detail various matters related to the choice of an ultraviolet cutoff scheme,<sup>62</sup> since this is a rather subtle matter, which can be elucidated more explicitly when using constructive rather than the more usual field-theoretic bosonization formalism. In Section A 1 we explain the need to reintroduce an ultraviolet cutoff after removing the fermionic bandwidth cutoff  $D$ , and in Section A 2 discuss how this is accomplished by the *bosonization cutoff scheme* used in the main text.

### 1. Extending the Bandwidth to Infinity

On physical grounds, the momentum sums in Eqs. (1) and (8) for  $H_0$  and  $H_{\text{int}}$  must be cut off at some large momenta ( $|k| \leq D \sim p_F$ ), to account for the finite width of the fermion conduction band and the fact that a realistic impurity potential always has non-zero range. However, the bosonization procedure used by us requires a single-particle Hilbert space with an *unbounded* fermion momentum spectrum.<sup>46</sup> To achieve this we have removed, following Haldane<sup>46</sup>, the implicit cutoff  $D$  in Eqs. (1) and (8), and used  $k \in [-\infty, \infty]$  instead. By doing so, we

extended the Hilbert space of single-electron states to include unphysical ‘‘positron’’ states with arbitrarily large negative momenta, but this should not change the low-energy physics of the system, since by construction they require very high energies ( $> \varepsilon_F$ ) for their excitation.

In the resulting single-particle Hilbert space with an unbounded fermion momentum spectrum, the fermion fields defined in (6) and the corresponding densities do not depend on any cutoff parameter. In this Appendix we shall denote this fact by a superscript  $(0)$ :

$$\psi_{\alpha j}^{(0)}(x) \equiv \sqrt{\frac{2\pi}{L}} \sum_{n_k \in \mathbb{Z}} e^{-ikx} c_{k\alpha j}, \quad (\text{A1})$$

$$\rho_{\alpha j}^{(0)}(x) \equiv : \frac{1}{2\pi} \psi_{\alpha j}^{(0)}(x) \psi_{\alpha j}^{(0)}(x) :, \quad (\text{A2})$$

In this notation, the position-space representation of the Hamiltonian, given here to facilitate comparison with field-theoretic treatments of the 2CK model, reads:

$$H_0 = \sum_{\alpha j} \int_{-L/2}^{L/2} \frac{dx}{2\pi} : \psi_{\alpha j}^{(0)\dagger}(x) i\partial_x \psi_{\alpha j}^{(0)}(x) :, \quad (\text{A3})$$

$$H_{\text{int}} = \sum_{\mu, \alpha, \alpha', j} \lambda_\mu S_\mu : \psi_{\alpha j}^{(0)\dagger}(0) \frac{1}{2} \sigma_{\alpha \alpha'}^\mu \psi_{\alpha' j}^{(0)}(0) :, \quad (\text{A4})$$

$$H_h = h_i S_z + h_e \sum_{\alpha j} \int_{-L/2}^{L/2} \frac{dx}{2\pi} \frac{\alpha}{2} : \psi_{\alpha j}^{(0)\dagger}(x) \psi_{\alpha j}^{(0)}(x) :. \quad (\text{A5})$$

Now, some physical quantities, such as the phase shift  $\delta$  of the outgoing relative to the incoming fields,

$$\psi_{\alpha j}^{(0)}(0^-) \equiv e^{i2\delta} \psi_{\alpha j}^{(0)}(0^+), \quad (\text{A6})$$

depend explicitly on an ultraviolet cutoff and in fact would be ill-defined without any. Therefore, the decision to use an infinite fermion band must always be accompanied by a *reintroduction*, in some other fashion, of an ultraviolet cutoff. Moreover, the precise way in which this is done is well-known<sup>53,63,64</sup> to strongly influence the meaning of the coupling constants in  $H_{\text{int}}$ . As an example, we consider the case of no spin-flip scattering ( $\lambda_\perp = 0$ ), and reintroduce an ultraviolet cutoff by replacing  $\lambda_z$  in Eq. (8) for  $H_{\text{int}}$  either<sup>63</sup> by the separable form  $\lambda_{z1} e^{-(|k|+|k'|)a/2}$ , or<sup>64</sup> by the nonseparable form  $\lambda_{z2} e^{-|k-k'|a/2}$ . Choice 1 restricts both momenta of a fermion scattering process separately to a band of width  $1/a$ , choice 2 only the momentum difference. They imply two different versions for  $H_z$  in position space, namely

$$H_{z1} = \lambda_{z1} S_z \sum_{\alpha j} \frac{\alpha}{2} \int_{-L/2}^{L/2} dx \int_{-L/2}^{L/2} dx' \delta_{a/2}(x) \delta_{a/2}(x') : \psi_{\alpha j}^{(0)\dagger}(x) \psi_{\alpha j}^{(0)}(x') :, \quad (\text{A7})$$

$$H_{z2} = \lambda_{z2} S_z \sum_{\alpha j} \frac{\alpha}{2} \int_{-L/2}^{L/2} dx \delta_{a/2}(x) : \psi_{\alpha j}^{(0)\dagger}(x) \psi_{\alpha j}^{(0)}(x) :, \quad (\text{A8})$$

as follows by noting that  $e^{-|k|a}$  is the Fourier-transform of the smeared  $\delta_a(x)$  function of (16):

$$\frac{1}{L} \sum_{n_k \in \mathbb{Z}} e^{-ikx} e^{-|k|a} = \delta_a(x) + \mathcal{O}(1/L^2). \quad (\text{A9})$$

Eq. (A7) shows that choice 1 separately smears out both  $\psi_{\alpha j}^{(0)\dagger}(x)$  and  $\psi_{\alpha j}^{(0)}(x)$  over a range  $a$ , i.e. corresponds to a zero-range potential in a finite band, whereas by (A8) choice 2 smears out the density  $\rho_{\alpha j}^{(0)}(x)$ , i.e. corresponds to a finite-range potential in an infinite band. Consequently, the equations of motions differ: Choice 1 yields

$$i(\partial_t - \partial_x) \psi_{\alpha j}^{(0)}(t, x) = \pi \alpha \lambda_{z1} S_z \delta_{a/2}(x) \int_{-L/2}^{L/2} dx' \delta_{a/2}(x') \psi_{\alpha j}^{(0)}(t, x') \quad (\text{A10})$$

$$\simeq \pi \alpha \lambda_{z1} S_z \delta(x) \frac{1}{2} [\psi_{\alpha j}^{(0)}(t, 0^-) + \psi_{\alpha j}^{(0)}(t, 0^+)] , \quad (\text{A11})$$

(we took  $a \rightarrow 0$  in the second line). This is solved by<sup>63</sup>

$$\psi_{\alpha j}^{(0)}(t, x) = e^{-ik(t+x)} [\theta(x) + \theta(-x) e^{2i\delta_1}] , \quad (\text{A12})$$

$$\delta_1 = -\arctan(\pi \alpha \lambda_{z1} S_z / 2) , \quad (\text{A13})$$

where  $\theta(x)$  is a sharp step function, and the phase shift agrees with that found in the Bethe Ansatz Kondo literature, or in non-1D treatments that use a finite bandwidth<sup>65</sup>. In contrast, the equation of motion for choice 2,

$$i(\partial_t - \partial_x) \psi_{\alpha j}^{(0)}(t, x) = \pi \alpha \lambda_{z2} S_z \delta_{a/2}(x) \psi_{\alpha j}^{(0)}(t, x) , \quad (\text{A14})$$

has the solution<sup>64</sup>

$$\psi_{\alpha j}^{(0)}(t, x) = e^{-ik(t+x)} e^{i\alpha \lambda_{z2} S_z \arctan(2x/a)} , \quad (\text{A15})$$

so that (for  $a \ll |0^\pm|$ ) the phase shift of (A6) is

$$\delta_2 = -\pi \alpha \lambda_{z2} S_z / 2 . \quad (\text{A16})$$

Evidently, regularization schemes 1 and 2 yield different relations between coupling constant and phase shift. Since the latter, being a physical quantity, must have the same value in both schemes,  $\delta_1 \equiv \delta_2$ , we thus conclude that the coupling constants must be related by  $\lambda_{z2} = \frac{4}{\pi} \arctan(\pi \lambda_{z1} / 4)$ .

Finally, note that after the removal of the fermion band cutoff  $D$ , even the free theory ( $H_{\text{int}} = 0$ ) requires the reintroduction of an ultraviolet cutoff: the free imaginary-time-ordered zero-temperature correlator,

$$\langle \mathcal{T} \psi_{\alpha j}^{(0)}(\tau, x) \psi_{\alpha j}^{(0)\dagger}(0, 0) \rangle = \frac{1}{\tau + ix} , \quad (\text{A17})$$

has a divergence at  $t = x = 0$ , which is often regularized by the replacement  $\tau \rightarrow \tau + \text{sgn}(\tau)a$ , where  $a \simeq 1/p_F$

(though we reuse the notation  $a$  here, this cutoff parameter in general need not be the same as that used in  $H_z$  above). Alternatively, one can introduce a bandwidth cutoff into the definition of the fermion field itself, e.g. replace  $\psi_{\alpha j}^{(0)}(x)$  by

$$\tilde{\psi}_{\alpha j}^{(a)}(x) \equiv \sqrt{\frac{2\pi}{L}} \sum_{n_k \in \mathbb{Z}} e^{-ikx} e^{-|k|a/2} c_{k\alpha j} \quad (\text{A18})$$

$$= \int_{-L/2}^{L/2} dx' \delta_{a/2}(x - x') \psi_{\alpha j}^{(0)}(x') , \quad (\text{A19})$$

i.e. by a smeared version of  $\psi_{\alpha j}^{(0)}(x)$ , which results in

$$\langle \mathcal{T} \tilde{\psi}_{\alpha j}^{(a)}(\tau, x) \tilde{\psi}_{\alpha j}^{(a)\dagger}(0, 0) \rangle = \frac{1}{\tau + ix + \text{sgn}(\tau)a} . \quad (\text{A20})$$

## 2. The Bosonization Cutoff Scheme

The *bosonization cutoff scheme* used in the main text constitutes yet another way, *alternative* to those just discussed, of reintroducing an ultraviolet cutoff after removing the fermion bandwidth cutoff  $D$ : one bosonizes the theory completely and introduces an ultraviolet cutoff  $e^{-q|a|/2}$  in the *boson* fields of Eq. (14), whose  $a$ -dependence we shall indicate in this appendix by an explicit superscript  $(a)$ :

$$\phi_{\alpha j}^{(a)}(x) \equiv \sum_{q>0} \frac{-1}{\sqrt{n_q}} \left( e^{-iqx} b_{q\alpha j} + e^{iqx} b_{q\alpha j}^\dagger \right) e^{-aq/2} . \quad (\text{A21})$$

Evidently,  $1/a$  can be viewed as “effective boson bandwidth” for the particle-hole excitations occurring in  $\phi^{(a)}$ . In this notation, the bosonization relations (18) and (19) used in the main text read

$$\psi_{\alpha j}^{(a)}(x) = F_{\alpha j} \Delta_L^{1/2} e^{-i(\hat{N}_{\alpha j} - P_0/2)2\pi x/L} :e^{-i\phi_{\alpha j}^{(a)}(x)}: \quad (\text{A22})$$

$$\rho_{\alpha j}^{(a)}(x) = \frac{1}{2\pi} \partial_x \phi_{\alpha j}^{(a)}(x) + \hat{N}_{\alpha j}/L \quad (\text{A23})$$

[un-normal-ordering the exponential in (A22), which is possible only for  $a \neq 0$ , yields a factor  $(a\Delta_L)^{-1/2}$  (see Eq. (42) of Ref. 44) and thus reproduces (18)]. The superscripts  $(a)$  emphasize that for  $a \neq 0$ ,  $\psi^{(a)}$  and  $\rho^{(a)}$  are *not* identically equal to the original  $\psi^{(0)}$  and  $\rho^{(0)}$  of (A1) of (A2), which do *not* depend on  $a$ . Instead, the rigorously exact bosonization identities for  $\psi^{(0)}$  and  $\rho^{(0)}$  are the  $a = 0$  versions of (A22) and (A23) (cf. Ref. 44, footnote 7). Correspondingly, the exact bosonized position-space version of  $H_0$  depends on  $\phi^{(0)}$  (not  $\phi^{(a)}$ ):

$$H_0 = \sum_{\alpha j} \Delta_L \hat{N}_{\alpha j} (\hat{N}_{\alpha j} + 1 - P_0)/2 + \sum_{\alpha j} \int_{-L/2}^{L/2} \frac{dx}{4\pi} : \left( \partial_x \phi_{\alpha j}^{(0)}(x) \right)^2 : . \quad (\text{A24})$$

By taking  $a \neq 0$  in (A22) and (A23) (but not in  $H_0$ ), as we do in the main text, we thus effectively make the replacement  $\psi^{(0)} \rightarrow \psi^{(a)}$ , i.e. we *redefine* the fermion fields to be explicitly cutoff dependent and thereby modify the ultraviolet behavior of the theory. Although this redefinition is not identical to the replacement  $\psi^{(0)} \rightarrow \tilde{\psi}^{(a)}$  of (A18) since  $\psi^{(a)} \neq \tilde{\psi}^{(a)}$ , it similarly *regularizes the correlation function*  $\langle \mathcal{T} \psi^{(a)} \psi^{(a)\dagger} \rangle$ , which turns out<sup>44</sup> to be given by (A20) too. Moreover, it *smears out the density* by  $a$ , since [by (A21) and (A9)]

$$\rho_{\alpha j}^{(a)}(x) = \Delta_L \sum_{k, k'} e^{-|k - k'|a/2} :c_{k\alpha j}^\dagger c_{k'\alpha}: \quad (\text{A25})$$

$$= \int_{-L/2}^{L/2} dx' \delta_{a/2}(x - x') : \psi_{\alpha j}^{(0)\dagger}(x') \psi_{\alpha j}^{(0)}(x') : , \quad (\text{A26})$$

and *thus also regularizes*  $H_z$ , which depends on the spin density (cf. (28) for  $H_z$  in the main text). In fact, comparison of (A26) with  $H_{z2}$  of (A8) shows that our bosonization cutoff scheme regularizes  $H_z$  precisely according to the choice 2 discussed above.

It is therefore not surprising that the phase shift for  $\psi_{\alpha j}^{(a)}$  found at the end of Section IV B via the EK-transformation  $U \equiv e^{i\lambda_z S_z \varphi_s^{(a)}(0)}$ , namely  $|\delta| = \pi/4$  for  $\lambda_z = 1$ , agrees with (A16) for choice 2. (Note that  $U$  would be undefined for  $a \neq 0$ , since its exponential, in order to be unitary, *must* be non-normal-ordered.) However, if one examines the phase shift more closely than for  $|x| \gg a$ , one discovers that the phase factor  $\arctan(2x/a)$  in (A15), obtained by solving the equation of motion for  $\psi_{\alpha j}^{(0)}$ , *differs* from the  $\arctan(x/a)$  in (35), obtained by EK-transforming  $\psi_{\alpha j}^{(a)}$ . This simply illustrates that  $\psi^{(0)} \neq \psi^{(a)}$ . Indeed, if one EK-transforms  $\psi^{(0)}$  instead of  $\psi^{(a)}$ , one recovers the  $\arctan(2x/a)$  of (A15), either by using  $\psi_{\alpha j}^{(0)}(x) \propto e^{-i\alpha \varphi_s^{(0)}(x)/2}$  and

$$U \varphi_s^{(0)}(x) U^\dagger = \varphi_s(x) - 2\lambda_z S_z \arctan(2x/a) , \quad (\text{A27})$$

or by using the *fermionic* definition (A1) for  $\psi^{(0)}$  to find

$$[i\varphi_s^{(a)}(0), \psi_{\alpha j}^{(0)}(x)] = \alpha i \arctan(2x/a) \psi_{\alpha j}^{(0)}(x) , \quad (\text{A28})$$

together with the fact that if  $[A, B] = cB$  with  $[c, A] = [c, B] = 0$ , then  $e^A B e^{-A} = B e^c$ .

This example illustrates the subtle difference between our bosonization cutoff scheme, which replaces  $\psi^{(0)}$  by  $\psi^{(a)}$  and thereby modifies  $H_z \rightarrow H_{z2}$ , and the regularization scheme of choice 2, which modifies only  $H_z \rightarrow H_{z2}$  but does not change  $\psi^{(0)}$ . As far as  $H_z$  is concerned, both schemes can be used with equal merit, but once one has chosen one of them, one must use it consistently throughout.

For the treatment of  $H_\perp$ , however, our bosonization cutoff scheme is distinctly more convenient. To see this,

note that the EK-transformed version of  $H_\perp$  differs, depending on whether  $H_\perp$  is expressed through  $\psi^{(a)}$  (as in the main text), or through  $\psi^{(0)}$ . In the former case the factor multiplying  $(\lambda_\perp/2)F_{\alpha j}^\dagger F_{-\alpha j}$  in (37) is

$$U \left[ \Delta_L : e^{i\alpha[\varphi_s^{(a)}(0) + j\varphi_x^{(a)}(0)]} : S_{-\alpha} \right] U^\dagger = \left( \frac{\Delta_L}{a} \right)^{1/2} : e^{i\alpha j\varphi_x^{(a)}(0)} : S_{-\alpha}, \quad (\text{A29})$$

(for  $\lambda_z = 1$ ), the latter case instead yields

$$U \left[ \Delta_L : e^{i\alpha[\varphi_s^{(0)}(0) + j\varphi_x^{(0)}(0)]} : S_{-\alpha} \right] U^\dagger = 2 \left( \frac{\Delta_L}{a} \right)^{1/2} : e^{i\alpha[\varphi_s^{(0)}(0) - \alpha\varphi_s^{(a)}(0) + j\varphi_x^{(0)}(0)]} : S_{-\alpha}. \quad (\text{A30})$$

Whereas in the former case the  $\varphi_s$ -dependence conveniently drops out for arbitrary  $a$ , in the latter it inconveniently drops out only in the limit  $a \rightarrow 0$ , in which the prefactor  $a^{-1/2}$  diverges (and moreover the fermion correlation functions are ultraviolet divergent). Note also that the extra prefactor of 2 in the latter case (which stems from normal-ordering the product of  $US_{-\alpha}U^\dagger = e^{-i\alpha\varphi_s^{(a)}(0)}S_{-\alpha}$  and  $:e^{i\alpha\varphi_s^{(0)}(0)}:$  instead of  $:e^{i\alpha\varphi_s^{(a)}(0)}:$ ) implies that the coupling constant must be reinterpreted such that  $2\lambda_\perp$  of the latter case corresponds to the  $\lambda_\perp$  used in the former. This illustrates once more how sensitively the meaning of the couplings depends on the choice of regularization scheme.

### 3. Point-Splitting vs. Normal-Ordering

In the literature the position-space versions of  $H_0$ , Eqs. (A3) or (A24), are used more frequently than the momentum-space versions of Eqs. (1) and (20), perhaps because the former may seem more concise. The product of two fields at the same point is then regularized using the point-splitting prescription

$$\lim_{x_0 \rightarrow 0} \left[ \hat{O}_1(x - ix_0) \hat{O}_2(x) - {}_0\langle \vec{0} | \hat{O}_1(x - ix_0) \hat{O}_2(x) | \vec{0} \rangle_0 \right],$$

which in most cases is equal to the normal-ordered product  $: \hat{O}_1(x) \hat{O}_2(x) :$ , evaluated by normal-ordering the  $c_{k\alpha j}$ 's in the Fourier expansions of these operators (see e.g. Appendix G of Ref. 44). However, when using point-split operators, great care is required if terms of order  $\Delta_L$  are to be treated correctly. Since in practice they are more easily dealt with by using normal-ordering in the momentum-space representation than point-splitting in the position-space representation, we use the former throughout this paper.

## APPENDIX B: CONSTRUCTING A BASIS FOR THE EXTENDED FOCK SPACE

In Section IV C 1 we transformed from an old to a new set of quantum numbers,  $\vec{N} \rightarrow \vec{\mathcal{N}}$ , and embedded the physical Fock space  $\mathcal{F}_{\text{phys}}$  in the extended Fock space  $\mathcal{F}_{\text{ext}}$  [all  $|\vec{\mathcal{N}}\rangle \in \mathcal{F}_{\text{phys}}$  satisfy both the free gluing conditions (22a) and (22b), but only (22a) is satisfied by all  $|\vec{\mathcal{N}}\rangle \in \mathcal{F}_{\text{ext}}$ ]. In this Appendix we show explicitly how such an embedding can be accomplished, by constructing a basis of  $\vec{\mathcal{N}}$ -particle ground states  $\{|\vec{\mathcal{N}}\rangle_0\}$  that spans  $\mathcal{F}_{\text{ext}}$ , in terms of ordered products of new Klein factors  $\mathcal{F}_y^\dagger$  acting on two reference states.

To begin, we fix the relative phases of the set  $\{|\vec{\mathcal{N}}\rangle_0\}$  of  $\vec{N}$  particle ground states that span  $\mathcal{F}_{\text{phys}}$ , by defining

$$|\vec{N}\rangle_0 \equiv F_{\uparrow 1}^{\dagger N_{\uparrow 1}} F_{\downarrow 1}^{\dagger N_{\downarrow 1}} F_{\uparrow 2}^{\dagger N_{\uparrow 2}} F_{\downarrow 2}^{\dagger N_{\downarrow 2}} |\vec{0}\rangle_0. \quad (\text{B1})$$

States with an even or odd total number of particles have  $P = 2\mathcal{N}_c \text{mod} 2 = 0$  or 1, respectively. Clearly, all even or odd states can be generated, respectively, from the even or odd reference states  $|\vec{0}\rangle_0$  or  $|\vec{\frac{1}{2}}\rangle_0 \equiv F_{\uparrow 1}^\dagger |\vec{0}\rangle_0$ , defined as

$$|\vec{\frac{P}{2}}\rangle_0 \equiv |\vec{\mathcal{N}} = \frac{P}{2}, \frac{P}{2}, \frac{P}{2}, \frac{P}{2}\rangle_0 \equiv |\vec{N} = P, 0, 0, 0\rangle_0, \quad (\text{B2})$$

by the application of a product of an *even number* of old Klein factors  $F_{\alpha j}^\dagger$  or  $F_{\alpha j}$ . By using Eqs. (40) and related bilinear relations, this product can be transcribed into a product of an even number of new Klein factors  $\mathcal{F}_y^\dagger$  or  $\mathcal{F}_y$ . The resulting state evidently is an eigenstate of  $\hat{\mathcal{N}}_y$ , and since Eqs. (40) by construction respect Eq. (21), its eigenvalues  $\vec{\mathcal{N}}$  are related to  $\vec{N}$  by Eq. (21). Therefore

$$|\vec{N}\rangle_0 = e^{i\Phi(\vec{\mathcal{N}})} |\vec{\mathcal{N}}\rangle_0, \quad (\text{B3})$$

where the  $\vec{\mathcal{N}}$  particle ground state  $|\vec{\mathcal{N}}\rangle_0$  is defined to be

$$|\vec{\mathcal{N}}\rangle_0 \equiv \mathcal{F}_c^{\dagger \bar{N}_c} \mathcal{F}_s^{\dagger \bar{N}_s} \mathcal{F}_f^{\dagger \bar{N}_f} \mathcal{F}_x^{\dagger \bar{N}_x} |\vec{\frac{P}{2}}\rangle_0 \quad (\text{B4})$$

for  $\vec{\mathcal{N}} \in (\mathbb{Z} + P/2)^4$ , the integers  $\bar{N}_y$  are defined by  $\bar{N}_y \equiv \mathcal{N}_y - P/2$ , and  $\sum_y \bar{N}_y$  is, by construction, an even number. The phase factor  $e^{i\Phi(\vec{\mathcal{N}})} = \pm 1$  can be determined, if necessary, by explicitly rearranging the above-mentioned even product of new Klein factors into the standard order of (B4). It ensures that the action of corresponding pairs of old or new Klein factors on the l.h.s. or r.h.s. of Eq. (B3), respectively, produces the same result.

Evidently, the set  $\{|\vec{\mathcal{N}}\rangle_0\}$  of all states with  $\sum_y \bar{N}_y = \text{even}$  constitutes a basis for the physical Fock space  $\mathcal{F}_{\text{phys}}$ , just as  $\{|\vec{N}\rangle_0\}$  does. The unphysical part of the extended Fock space  $\mathcal{F}_{\text{ext}}$  can now be formally constructed by using the definition (B4) also for integers with  $\sum \bar{N}_y = \text{odd}$ . Note once again that these new states violate the second free gluing condition (22b) and are purely mathematical constructs outside the original Fock space. Then the total extended Fock space can be formally written as

$$\mathcal{F}_{\text{ext}} = \sum_{\{\bar{N}_y\} \in \mathbb{Z}^4} \mathcal{F}_c^{\dagger \bar{N}_c} \mathcal{F}_s^{\dagger \bar{N}_s} \mathcal{F}_f^{\dagger \bar{N}_f} \mathcal{F}_x^{\dagger \bar{N}_x} (\{|\vec{0}\rangle\} \oplus \{|\frac{\vec{1}}{2}\rangle\}) ,$$

where  $\{|\vec{0}\rangle\}$  and  $\{|\frac{\vec{1}}{2}\rangle\}$  denote the set of all states that can be generated from the reference states by the action of bosonic excitations  $b_{qy}^\dagger$ .

Within  $\mathcal{F}_{\text{ext}}$ , which is the natural extension of the original physical Fock space  $\mathcal{F}_{\text{phys}}$ , the action of arbitrary (even *and* odd) products of new Klein factors evidently is trivially defined, and they leave the subspaces generated by  $|\vec{0}\rangle_0$  and  $|\frac{\vec{1}}{2}\rangle_0$  separately invariant. Note though, that it is impossible to reach  $|\vec{0}\rangle_0$  from  $|\frac{\vec{1}}{2}\rangle_0$  or vice versa using new Klein factors, simply because these change  $\mathcal{N}_y$  by  $\pm 1$ , whereas the  $\vec{\mathcal{N}}$  eigenvalues in the two subspaces “differ by  $\frac{\vec{1}}{2}$ ”. However, they *are* of course connected by the original Klein factors, e.g.  $|\frac{\vec{1}}{2}\rangle_0 = F_{\uparrow 1}^\dagger |\vec{0}\rangle_0$ . This shows again that there is no way to express an *individual* old Klein factor in terms of the new ones, or vice versa.

## APPENDIX C: EXPLICIT DIAGONALIZATION OF $H_x$ FOR 2CK MODEL

In this Appendix we diagonalize the Hamiltonian  $H_x$  of (59) in explicit detail. We also calculate the ground state energy shift  $\delta E_G$ , the  $\mathcal{N}_x$  fluctuations  $\langle \mathcal{N}_x \rangle$ , and do perturbation theory about the EK line.

### 1. Introducing Majorana Fermions

Our aim is to find the unitary transformation that brings the Hamiltonian  $H_x$  of (59) into the diagonal form (62), and to determine the discrete set of eigenenergies  $\varepsilon$ . This transformation will map the original set of orthonormal operators occurring in (59),  $\{\alpha_n; n = d, k \geq 0\}$  (with  $\{\alpha_n, \alpha_{n'}^\dagger\} = \delta_{nn'}$ ), onto the new orthonormal set occurring in Eqs. (62) to (66),  $\{\tilde{\alpha}_\varepsilon; \varepsilon \geq 0\}$  (with  $\{\tilde{\alpha}_\varepsilon, \tilde{\alpha}_{\varepsilon'}^\dagger\} = \delta_{\varepsilon\varepsilon'}$ ); however, the transformation does not involve the  $\beta_{\bar{k}}$ ’s in (59) at all, since they are completely decoupled and “just go along for the ride” below.

Since the hybridization term in Eq. (59) only contains the combinations  $(\alpha_{\bar{k}}^\dagger + \alpha_{\bar{k}})$  and  $(\alpha_d - \alpha_d^\dagger)$ , “*half of the impurity*”,  $(\alpha_d + \alpha_d^\dagger)$ , *is completely decoupled from conduction electrons* if  $\varepsilon_d = 0$ . (EK were the first to emphasize that this causes the model’s NFL behavior.) To exploit this fact, it is convenient to transform the two sets of fermions,  $\{\alpha_n\}$  and  $\{\tilde{\alpha}_\varepsilon\}$ , to two sets of Majorana fermions  $\{\gamma_{n\nu}\}$  and  $\{\tilde{\gamma}_{\varepsilon\nu}\}$  ( $\nu = \pm$ ), respectively:

$$\begin{pmatrix} \gamma_{n+} \\ \gamma_{n-} \end{pmatrix} \equiv \frac{1}{\sqrt{2}} \begin{pmatrix} 1 & 1 \\ -i & i \end{pmatrix} \begin{pmatrix} \alpha_n \\ \alpha_n^\dagger \end{pmatrix}, \quad (n = d, k \geq 0), \quad (C1)$$

$$\begin{pmatrix} \tilde{\gamma}_{\varepsilon+} \\ \tilde{\gamma}_{\varepsilon-} \end{pmatrix} \equiv \frac{1}{\sqrt{2}} \begin{pmatrix} 1 & 1 \\ -i & i \end{pmatrix} \begin{pmatrix} \tilde{\alpha}_\varepsilon \\ \tilde{\alpha}_\varepsilon^\dagger \end{pmatrix} \quad (\varepsilon \geq 0). \quad (C2)$$

By construction they are real ( $\gamma_{n\nu} = \gamma_{n\nu}^\dagger$ ,  $\tilde{\gamma}_{\varepsilon\nu} = \tilde{\gamma}_{\varepsilon\nu}^\dagger$ ) and obey the anticommutation relations

$$\{\gamma_{n\nu}, \gamma_{n'\nu'}\} = \delta_{nn'} \delta_{\nu\nu'}, \quad (C3)$$

$$\{\tilde{\gamma}_{\varepsilon\nu}, \tilde{\gamma}_{\varepsilon'\nu'}\} = \delta_{\varepsilon\varepsilon'} \delta_{\nu\nu'}. \quad (C4)$$

When rewritten in terms of these Majorana operators, the original form (59) for  $H_x$  becomes

$$H_x = \sum_{\bar{k} \geq 0} \bar{k} (i \gamma_{\bar{k}+} \gamma_{\bar{k}-} + 1/2) + |\varepsilon_d| (i \gamma_{d+} \gamma_{d-} + 1/2) + i \sum_{\bar{k} \geq 0} 2V_{\bar{k}} \gamma_{\bar{k}+} \gamma_{d-} + \sum_{\bar{k} \geq 0} \bar{k} \beta_{\bar{k}}^\dagger \beta_{\bar{k}}, \quad (C5)$$

[with  $\bar{k}$  and  $V_{\bar{k}}$  given by Eqs. (45) and (60)], and the sought-after diagonalized form (62) becomes

$$H_x = \sum_{\varepsilon \geq 0} \varepsilon (i \tilde{\gamma}_{\varepsilon+} \tilde{\gamma}_{\varepsilon-} + \frac{1}{2}) + \delta E_G + \sum_{\bar{k} \geq 0} \bar{k} \beta_{\bar{k}}^\dagger \beta_{\bar{k}}. \quad (C6)$$

To find the transformation that brings (C5) into the form (C6), we make a Ansatz for the  $\tilde{\gamma}_{\varepsilon\nu}$  [which by (C1) and (C2) is equivalent to the Bogoliubov Ansatz (64)]:

$$\tilde{\gamma}_{\varepsilon\nu} \equiv \sum_{n \in \{d, \bar{k} \geq 0\}} B_{\varepsilon n \nu} \gamma_{n\nu} \quad (\nu = \pm). \quad (C7)$$

It suffices for the Ansatz to be linear, since  $H_x$  is quadratic in  $\gamma_{n\nu}$ ’s, and for it to be diagonal in the index  $\nu$ , since both (C5) and (C6) are purely *off-diagonal* in  $\nu$ . Since the orthonormality conditions (C4) imply

$$\sum_n B_{\varepsilon n \nu} B_{\varepsilon' n \nu} = \delta_{\varepsilon \varepsilon'} \quad (\nu = \pm), \quad (C8)$$

the  $B_{\varepsilon n \nu}$ ’s are orthogonal matrices [with matrix indices  $(\varepsilon, n)$ ], so that Eq. (C7) can trivially be inverted:

$$\gamma_{n\nu} = \sum_{\varepsilon \geq 0} B_{\varepsilon n \nu} \tilde{\gamma}_{\varepsilon\nu}, \quad (\nu = \pm). \quad (C9)$$

We can deduce  $\delta E_G$  even without having determined the  $B_{\varepsilon n \nu}$  yet, by inserting (C9) into  $H_x$  to transform (C5) into (C6): since both equations are off-diagonal in  $\nu$ , no diagonal terms  $\tilde{\gamma}_{\varepsilon\nu} \tilde{\gamma}_{\varepsilon\nu}$  ( $= 1$ , i.e. no constants) can arise, so that the constants in both equations must be equal; this yields Eq. (68) for  $\delta E_G$ .

### 2. Determination of $B_{\varepsilon n \nu}$ ’s and $\varepsilon$ ’s

To determine the coefficients  $B_{\varepsilon n \nu}$ , we substitute the Ansatz (C7) it into the Heisenberg equation

$$[\tilde{\gamma}_{\varepsilon\nu}, H_x] = \nu i \varepsilon \tilde{\gamma}_{\varepsilon-\nu} \quad (\nu = \pm), \quad (C10)$$

[which follows from (C4) and (C6) and is equivalent to (65)], evaluate the commutator using (C3) and (C5), and equate the coefficients of  $\gamma_{n\nu}$ . This readily yields:

$$\varepsilon B_{\varepsilon\bar{k}+} = \bar{k}B_{\varepsilon\bar{k}-} + 2V_{\bar{k}}B_{\varepsilon d-}, \quad (\text{C11a})$$

$$\varepsilon B_{\varepsilon\bar{k}-} = \bar{k}B_{\varepsilon\bar{k}+}, \quad (\text{C11b})$$

$$\varepsilon B_{\varepsilon d+} = |\varepsilon_d|B_{\varepsilon d-}, \quad (\text{C11c})$$

$$\varepsilon B_{\varepsilon d-} = |\varepsilon_d|B_{\varepsilon d+} + \sum_{\bar{k} \geq 0} 2V_{\bar{k}}B_{\varepsilon\bar{k}+}. \quad (\text{C11d})$$

We consider the  $\varepsilon \neq 0$  and  $\varepsilon = 0$  solutions separately.

*a.  $\varepsilon \neq 0$  Solutions*

For  $\varepsilon \neq 0$  we write  $B_{\varepsilon d-} = \varrho(\varepsilon)\varepsilon$ , where  $\varrho(\varepsilon)$  is a normalization factor to be determined below. Then Eqs. (C11) yield Eqs. (69) after some simple algebra. Substituting these into (C11d) yields the eigenvalue equation

$$S_1(\varepsilon) = \varepsilon_d^2/\varepsilon^2 - 1, \quad (\text{C12})$$

where the infinite sum  $S_1(\varepsilon)$  can be evaluated as follows:

$$S_1(\varepsilon) \equiv \sum_{\bar{k} \geq 0} \frac{4V_{\bar{k}}^2}{\bar{k}^2 - \varepsilon^2} \quad (\text{C13})$$

$$= \sum_{n_{\bar{k}} \in \mathbb{Z}} \frac{-4V_0^2/\varepsilon}{\Delta_L(n_{\bar{k}} + \frac{1}{2} - \frac{P}{2}) + \varepsilon} \quad (\text{C14})$$

$$= (4\pi\Gamma/\varepsilon) \tan[\pi(\varepsilon/\Delta_L - P/2)]. \quad (\text{C15})$$

Equating Eqs. (C12) and (C15) gives the eigenvalue equation (67) that determines the allowed  $\varepsilon$ -values.

The normalization factor  $\varrho(\varepsilon)$  can be determined by writing the  $\varepsilon = \varepsilon' \neq 0$ ,  $\nu = +$  version of Eq. (C8) in the form [using Eq. (69)]

$$\varrho^2(\varepsilon) [\varepsilon_d^2 + \varepsilon^2 S_{2+}(\varepsilon)] = 1, \quad (\text{C16})$$

$$S_{2+}(\varepsilon) \equiv \sum_{\bar{k} \geq 0} \frac{4V_{\bar{k}}^2 \varepsilon^2}{(\bar{k}^2 - \varepsilon^2)^2}. \quad (\text{C17})$$

Noting from Eqs. (C13) and (C17) that  $S_{2+}(\varepsilon) = \frac{1}{2}\varepsilon\partial_{\varepsilon}S_1(\varepsilon)$ , evaluating this by reexpressing the derivative of  $S_1$ =(C15) in terms of  $\tan[]$ , and simplifying using  $\tan[] = (\varepsilon_d^2 - \varepsilon^2)/(\pi\varepsilon\Gamma)$  [by (C15)=(C12)], one readily finds Eq. (70) for  $\varrho(\varepsilon)$ .

Note that the eigenvalue equation (67) is symmetrical under the transformation  $\varepsilon \rightarrow -\varepsilon$  and therefore also has negative roots. However, from Eqs. (C11) the corresponding coefficients are given by  $B_{-\varepsilon n\nu} = \nu B_{\varepsilon n\nu}$ , thus the excitations corresponding to  $\varepsilon$  and  $-\varepsilon$  are not independent, but related by  $\tilde{\alpha}_{-\varepsilon} = \tilde{\alpha}_{\varepsilon}^{\dagger}$ . This confirms that only non-negative eigenvalues need to be considered [as was intuitively obvious already when writing down Eq. (62)].

*b.  $\varepsilon = 0$  Solutions*

There are three situations in which a root  $\varepsilon_{j,P}$  of the eigenvalue equation (67) can be equal to zero:

(i) For arbitrary  $\Gamma$ , the lowest root in the  $P = 0$  sector,  $\varepsilon_{0,0}$ , approaches 0 if and only if  $\varepsilon_d \rightarrow 0$ . For  $\varepsilon_d \neq 0$ , its asymptotic behavior close to 0 or  $\Delta_L/2$  is as follows:

$$\frac{\varepsilon_{0,0}}{\Delta_L} \simeq \frac{|\varepsilon_d|}{[\Delta_L^2 + 4\pi^2\Gamma\Delta_L]^{1/2}} \quad \text{for } \frac{\varepsilon_{0,0}}{\Delta_L} \rightarrow 0, \quad (\text{C18a})$$

$$\frac{\varepsilon_{0,0}}{\Delta_L} \simeq \frac{1}{2} - \frac{2\Gamma\Delta_L}{\varepsilon_d^2 - \Delta_L^2/4} \quad \text{for } \frac{\varepsilon_{0,0}}{\Delta_L} \rightarrow \frac{1}{2}. \quad (\text{C18b})$$

For  $\varepsilon_d = \varepsilon_{0,0} = 0$ , the coefficients  $B_{\varepsilon_{0,0}=0,n\nu}$  are simply the  $\varepsilon_d \rightarrow 0$  limits of the  $B_{\varepsilon_{0,0}n\nu}$  of Eqs. (69),

$$B_{\varepsilon_{0,0}n+} = \delta_{nd}, \quad B_{\varepsilon_{0,0}n-} = \frac{\delta_{nd} - (2V_{\bar{k}}/\bar{k})\delta_{n\bar{k}}}{[1 + 4\pi^2\Gamma/\Delta_L]^{1/2}}, \quad (\text{C19})$$

reflecting that  $\gamma_{d+}$  decouples from  $H_x$  for  $\varepsilon_d = 0$ .

(ii) The lowest root in the  $P = 1$  sector,  $\varepsilon_{0,1}$ , identically equals 0 for all  $\varepsilon_d = 0$  and  $\Gamma$ . Solving the  $\varepsilon = 0$ ,  $\Gamma \neq 0$  versions of (C11) *directly* (since (69), derived for  $\varepsilon \neq 0$ , can *not* be used here) gives

$$B_{\varepsilon_{0,1}n+} = \frac{2V_0 \delta_{nd} - |\varepsilon_d| \delta_{n0}}{[4V_0^2 + \varepsilon_d^2]^{1/2}}, \quad B_{\varepsilon_{0,1}n-} = \delta_{n0}, \quad (\text{C20})$$

reflecting that  $\gamma_{\bar{k}=0,-}$  decouples from  $H_x$ .

(iii) The second-lowest root in the  $P = 1$  sector,  $\varepsilon_{1,1}$ , approaches zero if and only if  $\Gamma \rightarrow 0$  at  $\varepsilon_d = 0$  (to be precise, in this limit  $\varepsilon_{1,1} \simeq 2\sqrt{\Gamma\Delta_L}$ ); this reflects the fact that  $H_x$  has *two* zero modes for  $\varepsilon_d = \Gamma = 0$ , namely  $\alpha_0$  and  $\alpha_d$ . Note, though, that in this limit  $\tilde{\gamma}_{\varepsilon_{1,1}\nu}$  [found using (69)] and  $\tilde{\gamma}_{\varepsilon_{0,1},\nu}$  do *not* reduce simply to  $\gamma_{d\nu}$  and  $\gamma_{\bar{k}=0,\nu}$  but to linear combinations of these (in Table I, this is indicated by braces). In the opposite limit of  $\Gamma/\Delta_L \rightarrow \infty$  at  $\varepsilon_d = 0$ , one has  $\varepsilon_{1,1} \simeq \Delta_L(\frac{1}{2} - \frac{\Delta_L}{4\pi^2\Gamma})$ .

### 3. Consistency Checks

Several consistency checks on the above solution are possible. Firstly, let us check Eq. (C8): In the special case that  $\varepsilon$  or  $\varepsilon'$  is  $\varepsilon_{0,1} = 0$ , Eq. (C20) is easily checked to be consistent with Eq. (C8). If  $\varepsilon$  and  $\varepsilon' \neq 0$ , one finds by writing out Eq. (C8) for  $(\varepsilon = \varepsilon', \nu = -)$  and  $(\varepsilon \neq \varepsilon', \nu = \pm)$ , respectively, that [analogously to (C16),(C17)] the following relations must hold:

$$\frac{1}{\varrho^2(\varepsilon)\varepsilon^2} - 1 = \sum_{\bar{k} \geq 0} \frac{4V_{\bar{k}}^2 \bar{k}^2}{(\bar{k}^2 - \varepsilon^2)^2} \quad [\equiv S_{2-}(\varepsilon)], \quad (\text{C21})$$

$$-\frac{\varepsilon_d^2}{\varepsilon\varepsilon'} = \sum_{\bar{k} \geq 0} \frac{4V_{\bar{k}}^2 \varepsilon\varepsilon'}{(\bar{k}^2 - \varepsilon^2)(\bar{k}^2 - \varepsilon'^2)} \quad [\equiv S_{3+}(\varepsilon, \varepsilon')],$$

$$-1 = \sum_{\bar{k} \geq 0} \frac{4V_{\bar{k}}^2 \bar{k}^2}{(\bar{k}^2 - \varepsilon^2)(\bar{k}^2 - \varepsilon'^2)} \quad [\equiv S_{3-}(\varepsilon, \varepsilon')].$$

One can verify that indeed they do, by noting from Eqs. (C13), (C17) that the sums defined above can be rewritten as  $S_{2-} = S_1 + S_{2+}$  and

$$S_{3\pm}(\varepsilon, \varepsilon') = \frac{1}{2} \left[ \frac{\varepsilon S_1(\varepsilon) - \varepsilon' S_1(\varepsilon')}{\varepsilon - \varepsilon'} \mp \frac{\varepsilon S_1(\varepsilon) + \varepsilon' S_1(\varepsilon')}{\varepsilon + \varepsilon'} \right]$$

and simplifying these using Eqs. (C12) and (C16).

Secondly, one can verify explicitly that our transformation does indeed diagonalize  $H_x$ : insert the inverse Bogoliubov transformation (C9) and Eqs. (69) for the coefficients  $B_{\varepsilon n \nu}$  into the original form (C5) for  $H_x$  and express the resulting  $\sum_{\bar{k}}$  sums in terms of  $S_1$ ,  $S_{2-}$  and  $S_{3-}$ :

$$\begin{aligned} H_x = & |\varepsilon_d|/2 + \sum_{k>0} k/2 + \sum_{\bar{k}>0} \bar{k} \beta_{\bar{k}}^\dagger \beta_{\bar{k}} \\ & + \sum_{\varepsilon, \varepsilon' > 0} i \tilde{\gamma}_\varepsilon + \tilde{\gamma}_{\varepsilon'} - \varrho(\varepsilon) \varrho(\varepsilon') \varepsilon' \left[ \varepsilon_d^2 - \varepsilon^2 S_1(\varepsilon) \right. \\ & \left. + \varepsilon^2 \left( \delta_{\varepsilon \varepsilon'} S_{2-}(\varepsilon) + (1 - \delta_{\varepsilon \varepsilon'}) S_{3-}(\varepsilon, \varepsilon') \right) \right]. \end{aligned} \quad (\text{C22})$$

(The terms with  $\varepsilon$  or  $\varepsilon' = 0$  can be checked to be zero.) Evaluating this using Eq. (C12) and the equations for  $S_{2-}$  and  $S_{3-}$  readily yields the sought-after diagonal form (C6) for  $H_x$  and confirms Eq. (68) for  $\delta E_G$ .

#### 4. Ground State Energy Shift $\delta E_G$

We now show how to calculate the ground state energy shift  $\delta E_G \equiv \delta E_G^0 + P \delta E_G^P$  of (68), for  $\Gamma/\Delta_L \gg 1$  and both  $T_h = 0$  and  $T_h/\Delta_L \gg 1$ , i.e. we derive Eqs. (77) and (78). As explained in Section VD, the coefficient of the  $P$ -dependent term,  $\delta E_G^P$ , must be extracted with care to obtain the correct finite-size spectrum.

In the notation of Eq. (71a), Eq. (68) becomes

$$\begin{aligned} \delta E_G = & \frac{1}{2} \left[ \sum_{j=1}^{N_{\max}} \Delta_L \left( j - \frac{1}{2} - \frac{P}{2} \right) + |\varepsilon_d| - \sum_{j=0}^{N_{\max}} \varepsilon_{j,P} \right] \\ = & \frac{1}{2} \left[ |\varepsilon_d| - \varepsilon_{0,P} - \Delta_L \sum_{j=1}^{N_{\max}} \delta_{j,P} \right] \end{aligned} \quad (\text{C23})$$

where we introduced a ‘‘band cutoff’’  $N_{\max} \equiv D/\Delta_L$  to regularize the sum (with  $D \sim 1/a$ ). The task at hand is to perform the sum on  $j$  sufficiently carefully to extract its leading  $P$ -dependence.

##### a. Zero magnetic field

We first consider the case  $\Gamma/\Delta_L \gg 1$  and  $T_h = 0$ . To isolate the  $P$ -dependence of  $\delta_{j,P}$ , we write Eq. (71b) as

$$\delta_{j,P} = 1/2 + g(j - P/2 + \delta_{j,P}), \quad (\text{C24})$$

$$g(x) \equiv -\frac{1}{\pi} \arctan \left[ \frac{\Delta_L(x - 1/2)}{4\pi\Gamma} \right], \quad (\text{C25})$$

and solve (C24) for  $\delta_{j,P}$  by expanding its r.h.s. in the small parameter  $(\delta_{j,P} - P/2)\Delta_L/\Gamma \ll 1$ , finding

$$\delta_{j,P} = \frac{1/2 + g(j)}{1 - g'(j)} - g'(j) \frac{P}{2} + \mathcal{O} \left( \frac{\Delta_L^2}{\Gamma^2} \right). \quad (\text{C26})$$

The first term is  $P$ -independent and gives the leading contribution to  $\delta E_G^0$ . The second term is  $\mathcal{O}(\Delta_L/\Gamma)$ , contains the full  $P$ -dependence of  $\delta_{j,P}$  to this order and contributes to  $\delta E_G^P$ . Inserting (C26) into (C23) gives

$$\delta E_G^0 = -\frac{\Delta_L}{2} \sum_{j=1}^{N_{\max}} \frac{1/2 + g(j)}{1 - g'(j)} \quad (\text{C27})$$

$$\begin{aligned} & = -\Gamma \left[ \int_0^{D/4\pi\Gamma} dy [\pi - 2 \arctan y] + \mathcal{O}(\Delta_L/\Gamma) \right] \\ & = -2\Gamma \left[ \ln(D/4\pi\Gamma) + 1 + \mathcal{O}(\Delta_L/\Gamma, \Gamma/D) \right], \end{aligned} \quad (\text{C28})$$

while the  $P$ -dependent part,  $\delta E_G^P$  is equal to

$$-\varepsilon_{0,P}/2 + (\Delta_L/4) \sum_{j=1}^{N_{\max}} g'(j) \quad (\text{C29})$$

$$\approx -\varepsilon_{0,P}/2 + (\Delta_L/4) [g(N_{\max}) - g(1)] \quad (\text{C30})$$

$$\approx -\Delta_L [1/8 + \mathcal{O}(\Delta_L/\Gamma)], \quad (\text{C31})$$

where for (C31) we used  $\varepsilon_{0,P} = 0$  for  $T_h = 0$  [by (72)].

##### b. Large magnetic field

Next we consider the case  $\Gamma/\Delta_L \gg 1$  and  $T_h/\Delta_L \gg 1$  (for arbitrary  $T_h/\Gamma$ ). This can be treated analogously, except that now (C25) must be replaced by [from (71b)]

$$g(x) \equiv \frac{1}{\pi} \arctan \frac{1}{4\pi} \left[ \frac{T_h}{\Delta_L(x - 1/2)} - \frac{\Delta_L(x - 1/2)}{\Gamma} \right]$$

[thus  $g'(x)$  is of order  $\mathcal{O}(\Delta_L/\Gamma, \Delta_L/T_h)$  for all  $x \geq 1$ ]. Since now  $\varepsilon_{0,P} = \Delta_L(1 - P)/2$  [by (72) and (C18b)], Eq. (C30) now yields  $\Delta_L[1/2 + \mathcal{O}(\Delta_L/\Gamma, \Delta_L/T_h)]$ , which is  $P$ -independent. This implies that  $\delta E_G^P = 0$  to this order, in other words that for  $T_h, \Gamma \gg \Delta_L$  (and independent of the ratio  $T_h/\Gamma$ ) the ground state energy shift  $\delta E_G$  is no longer  $P$ -dependent.

The  $P$ -independent part of the shift,  $\delta E_G^0$ , can be obtained from (C27), plus the  $|\varepsilon_d|/2$  of (C23):

$$\begin{aligned}\delta E_G^0 &= \frac{|\varepsilon_d|}{2} - \Gamma \left[ \int_0^{D/4\pi\Gamma} dy \left[ \pi - 2 \arctan \left( y - \frac{T_h}{16\pi^2\Gamma y} \right) \right] + \mathcal{O}(\Delta_L/\Gamma, \Delta_L/T_h) \right] \\ &= -2\Gamma \left[ \ln(D/|\varepsilon_d|) + 1 + \mathcal{O}(\Delta_L/\Gamma, \Delta_L/T_h, \Gamma/D, T_h/D, \Gamma/T_h) \right].\end{aligned}\quad (C32)$$

Although the integral can be evaluated for arbitrary values of its parameters using

$$\int dy \arctan(y - b/y) = y \arctan(y - b/y) - \frac{1}{4} \ln(y^4 + y^2 - 2y^2b + b^2) - \frac{1}{2} \sqrt{4b-1} \arctan \left( \frac{1+2y^2-2b}{\sqrt{4b-1}} \right), \quad (C33)$$

we gave in (C32) only the limit of large magnetic fields,  $T_h/\Gamma \gg 1$ .

### 5. Fluctuations in $\mathcal{N}_x$

The results for  $\langle \hat{\mathcal{N}}_x \rangle$  and  $\langle \hat{\mathcal{N}}_x^2 \rangle$  discussed and interpreted in Section V F are obtained as follows. We consider only  $\varepsilon_d = 0$  and the states  $|\tilde{0}\rangle_{\mathcal{S}_{\text{ext}}}$  and  $\tilde{\alpha}_{\varepsilon_{0,P}}^\dagger |\tilde{0}\rangle_{\mathcal{S}_{\text{ext}}}$ , which represent, respectively, the physical ground states in sectors with excitation parity  $\mathcal{P}_{\tilde{E}} = 0$  and 1. We express  $\hat{\mathcal{N}}_x$  through  $\alpha_{\bar{k}}$  and  $\beta_{\bar{k}}$ , using (51) and (58):

$$\hat{\mathcal{N}}_x = \sum_{\bar{k} > 0} i(\alpha_{\bar{k}}^\dagger \beta_{\bar{k}} - \beta_{\bar{k}}^\dagger \alpha_{\bar{k}}) + P(1/2 - \alpha_0^\dagger \alpha_0). \quad (C34)$$

Now, in a  $P = 1$  sector, we have [analogously to (C43)]

$$\begin{aligned}1/2 - \langle \alpha_0^\dagger \alpha_0 \rangle &= \frac{1}{2} \left[ \pm B_{\varepsilon_{0,1}0+} B_{\varepsilon_{0,1}0-} + \sum_{\varepsilon > \varepsilon_{0,1}} B_{\varepsilon 0+} B_{\varepsilon 0-} \right] \\ &= 0,\end{aligned}\quad (C35)$$

for all  $\Gamma/\Delta_L$  [using (69) and (C20)]. (Here and below the upper or lower signs in  $\pm$  (and  $\mp$ ) refer to  $\mathcal{P}_{\tilde{E}} = \langle \tilde{\alpha}_{\varepsilon_{0,P}}^\dagger \tilde{\alpha}_{\varepsilon_{0,P}} \rangle = 0$  or 1.) Since moreover  $\beta_{\bar{k}} |\tilde{0}\rangle_{\mathcal{S}_{\text{ext}}} = 0$ , we conclude from (C34) and (C35) that  $\langle \hat{\mathcal{N}}_x \rangle = 0$  for both  $P = 0$  and 1 and all  $\Gamma/\Delta_L$ .

The calculation of  $\langle \hat{\mathcal{N}}_x^2 \rangle$  is more involved:

$$\begin{aligned}\langle \hat{\mathcal{N}}_x^2 \rangle + P/4 &= \sum_{\bar{k} \geq 0} \langle \alpha_{\bar{k}}^\dagger \alpha_{\bar{k}} \rangle \\ &= \frac{1}{2} \sum_{\bar{k} \geq 0} \left[ 1 \mp B_{\varepsilon_{0,P}\bar{k}+} B_{\varepsilon_{0,P}\bar{k}-} - \sum_{j > 0} B_{\varepsilon_j,\bar{k}+} B_{\varepsilon_j,\bar{k}-} \right] \\ &= \frac{1}{2} \sum_{\bar{k} \geq 0} \left[ 1 - \sum_{\varepsilon > 0} \rho^2(\varepsilon) \varepsilon^2 \frac{4V_{\bar{k}}^2 \varepsilon \bar{k}}{(\varepsilon^2 - \bar{k}^2)^2} \right] \\ &= \sum_{\varepsilon > 0} \rho^2(\varepsilon) \varepsilon^2 \left[ \frac{1}{4} + \sum_{\bar{k} \geq 0} \frac{V_{\bar{k}}^2}{(\bar{k} + \varepsilon)^2} \right] + \frac{1}{2} \left[ \sum_{\bar{k} \geq 0} - \sum_{\varepsilon > 0} \right].\end{aligned}\quad (C36)$$

For the first equation we used (C34), (C35); for the second (58), (C1), (C9), (C2); for the third (69), (C19) or (C20); we tamed the “divergence” at  $\varepsilon \simeq \bar{k}$  using

$$\frac{\varepsilon \bar{k}}{(\varepsilon^2 - \bar{k}^2)^2} = \frac{\bar{k}^2}{(\bar{k}^2 - \varepsilon^2)^2} - \frac{1}{2(\bar{k}^2 - \varepsilon^2)} - \frac{1}{2(\bar{k} + \varepsilon)^2}$$

and performing the  $\sum_{\bar{k}}$  sums over the first two terms using (C12), (C21) and (C13), thus obtaining (C36), in which the last two (diverging) terms cancel exactly.

The limit  $\Gamma/\Delta_L \rightarrow 0$  of (C36) yields  $\langle \hat{\mathcal{N}}_x^2 \rangle \rightarrow P/4$  [for  $P = 1$  the mode  $\varepsilon_{1,1} \rightarrow 2\sqrt{\Gamma\Delta_L}$  (compare Section C2 b) makes a non-zero contribution]. To obtain the leading behavior of (C36) in the opposite limit  $\Gamma/\Delta_L \gg 1$ , we evaluate the sums as integrals:

$$\begin{aligned}\langle \hat{\mathcal{N}}_x^2 \rangle &\approx \int_{\Delta_L}^{\infty} d\varepsilon \frac{2\Gamma}{\frac{1}{4}\varepsilon^2 + 4\pi^2\Gamma^2} \left[ \frac{1}{4} + \int_0^{\infty} d\bar{k} \frac{2\Gamma}{(\bar{k} + \varepsilon)^2} \right] \\ &\approx \frac{1}{\pi^2} \ln(\Gamma L) + \mathcal{O}[(\Delta_L/\Gamma)^0].\end{aligned}\quad (C37)$$

### 6. Perturbing around EK line by $\delta H'_z$

In this section we determine the scaling dimension  $\gamma_{\delta\lambda_z}$  of the operator  $\delta H'_z$  of (38), which arises as soon as one leaves the EK line, i.e. when  $\lambda_z = 1 + \delta\lambda_z$ . To this end we perturbatively calculate, in a given subspace  $\mathcal{S}_{\text{phys}}(S_T, \mathcal{N}_c, \mathcal{N}_f)$  at  $\varepsilon_d = 0$ , the level shifts  $\delta\tilde{\mathcal{E}}(L)$  [see (90)] induced by  $\delta H'_z$ . As first step, we express  $\delta H'_z$  in terms of operators that diagonalize  $H'(\delta\lambda_z = 0)$ :

$$\partial_x \varphi_s(x) = \Delta_L \sum_{n_q > 0} \sqrt{n_q} i(b_{qs} - b_{qs}^\dagger), \quad (C38)$$

$$\hat{\mathcal{N}}_s S_z = S_T S_z - 1/4, \quad (C39)$$

$$S_z = \frac{1}{2} \sum_{\varepsilon \varepsilon'} B_{\varepsilon d+} B_{\varepsilon' d-} (\tilde{\alpha}_\varepsilon^\dagger + \tilde{\alpha}_\varepsilon)(\tilde{\alpha}_{\varepsilon'}^\dagger - \tilde{\alpha}_{\varepsilon'}). \quad (C40)$$

[Eq. (C38) follows from (14) and (26), Eq. (C39) from (23), and Eq. (C40) from (43), (58c), (C1), (C9) and (C2).] These relations show that although the NFL fixed point spectrum is highly degenerate, there is no need for degenerate perturbation theory, because  $\langle \tilde{E} | \delta H'_z | \tilde{E}' \rangle = 0$  whenever  $|\tilde{E}\rangle$  and  $|\tilde{E}'\rangle$  are degenerate but distinct eigenstates of  $H'$  [by inspection; compare Table I]. To first order in  $\delta\lambda_z$ , the dimensionless energy shift  $\delta\tilde{\mathcal{E}}(L)$  of (90) due to  $\delta H'_z$  is thus simply given by

$$\begin{aligned}\delta\tilde{\mathcal{E}}(L) &= \left[ \langle \tilde{E} | \delta H'_z | \tilde{E} \rangle - \langle \tilde{E}_{\text{min}} | \delta H'_z | \tilde{E}_{\text{min}} \rangle \right] / \Delta_L \\ &= \delta\lambda_z S_T \left[ \langle \tilde{E} | S_z | \tilde{E} \rangle - \langle \tilde{E}_{\text{min}} | S_z | \tilde{E}_{\text{min}} \rangle \right].\end{aligned}\quad (C41)$$

(Note that since  $\partial_x \varphi_s$  [by (C38)] is linear in  $b_{qs}$  and  $b_{qs}^\dagger$ , in (C41) only in the second, ‘‘zero-mode term’’ of  $\delta H'_z$  contributes, which does not occur in the continuum limit considered in Ref. 4.) Now,  $\tilde{E}_{\min}$  corresponds to the physical ground states in the two sectors  $\mathcal{S}_{\text{phys}}(S_T = \pm 1/2, \mathcal{N}_c = 0, \mathcal{N}_f = 0)$  [with  $\mathcal{E}_{\text{NFL}} = 0$  in Table I], namely

$$|\tilde{0}\rangle_{\mathcal{S}_{\text{ext}}(1/2,0,0)}, \quad \tilde{\alpha}_{\varepsilon_{0,0}}^\dagger |\tilde{0}\rangle_{\mathcal{S}_{\text{ext}}(-1/2,0,0)}. \quad (\text{C42})$$

From (C40), one readily finds for these, respectively,

$$S_T \langle S_z \rangle = \pm \frac{1}{4} \left( \pm B_{\varepsilon_{0,0}d+} B_{\varepsilon_{0,0}d-} + \sum_{j>0} B_{\varepsilon_{j,0}d+} B_{\varepsilon_{j,0}d-} \right). \quad (\text{C43})$$

Evaluating this using (69a) and (C19), the first term yields  $\frac{1}{4}[1 + 4\pi^2\Gamma/\Delta_L]^{-1/2}$  for both cases, and the second term vanishes for  $\varepsilon_d = 0$ . Thus the two-fold ground state degeneracy persists, in keeping with the fact that  $\delta H'_z$  respects spin reversal symmetry.

The first four excited states in Table I, with  $= \frac{1}{8}$ , all have  $S_T = 0$ , hence  $\langle S_T S_z \rangle = 0$ . They are thus not shifted by  $\delta H'_z$  themselves. Nevertheless, their *relative shift* w.r.t. the  $\mathcal{E}_{\text{NFL}} = 0$  physical ground states just discussed is non-zero, since the ground states were shifted upwards: by (C41), it is

$$\delta\tilde{\mathcal{E}}(L) = -\delta\lambda_z \frac{1}{4}[1 + 4\pi^2\Gamma/\Delta_L]^{-1/2} \sim L^{-1/2}. \quad (\text{C44})$$

It follows [from (90)] that the sought-after scaling dimension of  $\delta H'_z$  is  $\gamma_{\delta\lambda_z} = 1/2$ . Thus this perturbation is irrelevant, and the RG flow in the vicinity of the EK-line is always towards it. [It is easy to check that all 10 of the next-higher excited states in Table I, with  $\mathcal{E}_{\text{NFL}} = \frac{1}{2}$ , have  $\delta\tilde{\mathcal{E}}(L) = -\delta\lambda_z \frac{1}{2}[1 + 4\pi^2\Gamma/\Delta_L]^{-1/2}$ , which again is  $\sim L^{-1/2}$ , as expected.]

Let us now turn on a local magnetic field  $\varepsilon_d = h_i$ , in which case the second term of (C43) is non-zero and contributes to lifting the ground state degeneracy. In the continuum limit  $L \rightarrow \infty$  (so that  $\Delta_L \ll h_i, \Gamma$ ), it in fact gives a much larger contribution than the first term of (C43), namely  $\delta\tilde{\mathcal{E}}(L) = \pm \frac{\delta\lambda_z}{4} I(\bar{h})$ , where  $\bar{h} \equiv |h_i|/(2\pi\Gamma)$ , and  $I(\bar{h})$  is given, after the substitution  $x = \varepsilon_{j,0}^2/\varepsilon_d^2$ , by the following integral:

$$I(\bar{h}) = \frac{\bar{h}}{\pi} \int_0^\infty dx \frac{1}{\bar{h}^2(x-1)^2/2 + 2x} \quad (\text{C45})$$

$$= \begin{cases} \xrightarrow{\bar{h} \rightarrow 0} -\frac{2}{\pi} \bar{h} \ln(\bar{h}/2); \\ \xrightarrow{\bar{h} \rightarrow \infty} 1 - \frac{2}{\pi \bar{h}}. \end{cases}$$

## APPENDIX D: THE SINGLE-CHANNEL KONDO MODEL

This Appendix deals with the anisotropic *single-channel* Kondo (1CK) model, which is of interest not only as the most basic Kondo model, but also since it is equivalent to a dynamic two-state system coupled to an ohmic environment.<sup>66</sup> We shall solve the 1CK model along the so-called Toulouse line,<sup>67,53</sup> the 1CK analog of the EK line, calculating the crossover of the finite-size spectrum from the free Fermi liquid fixed point to the strong-coupling Fermi liquid fixed point, well-known from Wilson’s NRG calculations.<sup>60</sup> Since the 1CK calculation is a straightforward adaption of that developed above for the 2CK case, it will be presented in less detail than the latter, though technical differences will be pointed out.

### 1. Conserved Quantum Numbers

The 1CK model is defined by Eqs. (1) or (20) for  $H_0$ , (8) for  $H_{\text{int}}$  and (9) for  $H_h$ , the only difference being that the channel index only has the value  $j = 1$  and hence can be dropped throughout. To exploit the fact that the total charge is conserved, we transform from the  $\alpha = (\uparrow, \downarrow)$  basis to a  $y = (c, s)$  basis by writing:

$$b_{qc/s}^\dagger \equiv (b_{q\uparrow}^\dagger \pm b_{q\downarrow}^\dagger)/\sqrt{2}, \quad (\text{D1a})$$

$$\varphi_{c/s}(x) \equiv (\phi_\uparrow(x) \pm \phi_\downarrow(x))/\sqrt{2}. \quad (\text{D1b})$$

$$\hat{\mathcal{N}}_{c/s} \equiv (\hat{N}_\uparrow \pm \hat{N}_\downarrow)/2, \quad (\text{D1c})$$

Note that the normalization constants in Eqs. (D1a) and (D1b) differ from that of (D1c) [this contrasts with the 2CK case, and affects many of the equations below]: the  $1/\sqrt{2}$  in the former ensures that the transformations for  $b_{qy}^\dagger$  and  $\varphi_y$  are unitary, so that these operators satisfy commutation relations analogous to those of  $b_{q\alpha}$  and  $\phi_\alpha$  [namely (12) and (15)]; the  $1/2$  in (D1c) ensures that  $\hat{\mathcal{N}}_c$  and  $\hat{\mathcal{N}}_s$  can be interpreted as half the total charge and the total electron spin, whose eigenvalues are either both integers or both half-integers (whereas a  $1/\sqrt{2}$  in (D1c) would have yielded irrational eigenvalues):

$$\vec{\mathcal{N}} \equiv (\mathcal{N}_c, \mathcal{N}_s) \in (\mathbb{Z} + P/2)^2. \quad (\text{D2})$$

Here the *parity index*  $P$  equals 0 or 1 if the total number of electrons is even or odd, respectively. Eq. (D2) is the *free gluing condition* for the 1CK model.

Evidently, the total charge  $\mathcal{N}_c$  and the total spin,

$$S_T = \mathcal{N}_s + S_z, \quad (\text{D3})$$

are conserved, where (D3) will be called the *spin-conservation condition*. Hence we can restrict our attention to the invariant subspace

$$\mathcal{S}_{\text{phys}}(S_T, \mathcal{N}_c) \equiv \{|\mathcal{N}_c, S_T - \frac{1}{2}; \uparrow\rangle \oplus |\mathcal{N}_c, S_T + \frac{1}{2}; \downarrow\rangle\}. \quad (\text{D4})$$

The difference between Eqs. (D4) and (25) makes explicit a major difference between the 1CK and 2CK models: though for both the quantum number  $\mathcal{N}_s$  fluctuates “mildly” between  $S_T \mp 1/2$ , the *1CK model lacks a “wildly” fluctuating quantum number* such as  $\mathcal{N}_x$ ; this is the “deep reason” why it also lacks NFL behavior.

In the new charge-spin basis, the bosonized form of the 1CK Hamiltonian takes the following simple form:

$$H_0 = \Delta_L \left[ \hat{\mathcal{N}}_c (1 - P_0) + \hat{\mathcal{N}}_c^2 + \hat{\mathcal{N}}_s^2 \right] + \sum_{q>0} q (b_{qc}^\dagger b_{qc} + b_{qs}^\dagger b_{qs}) , \quad (D5)$$

$$H_z = \lambda_z \left[ \partial_x \varphi_s(0) / \sqrt{2} + \Delta_L \hat{\mathcal{N}}_s \right] S_z , \quad (D6)$$

$$H_\perp = \frac{\lambda_\perp}{2a} \left[ e^{-i\sqrt{2}\varphi_s(0)} S_+ F_\downarrow^\dagger F_\uparrow + \text{h.c.} \right] . \quad (D7)$$

## 2. EK transformation

To simplify  $H_z$ , we use the same Emery-Kivelson transformation  $U(\lambda) = e^{i\gamma S_z \varphi_s(0)}$  of (31) as for the 2CK model, but now with  $\varphi_s(x)$  given by Eq. (D1b) instead of (26). The impurity spin operators  $S_\pm$  and the spin field  $\varphi_s$  transform according to Eqs. (32) and (34), just as in the 2CK case, but in contrast to the latter,

$$U(H_0 + H_z)U^{-1} = H_0 + (\lambda_z / \sqrt{2} - \gamma) \partial_x \varphi_s(0) S_z + \lambda_z \Delta_L \hat{\mathcal{N}}_s S_z + \text{const} , \quad (D8)$$

$$\psi_\alpha(x) \rightarrow \psi_\alpha(x) e^{i\sqrt{2}\alpha\gamma S_z \arctan(x/a)} , \quad (|x| \ll L) . \quad (D9)$$

Moreover, since in the 1CK case the spin density is  $\partial_x \varphi_s(x) / (2\pi\sqrt{2})$ , a spin  $-\gamma S_z / \sqrt{2}$  from the conduction band is tied to the impurity. To eliminate the  $S_z \partial_x \varphi_s$  term, we choose  $\gamma \equiv \lambda_z / \sqrt{2}$  (in contrast to  $\gamma \equiv \lambda_z$  for the 2CK case). Then

$$H'(\lambda_\perp = 0) = \Delta_L \left[ \hat{\mathcal{N}}_c (\mathcal{N}_c + 1 - P_0) + \hat{\mathcal{N}}_s^2 + \lambda_z \hat{\mathcal{N}}_s S_z \right] + \sum_{q>0} q (b_{qc}^\dagger b_{qc} + b_{qs}^\dagger b_{qs}) + H_h + \text{const} , \quad (D10)$$

and  $H'_\perp$  contains the factors  $e^{\pm i(\sqrt{2} - \lambda_z / \sqrt{2})\varphi_s(0)}$ .

These factors simplify for two special values of  $\lambda_z$ . The first case,  $\lambda_z = 2$  (i.e.  $\gamma = \sqrt{2}$ ), is called the *decoupling point*, since the  $\varphi_s$ -dependence drops out completely:

$$H'_\perp = \frac{\lambda_\perp}{2a} (S_+ F_\downarrow^\dagger F_\uparrow + \text{h.c.}) . \quad (D11)$$

In this case, the spin  $-\gamma S_z / \sqrt{2}$  from the conduction band that is tied to the impurity is precisely  $-S_z$ , thus we have perfect screening. Indeed, by (D9) the phase shift  $\delta$  in  $\psi_\alpha(0^-) \equiv e^{i2\delta} \psi_\alpha(0^+)$  is  $|\delta| = \pi/2$ , corresponding to the unitarity limit. The dynamics of the electron-hole excitations described by the  $\varphi_{s,c}$  fields evidently decouples from

$S_z$  [by (D11)]. Thus it is trivial to find the spectrum, which turns out to coincide with the fixed-point spectrum shown in the strong-coupling limit of Fig.7. Note, incidentally, that at the decoupling point the model can be mapped to a two-level system without dissipation.<sup>68,41</sup>

The other solvable point is the *Toulouse point*, with

$$\lambda_z^* \equiv 2 - \sqrt{2} , \quad \gamma^* \equiv \sqrt{2} - 1 , \quad (D12)$$

$$H'_\perp = \frac{\lambda_\perp}{2a} (S_+ F_\downarrow^\dagger F_\uparrow e^{-i\varphi_s(0)} + \text{h.c.}) . \quad (D13)$$

We henceforth focus on this point, which is the analog of the EK line in the 2CK context, since the factors  $e^{i\varphi_s}$  can be treated by refermionization, as shown below. Note, though, that the spin  $-\gamma^* S_z / \sqrt{2}$  from the conduction band that is tied to the impurity does not fully screen the latter.

## 3. Refermionization

To ensure proper anticommutation relations for the pseudofermions to be defined below, it is convenient to make one more unitary transformation with the operator  $U_2 = e^{i\pi \hat{\mathcal{N}}_s S_z}$ , which changes the phases of the Klein factors and the spin operators (and of the basis states in Fock space):

$$U_2 F_\downarrow^\dagger F_\uparrow U_2^{-1} = e^{-i\pi S_z} F_\downarrow^\dagger F_\uparrow , \quad (D14)$$

$$U_2 S_\pm U_2^{-1} = e^{\pm i\pi \hat{\mathcal{N}}_s} S_\pm . \quad (D15)$$

Then  $H'_\perp$  of Eq. (D13) takes the very simple form

$$U_2 H'_\perp U_2^{-1} = \frac{\lambda_\perp}{2\sqrt{a}} (c_d^\dagger \psi_s(0) + \psi_s^\dagger(0) c_d) , \quad (D16)$$

where we introduced the following pseudofermions,

$$c_d^\dagger \equiv S_+ e^{i\pi(\hat{\mathcal{N}}_s - S_z)} , \quad c_d^\dagger c_d = S_z + 1/2 , \quad (D17)$$

$$\psi_s(x) \equiv \frac{F_\downarrow^\dagger F_\uparrow}{a^{1/2}} e^{-i(\hat{\mathcal{N}}_s - \text{sgn}(S_T)[1+P]/2)2\pi x/L - i\varphi_s(x)} \quad (D18)$$

$$\equiv \sqrt{2\pi/L} \sum_{\bar{k}} c_{\bar{k}s} e^{-i\bar{k}x} , \quad (D19)$$

with  $\text{sgn}(S_T = 0) \equiv 1$ . By including the factor  $e^{i[1+\text{sgn}(S_T)\bar{P}]\pi x/L}$  in the definition (D18) of  $\psi_s$ , we purposefully ensured that  $\psi_s$  has the *same* boundary conditions (namely periodic) for both  $P = 0$  and  $1$ , in order not to have to distinguish between these two sectors (the reason for the  $\text{sgn}(S_T)$  factor is explained below). As a consequence, the  $\bar{k}$ ’s in Eq. (D19) must be of the form

$$\bar{k} = \Delta_L [n_{\bar{k}} - \text{sgn}(S_T)1/2] , \quad n_{\bar{k}} \in \mathbb{Z} . \quad (D20)$$

[i.e. the periodicity parameter  $P_0$  of (4) here equals 1].

By Eqs. (39), these pseudofermions have the properties

$$\{c_{\bar{k}s}, c_{\bar{k}'s}^\dagger\} = \delta_{\bar{k}\bar{k}'} , \quad (D21)$$

$$\{c_d, c_d^\dagger\} = 1 , \quad (D22)$$

$$\{c_d, c_{\bar{k}s}^\dagger\} = \{c_d, c_{\bar{k}s}\} = 0 , \quad (D23)$$

$$[c_d, \hat{\mathcal{N}}_s] = c_d . \quad (D24)$$

Note in particular that the anticommutation of  $c_d$  and  $c_{\bar{k}s}$  is ensured by the factor  $e^{-i\pi\hat{\mathcal{N}}_s}$  in the definition (D17) of  $c_d$ . Note further that the individual action of both  $c_d$  and  $\psi_s$  violates the conservation (D3) of the total spin  $S_T = \mathcal{N}_s + S_z$ . When diagonalizing  $H'$ , we shall therefore work not in the physical subspace  $\mathcal{S}_{\text{phys}}(S_T, \mathcal{N}_c)$  of (D4), but in a correspondingly extended subspace  $\mathcal{S}_{\text{ext}}(\mathcal{N}_c)$ , in which  $\mathcal{N}_s$  is unrestricted and not linked to  $S_z$ . At the end of the calculation we shall retain only the physical states in  $\mathcal{S}_{\text{ext}}(\mathcal{N}_c)$ , which we identify using a *generalized spin-conservation condition* to be derived from (D3).

Let  $|0\rangle_{\mathcal{S}_{\text{ext}}}$  be a free reference ground state in  $\mathcal{S}_{\text{ext}}$  defined as in (50), and let  $:\cdot:$  denote normal ordering w.r.t. it. Then  $:c_d^\dagger c_d := c_d^\dagger c_d - n_d^{(0)}$ . Moreover  $\hat{N}_s \equiv \sum_{\bar{k}} :c_{\bar{k}s}^\dagger c_{\bar{k}s}:$ , which counts the number of  $s$ -pseudofermions, is related to  $\hat{\mathcal{N}}_s$  by [compare (51)]

$$\hat{N}_s = \hat{\mathcal{N}}_s - \text{sgn}(S_T)P/2 . \quad (D25)$$

The  $\text{sgn}(S_T)$  factors above are needed because we purposefully included one in the refermionization relation (D18); we did this to ensure that the spin reversal transformation  $(S_z, \mathcal{N}_s, \varphi_s) \rightarrow (-S_z, -\mathcal{N}_s, -\varphi_s)$  can also be simply implemented in terms of the new pseudo-fermions, for which it implies

$$(S_T, c_d, \psi_s, \bar{N}_s) \rightarrow (-S_T, c_d^\dagger, \psi_s^\dagger, -\bar{N}_s) . \quad (D26)$$

The pseudofermions' kinetic energy is [compare (52)]

$$\sum_{\bar{k}} \bar{k} :c_{\bar{k}s}^\dagger c_{\bar{k}s} := \Delta_L \hat{N}_s^2/2 + \sum_q q b_{qs}^\dagger b_{qs} . \quad (D27)$$

This result can be used to rewrite  $H_0$  in (D5) in terms of the new pseudofermions  $c_{\bar{k}s}$  and  $c_d$ . Though (D27) differs from (D5) by terms in both  $\hat{\mathcal{N}}_s^2$  and  $\hat{\mathcal{N}}_s$ , the difference can be expressed in terms of  $c_d^\dagger c_d$  using the spin-conservation condition (D3), namely  $\hat{\mathcal{N}}_s = S_T + \frac{1}{2} - c_d^\dagger c_d$  (those states in  $\mathcal{S}_{\text{ext}}$  for which (D3) does not hold will be discarded at the end anyway). In this way, the EK-transformed Hamiltonian of Eqs. (D5), (D8) and (D16) can be brought into the following refermionized form:

$$U_2 H' U_2^{-1} = H_c + H_s + E_G + \text{const.}, \quad (D28)$$

$$H_c = \sum_q q b_{qc}^\dagger b_{qc} , \quad (D29)$$

$$H_s = \sum_{\bar{k}} \bar{k} :c_{\bar{k}s}^\dagger c_{\bar{k}s} + \varepsilon_d :c_d^\dagger c_d: + \sqrt{\Delta_L \Gamma} \sum_{\bar{k}} (c_{\bar{k}s}^\dagger c_d + c_d^\dagger c_{\bar{k}s}) , \quad (D30)$$

$$E_G = \Delta_L \left[ \mathcal{N}_c (\mathcal{N}_c + 1 - P_0) + \frac{1}{2} S_T [S_T + \text{sgn}(S_T)P] + \frac{1-P}{8} - \frac{\lambda_z^*}{4} \right] + S_T h_e + \varepsilon_d \left[ n_d^{(0)} - \frac{1}{2} \right] , \quad (D31)$$

$$\varepsilon_d = \Delta_L \mathcal{E}_{d,0} + h_i - h_e , \quad (D32)$$

$$\mathcal{E}_{d,0} = (\lambda_z^* - 1) S_T - \text{sgn}(S_T)P/2 . \quad (D33)$$

Evidently, the charge sector decouples completely. In the spin sector,  $H_s$  corresponds to a quadratic resonant level model, whose “resonant level” has energy  $\varepsilon_d$  and width  $\Gamma \equiv \lambda_\perp^2/4a$ , and  $E_G$  is the “free ground state energy” of the spin sector in the extended subspace  $\mathcal{S}_{\text{ext}}$ , in the presence of magnetic fields. Note that in the absence of magnetic fields, i.e.  $h_i = h_e = 0$ , we also have  $\text{sgn}(\varepsilon_d) = -\text{sgn}(S_T)$ ; thus it follows by inspection that in this case  $H_s$  and  $E_G$  are invariant under the spin reversal transformation (D26), as they should be. As for the 2CK case, we henceforth set  $h_e = 0$ , the generalization to  $h_e \neq 0$  being straightforward.

#### 4. Diagonalization of $H_s$

We wish to bring  $H_s$  into the diagonal form

$$H_s = \sum_{\varepsilon} \varepsilon : \tilde{c}_{\varepsilon}^\dagger \tilde{c}_{\varepsilon} : + \delta E_G . \quad (D34)$$

Here  $:\cdot:$  denotes normal ordering of the  $\tilde{c}_{\varepsilon}$  operators with respect to an exact reference ground state  $|0\rangle_{\mathcal{S}_{\text{ext}}}$  of the subspace  $\mathcal{S}_{\text{ext}}$ , defined by the conditions  $\tilde{c}_{\varepsilon} |0\rangle_{\mathcal{S}_{\text{ext}}} = 0$  for  $\varepsilon > 0$  and  $\tilde{c}_{\varepsilon}^\dagger |0\rangle_{\mathcal{S}_{\text{ext}}} = 0$  for  $\varepsilon \leq 0$ . This may be accomplished by a unitary transformation of the form

$$\tilde{c}_{\varepsilon}^\dagger = \sum_{n=\{\bar{k},d\}} B_{\varepsilon n} c_n^\dagger . \quad (D35)$$

Analogously to Appendix C, the  $B_{\varepsilon n}$ 's and  $\varepsilon$ 's can be determined starting from the relations

$$[H_s, \tilde{c}_{\varepsilon}^\dagger] = \varepsilon \tilde{c}_{\varepsilon}^\dagger, \quad \{\tilde{c}_{\varepsilon}, \tilde{c}_{\varepsilon'}^\dagger\} = \delta_{\varepsilon\varepsilon'} . \quad (D36)$$

One readily finds the following results:

$$\frac{\pi\Gamma}{\varepsilon - \varepsilon_d} = -\cot(\pi\varepsilon/\Delta_L) , \quad (D37)$$

$$B_{\varepsilon d} = \left[ \frac{\Gamma \Delta_L}{\Gamma^2 \pi^2 + \Gamma \Delta_L + (\varepsilon - \varepsilon_d)^2} \right]^{1/2} , \quad (D38)$$

$$B_{\varepsilon \bar{k}} = \sqrt{\Delta_L \Gamma} \frac{1}{\varepsilon - \bar{k}} B_{\varepsilon d} , \quad (D39)$$

$$\delta E_G = \sum_{\varepsilon < 0} \varepsilon - \sum_{\bar{k} < 0} \bar{k} - \varepsilon_d n_d^{(0)} . \quad (D40)$$

The eigenenergies  $\varepsilon$  are the roots of Eq. (D37). Their general behavior as functions of  $\Gamma$  and  $\varepsilon_d$  can be determined graphically, similarly to Fig. 3. To identify the

crossover scales of the problem, we write a general solution, in analogy to (71), as

$$\varepsilon_j = \Delta_L(j - 1/2 + \delta_j), \quad (\text{D41a})$$

$$\delta_j = \frac{1}{\pi} \arctan \left[ \frac{\pi \Gamma}{\varepsilon_j - \varepsilon_d} \right]. \quad (\text{D41b})$$

Evidently, all solutions with  $|\varepsilon_j - \varepsilon_d| \ll \Gamma$  are strongly perturbed, with upward or downward shifts  $\delta_j \simeq \pm 1/2$  for  $\varepsilon_j >$  or  $< \varepsilon_d$ , whereas those with  $|\varepsilon_j - \varepsilon_d| \gg \Gamma$  are only weakly perturbed, with  $\delta_j \simeq 0$ . (The solution  $\varepsilon_j$  closest to  $\varepsilon_d$  can be associated with the  $d$  level, which, measured in units of  $\Delta_L$ , is pushed to the integer closest to it as  $\Gamma/\Delta_L \rightarrow \infty$ .)

This implies the following crossover scales:

(i) Without magnetic fields ( $h_i = h_e = 0$ , so that  $\varepsilon_d = \Delta_L \mathcal{E}_{d,0}$ ) and in the limit  $\Gamma \gg \Delta_L$  (i.e. also  $\Gamma \gg |\varepsilon_d|$ ), the crossover scale separating the strongly and weakly perturbed spectral regimes is  $\Gamma$ , which can thus again be associated with the Kondo temperature, i.e.  $T_K \simeq \Gamma$ .

(ii) For a large local magnetic field  $h_i \gg \Delta_L$  (so that  $\varepsilon_d \simeq h_i$ ), the  $h_i$ -induced shifts in the lowest-lying levels with  $|\varepsilon_j| \ll \Gamma$  become large ( $\simeq 1/2$ ) roughly when  $h_i$  reaches the crossover field  $h_c \simeq \Gamma$ . In other words, for  $h_i \gg h_c$ , the local magnetic field is strong enough to effectively erase the effects of spin-flip scattering from the lowest-lying part of spectrum. Note the contrast to the 2CK case, where the crossover field is smaller, namely  $h_c \simeq \sqrt{\Gamma \Delta_L}$ .

For  $\Gamma \gg \varepsilon_d, \Delta_L$ , the ground state energy shift  $\delta E_G$ , calculated similarly to Appendix C4, turns out to be  $\delta E_G = \delta E_G^0 + \delta E_G^d$ , where  $\delta E_G^0 \approx -\Gamma \ln(D/\Gamma)$  is the “binding energy”, and

$$\delta E_G^d = \varepsilon_d [1/2 - n_d^{(0)}] + \dots \quad (\text{D42})$$

where the dots represent terms that are either independent of  $P$  and  $\varepsilon_d$ , or of order  $\mathcal{O}(\varepsilon_d^2/\Gamma, \Delta_L^2/\Gamma, \Delta_L \varepsilon_d/\Gamma)$ . Note that  $\delta E_G^d$  precisely cancels the  $\varepsilon_d$  term in  $E_G$  of (D31), thus the fixed point spectrum at  $\Gamma/\Delta_L = \infty$  satisfyingly does not depend on the parameter  $\lambda_z^* = 2 - \sqrt{2}$  occurring in  $\varepsilon_d$ .

## 5. Generalized Spin-Conservation Conditions

To identify and discard all states in  $\mathcal{S}_{\text{ext}}$  that violate the total-spin-conservation condition (D3), we now derive a *generalized spin-conservation condition*. The argument is analogous to that for the 2CK generalized gluing condition in Section V C, but more straightforward, since  $H_s$  conserves the *number* of  $c_n$  excitations (not only their number parity).

The number of excitations of a general eigenstate  $|\tilde{E}\rangle$  of  $H_s$  relative to  $\mathcal{S}_{\text{ext}}$  is

$$\mathcal{N}_{\tilde{E}} = \langle \tilde{E} | \sum_{\varepsilon} : \tilde{c}_{\varepsilon}^{\dagger} \tilde{c}_{\varepsilon} : | \tilde{E} \rangle. \quad (\text{D43})$$

When  $\Gamma$  is turned off adiabatically and  $|\tilde{E}\rangle$  reduces to  $|E\rangle = \lim_{\Gamma \rightarrow 0} |\tilde{E}\rangle$ , its excitation number  $\mathcal{N}_{\tilde{E}}$  remains fixed. It hence equals  $\mathcal{N}_{\tilde{E}}(\Gamma \rightarrow 0)$ , which can be written as

$$\begin{aligned} \langle E | \sum_{\bar{k}} : c_{\bar{k}s}^{\dagger} c_{\bar{k}s} : + : c_d^{\dagger} c_d : | E \rangle \\ = \langle E | \left[ \hat{N}_s + S_z + 1/2 - n_d^{(0)} \right] | E \rangle. \end{aligned}$$

Using (D25) for  $\hat{N}_s$  and imposing the condition that any physical  $|E\rangle$  must satisfy the total-spin-conservation condition (D3), we obtain

$$\mathcal{N}_{\tilde{E}} = \begin{cases} S_T - [\text{sgn}(S_T)P - 1]/2 & (\varepsilon_d > 0) \\ S_T - [\text{sgn}(S_T)P + 1]/2 & (\varepsilon_d \leq 0) \end{cases}. \quad (\text{D44})$$

This *generalized spin-conservation condition* specifies which of all the possible states in  $\mathcal{S}_{\text{ext}}$  are physical; it supplements the free gluing condition (D2), which stipulates that  $S_T \mp 1/2$  must be integer (half-integer) if  $\mathcal{N}_c$  is integer (half-integer).

## 6. Finite-Size Spectrum

We consider here only the case  $P_0 = 1$  of anti-periodic boundary conditions ( $P_0 = 0$  is analogous), and zero magnetic fields,  $h_i = h_e = 0$ . The construction of the finite-size spectrum is entirely analogous to the 2CK case of Section V E, but a little more cumbersome, since  $\mathcal{E}_{d,0}$  of (D33) and hence also  $\varepsilon_d$  is not equal to zero; instead it depends on  $S_T$ , i.e. changes from one sector  $\mathcal{S}_{\text{ext}}$  to the next. The results are summarized in Fig. 7 and Table III. The latter’s caption also summarizes the technical details of the construction.

(i) *Phase-Shifted Spectrum*:— The evolution of the phase-shifted spectrum  $\mathcal{E}_{\text{phase}}$  for  $\lambda_z \in [0, \lambda_z^*]$  at  $\lambda_{\perp} = 0$  is given by  $H'(\lambda_{\perp} = 0)$  of (D10); it evolves linearly with increasing  $\lambda_z$ , from  $\mathcal{E}_{\text{free}}$  at  $\lambda_z = 0$  to  $\mathcal{E}_{\text{phase}}$  at  $\lambda_z = \lambda^* = 2 - \sqrt{2}$ , as shown in Fig. 7(a).

(ii) *Crossover Spectrum*:— The crossover spectrum as function of  $\Gamma/\Delta_L \in [0, \infty]$  at the Toulouse point  $\lambda_z = \lambda_z^*$  is shown in Fig. 7(b). The spectrum evolves continuously from the phase-shifted values  $\mathcal{E}_{\text{phase}}$  at  $\Gamma = 0$  to a Fermi liquid fixed-point spectrum  $\mathcal{E}_{\text{FL}}$  at  $\Gamma/\Delta_L = \infty$ , which is constructed analytically in Table III. The fixed-point spectrum corresponds precisely to the Fermi-liquid spectrum of free fermions [of (D5)] obeying the periodic boundary condition  $P_0 = 0$ . This agrees with the standard results of Wilson’s numerical renormalization group calculations,<sup>60</sup> and is expected, because at  $\Gamma = \infty$  one electron is bound so tightly to the impurity that the total number of free electrons effectively changes by one, and hence the chemical potential shifts by  $\Delta_L/2$ .<sup>60</sup>

The fact that all  $\mathcal{E}_{\text{FL}}$ ’s are integers or half-integers is a very direct sign of Fermi liquid physics, since it implies the absence of non-fermionic operators.

Finally, it is instructive to deduce another well-known fact, namely that a local magnetic field  $h_i$  is a marginal perturbation, from the deviations from  $\mathcal{E}_{\text{FL}}$  which it produces: For the lowest-lying levels, the value of the shift  $\delta_j$  of (D41) at the Fermi liquid fixed point ( $h_i = 0, \Gamma \gg \Delta_L$ ) is  $|\langle \delta_j \rangle_{\text{FL}}| = 1/2$ . For a small local field  $h_i \ll \Delta_L$ , an expansion in powers of  $h_i/\Delta_L$  and  $\Delta_L/\Gamma$  yields

$$\delta_j - \langle \delta_j \rangle_{\text{FL}} = \frac{h_i}{\pi^2 \Gamma} \left[ 1 - \frac{(j - 1/2 + \delta_j - \mathcal{E}_{0,d})^2 \Delta_L^2}{\pi^2 \Gamma^2} \right].$$

Since the  $L$ -dependence of the leading term is  $\sim h_i L^0$ , the local magnetic field has scaling dimension  $\gamma_{h_i} = 0$  [cf. (90)] and hence is a *marginal* perturbation (in contrast to the 2CK case, where it is relevant with  $\gamma_{h_i} = -1/2$ , cf. Section VI C). A marginal perturbation always implies the existence of a line of fixed points, parameterized by a *non-universal quantity*. Indeed, for  $h_i$  non-zero, the fixed point spectrum obtained for  $L \rightarrow \infty$  is non-universal, since in this limit (D41b) yields non-universal shifts for the lowest-lying levels, namely  $\delta_j \rightarrow -\frac{1}{\pi} \arctan(\pi \Gamma / h_i)$ . In contrast, for the 2CK case with  $\Gamma, h_i \neq 0$ , the limit  $L \rightarrow \infty$  necessarily implies  $\Gamma, T_h \gg \Delta_L$ ; hence (71b) yields universal shifts  $\delta_{j,P} \rightarrow 1$  [see Fig. 4], which is why along the EK line the phase-shifted fixed point spectrum  $\mathcal{E}_{\text{ph}}$  of Fig. 6(c) is independent of  $\Gamma$  and  $h_i$  too (though away from the EK line it does acquire a dependence on  $h_i/\Gamma$ , see Section VI C).

- <sup>1</sup> D. L. Cox, Phys. Rev. Lett. **59**, 1240 (1987); Physica (Amsterdam) **153-155C**, 1642 (1987); J. Magn. Magn **76 & 77**, 53 (1988); D.L. Cox et al., Phys. Rev. Lett. **62**, 2188 (1989).
- <sup>2</sup> C. L. Seaman, M. B. Maple, B. W. Lee, S. Ghamaty, M. S. Torikachvili, J.-S. Kang, L. Z. Liu, J. W. Allen and D. L. Cox, Phys. Rev. Lett. **67** (1991), 2882.
- <sup>3</sup> B. Andraka and A. M. Tsvelick, Phys. Rev. Lett. **67**, 2886 (1991).
- <sup>4</sup> V. J. Emery and S. Kivelson, Phys. Rev. B **46**, 10812 (1992); Phys. Rev. Lett. **71**, 3701 (1993).
- <sup>5</sup> T. Giamarchi, C. M. Varma, A. E. Ruckenstein and P. Nozières, Phys. Rev. Lett. **70**, 3967 (1993).
- <sup>6</sup> K. Vladar and A. Zawadowski, Phys. Rev. B **28**, (a) 1564; (b) 1582; (c) 1596 (1983).
- <sup>7</sup> A. Muramatsu and F. Guinea, Phys. Rev. Lett. **57**, 2337 (1986).
- <sup>8</sup> G. Zaránd and A. Zawadowski, Phys. Rev. Lett. **72**, 542 (1994); Phys. Rev. B **50**, 932 (1994).
- <sup>9</sup> A. L. Moustakas and D. S. Fisher, Phys. Rev. **B53**, 4300 (1996); see also Phys. Rev. B **51**, 6908 (1995).
- <sup>10</sup> G. Zaránd and K. Vladár, Phys. Rev. Lett. **76**, 2133 (1996); G. Zaránd, Phys. Rev. Lett. **77**, 3609 (1996).
- <sup>11</sup> T. Pruschke et al., Adv. in Physics **42**, 187 (1995); A. Georges et al., Rev. Mod. Phys. **68**, 1 (1996).
- <sup>12</sup> P. Nozières and A. Blandin, J. Phys. (Paris) **41**, 193 (1980).
- <sup>13</sup> D. C. Ralph, A. W. W. Ludwig, J. von Delft, and R. A. Buhrman, Phys. Rev. Lett. **72** (1994), 1064.
- <sup>14</sup> R. J. P. Keijsers, O. I. Shklyarevskii, and H. van Kempen, Phys. Rev. Lett., **77** (1996), 3411.
- <sup>15</sup> S. K. Upadhyay, R. N. Louie and R. A. Buhrman, Phys. Rev. **B56**, 12033 (1997).
- <sup>16</sup> G. Zaránd, Jan von Delft, and A. Zawadowski, Comment on "Point-contact study of fast and slow two-level fluctuators in metallic glasses", Phys. Rev. Lett. **80**, 1353 (1998).
- <sup>17</sup> J. von Delft, D. C. Ralph, R. A. Buhrman, S. K. Upadhyay, R. N. Louie, A. W. W. Ludwig and V. Ambegaokar, Ann. Phys. **263**, 1, (1998).
- <sup>18</sup> D. L. Cox and A. Zawadowski, Advances in Physics, **47**, 599 (1998) [cond-mat/9704103].
- <sup>19</sup> A. A. Abrikosov and A. A. Migdal, J. Low Temp. Phys. **3**, 519 (1970); M. Fowler and A. Zawadowski, Solid State Commun. **9**, 471 (1971).
- <sup>20</sup> K. Vladar, A. Zawadowski and G. T. Zimányi, Phys. Rev. B **37**, 2001, 2015 (1988).
- <sup>21</sup> M. Fabrizio, A. Gogolin, and Ph. Nozières, Phys. Rev. Lett. **74**, 4503 (1995); Phys. Rev. B **51** 16088 (1995).
- <sup>22</sup> D. L. Cox and A. E. Ruckenstein, Phys. Rev. Lett. **71**, 1613 (1993).
- <sup>23</sup> M. H. Hettler, J. Kroha, and S. Hershfield, Phys. Rev. Lett. **73**, 1967 (1994); preprint cond-mat/9707209.
- <sup>24</sup> T. S. Kim and D. L. Cox, Phys. Rev. B **55**, 12594 (1997); Phys. Rev. B **54**, 6494 (1996); Phys. Rev. Lett. **75**, 1622 (1995).
- <sup>25</sup> P. Coleman, L.B. Ioffe, and A. M. Tsvelick, Phys. Rev. B **52**, 6611 (1995).
- <sup>26</sup> P. Coleman and A. Schofield, Phys. Rev. Lett. **75** 2184 (1995).
- <sup>27</sup> R. Bulla, A. C. Hewson, and G. M. Zhang, Phys. Rev. B **56**, 11721 (1997); R. Bulla and A. C. Hewson, Zeitschrift für Physik B **104**, 333 (1997). G.-M. Zhang and A.C. Hewson, Phys. Rev. Lett. **76**, 2137 (1996);
- <sup>28</sup> D. M. Cragg, P. Lloyd and P. Nozières, J. Phys. **13**, 245 (1980).
- <sup>29</sup> H.-B. Pang, Ph.D. dissertation, The Ohio State University, unpublished (1992); H.-B. Pang and D. L. Cox, Phys. Rev. B **44**, 9454 (1991).
- <sup>30</sup> I. Affleck, A. W. W. Ludwig, H.-B. Pang and D. L. Cox, Phys. Rev. B **45**, 7918 (1992).
- <sup>31</sup> N. Andrei and C. Destri, Phys. Rev. Lett. **52**, 364 (1984).
- <sup>32</sup> P. B. Wiegmann and A. M. Tsvelick, Z. Physik **B54**, 201 (1985).
- <sup>33</sup> N. Andrei and A. Jerez, Phys. Rev. Lett. **74**, 4507 (1995).
- <sup>34</sup> I. Affleck, Nucl. Phys. **B336**, 517 (1990).
- <sup>35</sup> I. Affleck and A. W. W. Ludwig, Nucl. Phys. **B352**, 849 (1991).
- <sup>36</sup> I. Affleck and A. W. W. Ludwig, Nucl. Phys. **B360**, 641 (1991).
- <sup>37</sup> I. Affleck and A. W. W. Ludwig, Phys. Rev. B **48**, 7297 (1993).
- <sup>38</sup> I. Affleck and A. W. W. Ludwig, Nucl. Phys. **B428**, 545 (1994).
- <sup>39</sup> A. W. W. Ludwig, Int. J. Mod. Phys. **B8**, 347 (1994).
- <sup>40</sup> A. M. Sengupta and A. Georges, Phys. Rev. B **49**, 10020 (1994).
- <sup>41</sup> G. Kotliar and Q. Si, Phys. Rev. B **53**, 12373 (1996).

<sup>42</sup> J. M. Maldacena and A. W. W. Ludwig, preprint cond-mat/9502109, Nucl. Phys. **B506**, 565 (1997).

<sup>43</sup> J. W. Ye, Nucl. Phys. B **512**, 543 (1998); J. W. Ye, Phys. Rev. Lett. **77**, 3224 (1996); J. W. Ye, Phys. Rev. Lett. **79**, 1385 (1997).

<sup>44</sup> Jan von Delft and H. Schoeller, Annalen der Physik (Leipzig), **7**, 225-306 (1998) [cond-mat/9805275]. This review gives an elementary, non-field-theoretic derivation of bosonization, by noting that  $\psi_{\alpha j}(x)|\vec{N}\rangle$  is an eigenstate of  $b_{q\alpha\bar{j}}$  and hence has a coherent state representation in terms of  $b_{\alpha j}^\dagger$ 's.

<sup>45</sup> Jan von Delft, G. Zaránd and M. Fabrizio, Phys. Rev. Lett. **81**, 196 (1998).

<sup>46</sup> F. D. M. Haldane, J. Phys. C., **14**, 2585, (1981).

<sup>47</sup> J. von Delft and G. Zaránd, in preparation.

<sup>48</sup> M. Fabrizio and A. Gogolin, Phys. Rev. Lett. **78**, 4527 (1997).

<sup>49</sup> A. Furusaki, Phys. Rev. B **56**, 9352 (1997).

<sup>50</sup> A.A. Abrikosov, Physics **2**, 5 (1965).

<sup>51</sup> Y. Shimizu, O. Sakai, S. Susuki, **67**, 2395 (1998); M. Koga and D. Cox, (submitted to Phys. Rev. Lett.).

<sup>52</sup> P. D. Sacramento and P. Schlottman, Phys. Rev. B **43**, 13294 (1991).

<sup>53</sup> V. J. Emery and S. A. Kivelson, in *Fundamental Problems in Statistical Mechanics VIII*, edited by H. van Beijeren and M. H. Ernst, pp. 1-24, Elsevier, Amsterdam, (1994).

<sup>54</sup> J. Cardy, in *Phase Transition and Critical Phenomena II*, (Academic Press), 55 (1987).

<sup>55</sup> A. V. Rozhkov, cond-mat/9711181.

<sup>56</sup> I. Affleck and A. W. W. Ludwig, Phys. Rev. Lett. **67**, 3160 (1991).

<sup>57</sup> P. W. Anderson, J. Phys. C **3**, 2346 (1970).

<sup>58</sup> G. Yuval and P. W. Anderson, Phys. Rev. B **1**, 1522 (1970); P. W. Anderson, G. Yuval, and D. R. Hamann, Phys. Rev. B **1**, 4464 (1970).

<sup>59</sup> J. Gan, N. Andrei, and P. Coleman, Phys. Rev. Lett. **74**, 2583 (1993).

<sup>60</sup> K.G. Wilson and J. Kogut, Rev. Mod. Phys. **47**, 773 (1975).

<sup>61</sup> C. Dobler, *On the Stability of the 2-Channel Kondo Model*, Diplomthesis, Universität Karlsruhe, (1998).

<sup>62</sup> A careful discussion of cutoff-related matters is also given by K. Schönhammer in cond-mat/9710330.

<sup>63</sup> P. Nozières and C. T. De Dominicis, Phys. Rev. **178**, 1097 (1969).

<sup>64</sup> K. D. Schotte and U. Schotte, Phys. Rev. **182**, 479 (1969).

<sup>65</sup> A. C. Hewson *The Kondo Problem to Heavy Fermions*, Cambridge University Press (1993).

<sup>66</sup> F. Guinea, V. Hakim and A. Muramatsu, Phys. Rev. **B32** 4410, (1985); T. A. Costi and C. Kieffer, Phys. Rev. Lett. **76**, 1683 (1996).

<sup>67</sup> G. Toulouse, C. R. Acad. Sci. **268**, 1200 (1969).

<sup>68</sup> A. J. Leggett *et al.*, Rev. Mod. Phys. **59**, 1 (1987).

<sup>69</sup> The limit  $a \rightarrow 0$  must be taken first (before  $x_0 \rightarrow 0$ ), since the bosonization and repermionization identities (18) and (44) are exact only for  $a = 0$ , as discussed in Appendix A 2. A detailed evaluation of such point-split products is given in Appendix G.3 of Ref. 44, where, however, it was mistakenly stated (and even emphasized) that the “point-splitting” parameter  $x_0$  should be set equal to the

bosonization cutoff parameter  $a$ . This is incorrect. The calculations in Appendix G.3 of Ref. 44 can be corrected by first replacing the explicit occurrence of  $a$  by  $x_0$ , then setting  $a = 0$  in the boson fields  $\phi_\eta$ , and then taking  $x_0 \rightarrow 0$ .

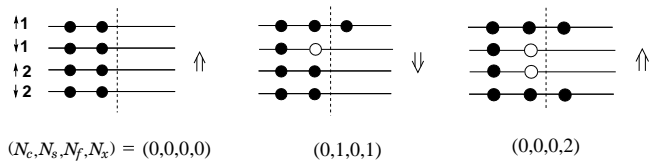


FIG. 1. Under a succession of spin flips,  $N_s$  fluctuates *mildly* between  $S_T \mp 1/2$  (here  $S_T = 1/2$ ); in contrast,  $N_x$  fluctuates *wildly*, since it can acquire *any* value consistent with the gluing conditions (22). The dotted line represents the reference energy 0 up to which the free Fermi sea is filled for  $P_0 = 1$ , the filled and empty circles represent filled and empty single-particle states with energy  $k$ .

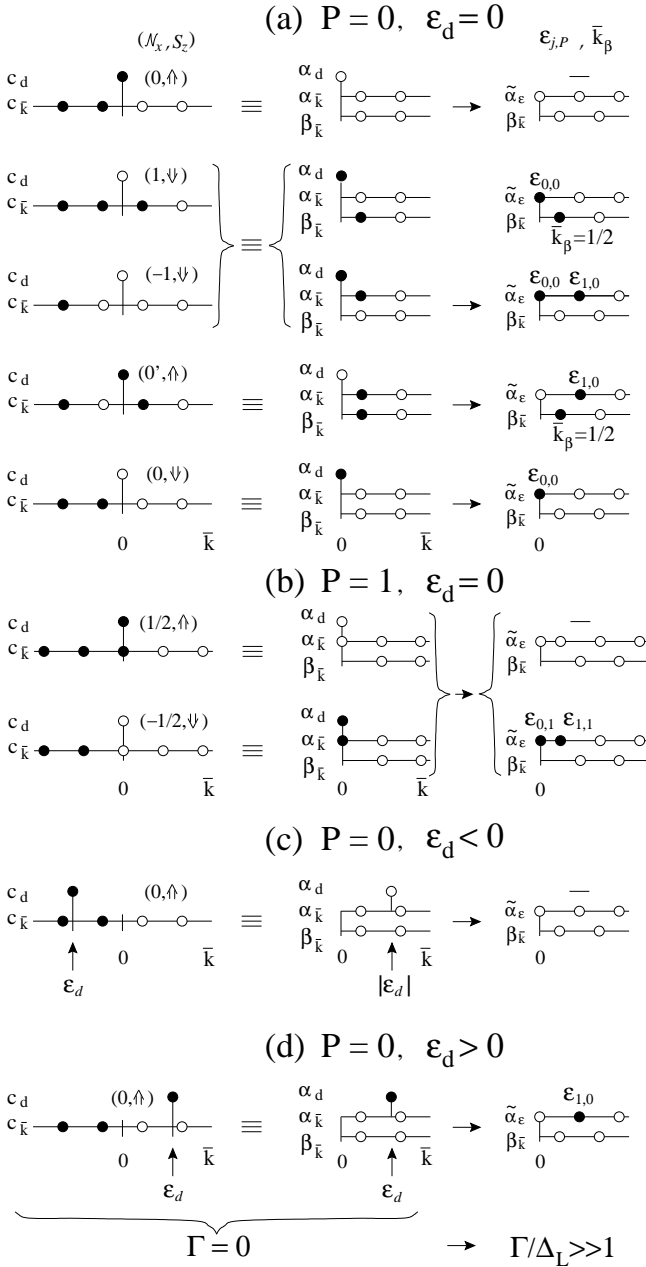


FIG. 2. The left and middle columns show, for various combinations of  $(N_x, S_z)$ , some representative free many-body states [eigenstates of  $H'(\lambda_\perp = 0)$  of (36)] in a general physical subspace  $\mathcal{S}_{\text{phys}}(S_T, N_c, N_f)$ , constructed in terms of both  $c_n$ 's and  $\alpha_n$ 's, thus illustrating the transformation (58) between these operators. The braces between these two columns indicate that the states to their left and right are not in one-to-one correspondence, but linear combinations of each other. The right column shows some of the exact physical many-body eigenstates  $|\tilde{E}\rangle$  of the full  $H'$  of (73) at  $\Gamma/\Delta_L \gg 1$ . Each  $|\tilde{E}\rangle$  is labeled by the excitation energies  $\varepsilon_{j,P}$  and  $\bar{k}_\beta$  of its occupied single-particle states. When  $\Gamma$  is turned off to 0, each state in the right column reduces to the free state in the same row in the middle column, unless they are separated by braces, in which case it reduces to a linear combination of the two degenerate free states grouped within the braces to its left. The first four rows in (a) and the two rows in (b) correspond, in that order, to the first four  $S_T = 1/2$  states and the two  $S_T = 0$  states listed in Table I; the fifth row in (a) is the spin-reversed partner of the first row in (a), illustrating how the two-fold degeneracy guaranteed by spin-reversal symmetry comes about due to the presence or absence of a  $\varepsilon_{0,P} = 0$  excitation; (c) and (d) illustrate the case  $\varepsilon_d \neq 0$  relevant for non-zero magnetic fields.

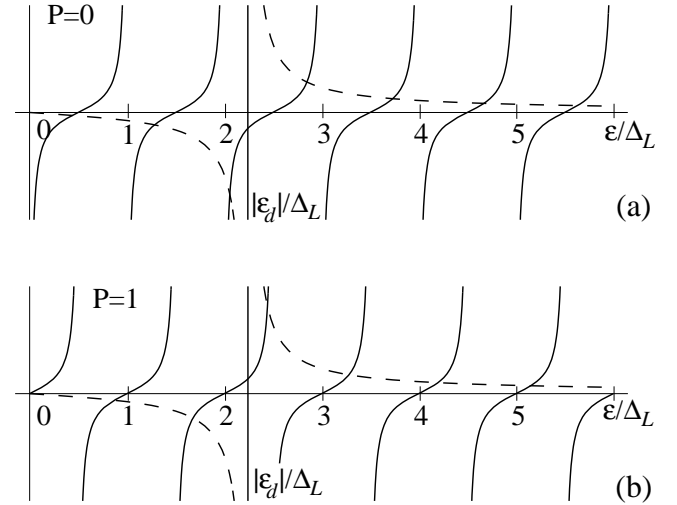


FIG. 3. Graphical solution of the eigenvalue equation (67) for (a)  $P = 0$  and (b)  $P = 1$ . The vertical solid line marks the position of  $|\varepsilon_d|$ . Dashed and solid lines represent the left- and right-hand sides of (67); their intersections give the allowed eigenvalues  $\varepsilon$ . The “amplitude” of the dashed lines is proportional to  $\Gamma/\Delta_L$ ; if this increases from 0, the  $\varepsilon$ 's thus shift away from their free values  $|\varepsilon_d|$  or  $\bar{k} = \Delta_L[n_{\bar{k}} - (1 - P)/2]$ .

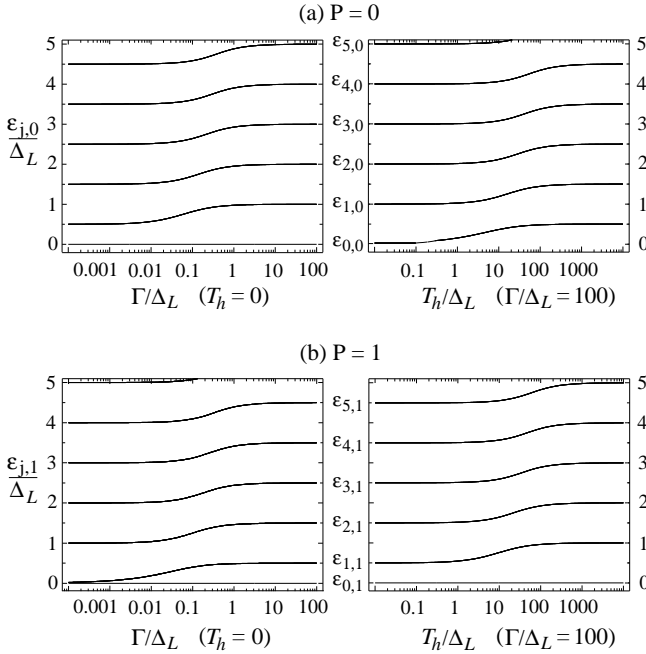


FIG. 4. (a) Evolution of the excitation energies  $\varepsilon_{j,P}$ , found by numerically solving the eigenvalue equation (67) (or by a graphical analysis as in Fig. 3). On the left the evolution is shown as function of  $\Gamma/\Delta_L \in [0, \infty)$  at  $T_h = 0$ , and on the right as function of  $T_h/\Delta_L \in [0, \infty)$  at fixed  $\Gamma/\Delta_L \gg 1$ , for (a)  $P = 0$  and (b)  $P = 1$ . These excitation energies are combined in Table I with excitations in the charge, spin and flavor sectors to obtain the evolution of the full finite-size spectrum shown in Fig. 6.

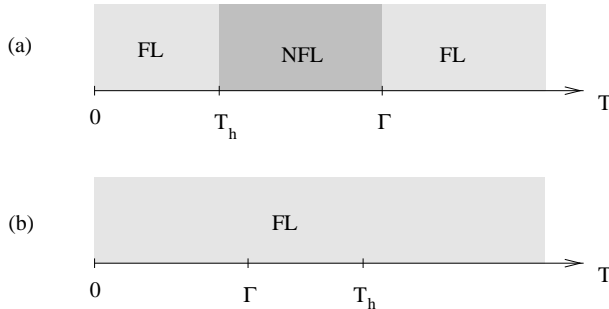


FIG. 5. Sketch of the different Fermi liquid and non-Fermi liquid regions for a finite magnetic field on the EK line.

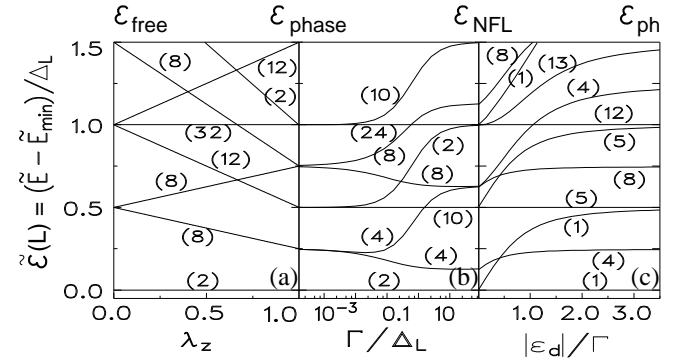


FIG. 6. Evolution of the many-body finite-size spectrum of the 2CK model, for antiperiodic boundary conditions ( $P_0 = 1$ ), from the free Fermi liquid fixed point to the NFL fixed point, and the additional crossover induced by a local magnetic field to a phase-shifted Fermi liquid fixed point. All eigenstates of  $H'$  of Eq. (54) are shown for which  $\mathcal{E}_{\text{NFL}} \leq 1$ , as well as some higher-lying states, with degeneracies given in brackets (in Ref.<sup>45</sup>, the degeneracies for  $\mathcal{E}_{\text{NFL}} = 1$  were incorrect). (a) When  $\lambda_z$  is tuned from 0 to its Emery-Kivelson value  $\lambda_z = 1$ , with  $\lambda_{\perp} = \varepsilon_d = 0$ , the free Fermi-liquid spectrum  $\mathcal{E}_{\text{free}}$  at  $\lambda_z = 0$  evolves smoothly into a simple phase-shifted spectrum  $\mathcal{E}_{\text{phase}}$  at  $\lambda_z = 1$ . (b) When  $\Gamma/\Delta_L = \lambda_{\perp}^2/(4a\Delta_L)$  is tuned from 0 to  $\infty$  along the EK line, i.e. with  $\lambda_z = 1$  and  $\varepsilon_d = 0$ , the spectrum crosses over from  $\mathcal{E}_{\text{phase}}$  to the non-Fermi liquid spectrum  $\mathcal{E}_{\text{NFL}}$  at  $\Gamma/\Delta_L = \infty$ , which agrees with NRG and CFT results. (c) Turning on a local magnetic field  $\varepsilon_d = h_i$  (with  $h_e = 0$ ) by tuning  $|\varepsilon_d|/\Gamma$  from 0 to  $\infty$  with  $\lambda_z = 1$ ,  $\Gamma \gg \Delta_L$  fixed, then induces a further crossover from  $\mathcal{E}_{\text{NFL}}$  to  $\mathcal{E}_{\text{ph}}$ . For the lowest levels this crossover occurs when  $|\varepsilon_d|/\Gamma \gtrsim 1$ , since then the crossover parameter used in Fig. 4, namely  $T_h/\Delta_L = (\varepsilon_d/\Gamma)^2(\Gamma/\Delta_L)$ , is  $\gg 1$ . The  $\mathcal{E}_{\text{ph}}$  spectrum is identical to the phase-shifted spectrum  $\mathcal{E}_{\text{phase}}$  of  $\lambda_z = 1$  and  $\lambda_{\perp} = \varepsilon_d = 0$ , apart from a degeneracy factor of two due to the lack of spin reversal symmetry.

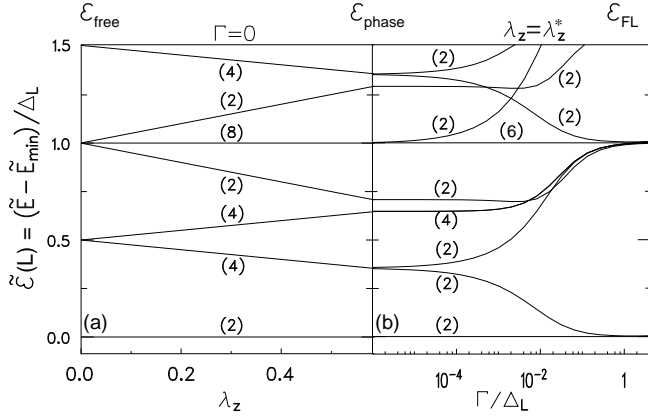


FIG. 7. Evolution of the many-body finite-size spectrum of the 1CK model, for anti-periodic boundary conditions ( $P_0 = 1$ ), from the free Fermi liquid fixed point to the strong-coupling Fermi liquid fixed point. All eigenstates of  $H'$  of Eq. (D28) are shown for which  $\mathcal{E}_{\text{FL}} \leq 1$ , as well as some higher-lying states, with degeneracies given in brackets. (a) When  $\lambda_z$  is tuned from 0 to its Toulouse-point value  $\lambda^* = 2 - \sqrt{2}$ , with  $\lambda_{\perp} = \varepsilon_d = 0$ , the free Fermi-liquid spectrum  $\mathcal{E}_{\text{free}}$  at  $\lambda_z = 0$  evolves smoothly into a simple phase-shifted spectrum  $\mathcal{E}_{\text{phase}}$  at  $\lambda_z = \lambda_z^*$ . (b) When  $\Gamma/\Delta_L = \lambda_{\perp}^2/(4a\Delta_L)$  is tuned from 0 to  $\infty$  at the Toulouse point, i.e. with  $\lambda_z = \lambda_z^*$  and  $\varepsilon_d = 0$ , the spectrum crosses over from  $\mathcal{E}_{\text{phase}}$  to the strong-coupling Fermi liquid spectrum  $\mathcal{E}_{\text{FL}}$  at  $\Gamma/\Delta_L = \infty$ . The latter is identical to the free Fermi-liquid spectrum ( $\lambda_z = \lambda_{\perp} = \varepsilon_d = 0$ ) for periodic boundary conditions ( $P_0 = 0$ ), in agreement with Wilson's NRG results.

$S_T$	$\mathcal{N}_c$	$\mathcal{N}_f$	$\mathcal{N}_s$	$\mathcal{N}_x$	$S_z$	$\mathcal{E}_{\text{free}}$ Eq. (27)	$\mathcal{E}_{\text{phase}}$ Eq. (36)	$\mathcal{E}_G$ Eq. (57)	excitations w.r.t. $ \tilde{0}\rangle_{\mathcal{S}_{\text{ext}}}$ $\mathcal{E}_{\text{ex}}(0) \rightarrow \mathcal{E}_{\text{ex}}(\infty)$	$\delta\mathcal{E}_G^P$ Eq. (77)	$\mathcal{E}_{\text{NFL}}$
$1/2$	0	0	0	0	$\uparrow$	0	0 (1)	0	$\varepsilon_{0,0}: 0 \rightarrow 0, \bar{k}_\beta = 1/2$ $\varepsilon_{0,0}: 0 \rightarrow 0, \varepsilon_{1,0}: 1/2 \rightarrow 1$ $\varepsilon_{1,0}: 1/2 \rightarrow 1, \bar{k}_\beta = 1/2$ $q_s = 1$ $q_f = 1$ $q_c = 1$	0 (1)	
	0	0	1	1	$\downarrow$	1	1/2 (1)			$1/2$ (1)	
	0	0	1	-1	$\downarrow$	1	1/2 (1)			1 (1)	
	0	0	0	0'	$\uparrow$	1	1 (1)			$3/2$ (1)	
	0	0	0'	0	$\uparrow$	1	1 (1)			1 (1)	
	0	0'	0	0	$\uparrow$	1	1 (1)			1 (1)	
	0'	0	0	0	$\uparrow$	1	1 (1)			1 (1)	
	0	$\pm 1/2$	$\mp 1/2$	$-1/2$	$1/2$	$1/2$	$1/4$ (4)			$1/8$ (2)	
	0	$\pm 1/2$	$\mp 1/2$	$1/2$	$-1/2$	$\downarrow$	$1/2$	$1/4$	$\varepsilon_{0,1}: 0 \rightarrow 0, \varepsilon_{1,1}: 0 \rightarrow 1/2$ $\varepsilon_{0,1}: 0 \rightarrow 0, \varepsilon_{1,1}: 0 \rightarrow 1/2$	$5/8$ (2)	
1	$\pm 1/2$	$\pm 1/2$	$1/2$	$1/2$	$\uparrow$	$1/2$	$3/4$ (4)			$5/8$ (2)	
$-1$	$\pm 1/2$	$\pm 1/2$	$3/2$	$-1/2$	$\downarrow$	$3/2$	$3/4$ (4)	$3/4$	$\varepsilon_{0,1}: 0 \rightarrow 0, \varepsilon_{1,1}: 0 \rightarrow 1/2$ $\varepsilon_{0,1}: 0 \rightarrow 0, \varepsilon_{1,1}: 0 \rightarrow 1/2$	$9/8$ (2)	
			$-3/2$	$1/2$	$\uparrow$	$3/2$	$3/4$ (4)			$5/8$ (2)	
$-1/2$	$\pm 1$	0	$-1/2$	$-1/2$	$\downarrow$	$1/2$	$1/2$ (2)	$1/2$	$\varepsilon_{0,0}: 0 \rightarrow 0, \bar{k}_\beta = 1/2$ $\varepsilon_{0,0}: 0 \rightarrow 0, \varepsilon_{1,0}: 1/2 \rightarrow 1$	$1/2$ (2)	
			0	1	$\downarrow$	1	1 (2)			1 (2)	
			0	-1	$\downarrow$	1	1 (2)			$3/2$ (2)	
$-1/2$	0	$\pm 1$	-1	0	$\uparrow$	$1/2$ (2)	$1/2$	$1/2$	$\varepsilon_{0,0}: 0 \rightarrow 0, \bar{k}_\beta = 1/2$ $\varepsilon_{0,0}: 0 \rightarrow 0, \varepsilon_{1,0}: 1/2 \rightarrow 1$	$1/2$ (2)	
			0	1	$\downarrow$	1	1 (2)			1 (2)	
			0	-1	$\downarrow$	1	1 (2)			$3/2$ (2)	
$1/2$	$\pm 1$	$\pm 1$	0	0	$\uparrow$	1	1 (2)	1	—	0	$1$ (2)
$1/2$	$\pm 1$	$\mp 1$	0	0	$\uparrow$	1	1 (2)	1	—	0	$1$ (2)
$-3/2$	0	0	-2	0	$\uparrow$	2	1 (1)	1	—	0	$1$ (1)

TABLE I. Construction of the 2CK model's finite-size spectrum for  $P_0 = 1$ , corresponding to Fig. 6. The table shows all states that have excitation parity  $\mathcal{P}_{\tilde{E}} = 0$  [see (75)] and a NFL fixed-point energy  $\mathcal{E}_{\text{NFL}}$  that is  $\leq 1$ , as well as some higher-lying states. (The states with  $P_{\tilde{E}} = 1$  double the degeneracies of those with  $P_{\tilde{E}} = 0$  listed here, as explained below.) All energies are given in units of  $\Delta_L$ , e.g.  $\mathcal{E}_G \equiv E_G/\Delta_L$ , with degeneracies in brackets. States in the same sector  $\mathcal{S}_{\text{phys}}(S_T, \mathcal{N}_c, \mathcal{N}_f)$  are grouped together between a pair of horizontal lines and have the same  $\mathcal{E}_G$  and  $\delta\mathcal{E}_G^P$ . (i) The construction of the *phase-shifted spectrum* for  $\lambda_{\perp} = 0$  and  $\varepsilon_d = 0$  is shown to the left of the brace column: in each sector, we list the lowest-lying free eigenstates of  $H'(\lambda_{\perp} = 0)$ , some of which are illustrated in the left and middle columns of Fig. 2. Each such state is labeled by the further quantum numbers  $(\mathcal{N}_s, \mathcal{N}_x, S_z)$ , satisfies the free gluing conditions (22), and has energy  $\mathcal{E}_{\text{free}}$  or  $\mathcal{E}_{\text{phase}}$  for  $\lambda_z = 0$  or 1, respectively, as shown in Fig. 6(a). ( $\mathcal{N}_y = 0'$  here denotes a particle-hole excitation with  $\mathcal{N}_y = 0$ ,  $\langle b_{1y}^\dagger b_{1y} \rangle = 1$  and dimensionless energy  $q_y = 1$ .) (ii) The construction of the *crossover spectrum* for  $\lambda_{\perp} \neq 0$  at  $\lambda_z = 1$  and  $\varepsilon_d = 0$  is shown to the right of the brace column: in each sector, we list the lowest-lying physical eigenstates  $|\tilde{E}\rangle$  of the full  $H'(\lambda_{\perp} \neq 0)$ , some of which are illustrated in the right column of Fig. 2. Each such  $|\tilde{E}\rangle$  is characterized by the excitation energies  $\mathcal{E}_{\text{ex}} = \varepsilon_{j,P}, \bar{k}_\beta$  or  $q_y$  of those excitations  $\tilde{\alpha}_{\varepsilon_{j,P}}^\dagger, \beta_{\bar{k}}^\dagger$  or  $b_{qy}^\dagger$  which it contains relative to the reference state  $|\tilde{0}\rangle_{\text{ext}}$  in  $\mathcal{S}_{\text{ext}}(S_T, \mathcal{N}_c, \mathcal{N}_f)$  [see (63)], and satisfies the generalized gluing condition (75). As  $\Gamma/\Delta_L$  increases from 0 to  $\infty$ , the excitation energies evolve from  $\mathcal{E}_{\text{ex}}(0) \rightarrow \mathcal{E}_{\text{ex}}(\infty)$  [as can be read off from Fig. 4(a)]; correspondingly, the energy of each eigenstate  $|\tilde{E}\rangle$  evolves from  $\mathcal{E}_{\text{phase}} = \mathcal{E}_G + \sum \mathcal{E}_{\text{ex}}(0)$  to  $\mathcal{E}_{\text{NFL}} = \mathcal{E}_G + \sum \mathcal{E}_{\text{ex}}(\infty) + \delta\mathcal{E}_G^P$  (the sum goes over all excitations listed), as shown in Fig. 6(b). When  $\Gamma$  is turned off, each  $|\tilde{E}\rangle$  reduces to the free state on its left in the same row, unless they are separated by braces, in which case  $|\tilde{E}\rangle$  reduces to a linear combination of the two degenerate free states grouped within the braces to its left (as illustrated in Fig. 2 and Section C 2 b). By spin reversal symmetry, for each state shown here (all have  $\mathcal{P}_{\tilde{E}} = 0$ ) there exists a degenerate partner with  $\mathcal{P}_{\tilde{E}} = 1$ , obtained by setting  $(S_T, \mathcal{N}_f) \rightarrow (-S_T, -\mathcal{N}_f)$  and either, for  $\lambda_{\perp} = 0$ ,  $(\mathcal{N}_s, \mathcal{N}_x, S_z) \rightarrow (-\mathcal{N}_s, -\mathcal{N}_x, -S_z)$ , or, for  $\lambda_{\perp} \neq 0$ , by adding (or removing) a  $\varepsilon_{0,P} = 0$  excitation if it was absent (or present), as illustrated by the first and fifth rows of Fig. 2(a). The degeneracies in Fig. 6(a) and (b), and summarized in Table II, are thus twice those listed here. (iii) A *crossover induced by a local magnetic field*  $\varepsilon_d = h_i$  (with  $h_e = 0$ ) occurs as  $T_h/\Delta_L = \varepsilon_d^2/(\Gamma\Delta_L)$  increases from 0 to  $\infty$  (at fixed  $\Gamma/\Delta_L \gg 1$ ), as shown in Fig. 6(c). It results from the further evolution of the listed excitations' energies  $\mathcal{E}_{\text{ex}}$  with  $T_h/\Delta_L$  [as can be read off from Fig. 4(b)]. The fixed-point spectrum at  $T_h/\Delta_L = \infty$  is given by  $\mathcal{E}_{\text{ph}} = \mathcal{E}_G + \sum \mathcal{E}_{\text{ex}}(\Gamma/\Delta_L = \infty, T_h/\Delta_L = \infty)$  (note from (77) that  $\delta\mathcal{E}_G^P = 0$  for  $T_h/\Delta_L \gg 1$ ).

$\mathcal{E}_{\text{free}}$		$\mathcal{E}_{\text{phase}}$		$\mathcal{E}_{\text{NFL}}$		$\mathcal{E}_{\text{ph}}$	
0	(2)	0	(2)	0	(2)	0	(1)
1/2	(16)	1/4	(8)	1/8	(4)	1/4	(4)
1	(54)	1/2	(12)	1/2	(10)	1/2	(6)
		3/4	(16)	5/8	(12)	3/4	(8)
		1	(34)	1	(26)	1	(17)

TABLE II. Summary of the finite-size spectrum of Fig. 6 for the 2CK model, at the four points  $\lambda_z = \lambda_{\perp} = \varepsilon_d = 0$  ( $\mathcal{E}_{\text{free}}$ );  $\lambda_z = 1, \lambda_{\perp} = \varepsilon_d = 0$  ( $\mathcal{E}_{\text{phase}}$ );  $\lambda_z = 1, \Gamma/\Delta_L = \infty, \varepsilon_d = 0$  ( $\mathcal{E}_{\text{NFL}}$ ); and  $\lambda_z = 1, \Gamma/\Delta_L = \infty, T_h/\Delta_L = \infty$  ( $\mathcal{E}_{\text{ph}}$ ). We list all energies  $\mathcal{E} \leq 1$  (in units of  $\Delta_L$ ) and give their total degeneracies in brackets.

$S_T$	$\mathcal{N}_c$	$\mathcal{N}_s$	$S_z$	$\mathcal{E}_{d,0}$ (D33)	$\mathcal{N}_{\tilde{E}}$ (D44)	$\mathcal{E}_{\text{free}}$ (D5)	$\mathcal{E}_{\text{phase}}$ (D10)	$\mathcal{E}_G$ (D31)	excitations w.r.t. $ \tilde{0}\rangle_{\mathcal{S}_{\text{ext}}}$ $\mathcal{E}_{\text{ex}}(0) \rightarrow \mathcal{E}_{\text{ex}}(\infty)$	$\delta\mathcal{E}_G^d - \frac{1-\lambda^*}{4}$ (D42)	$\mathcal{E}_{\text{FL}}$
0	$\pm 1/2$	-1/2	$\uparrow$			1/2	$1/2 - \lambda^*/4$ (4)	$\left\{ \begin{array}{l}   -1/2 \rangle \rightarrow   0 \rangle \\   -1/2 \rangle \rightarrow   -1 \rangle \\   -1/2 \rangle \rightarrow   0 \rangle, \quad q_c = 1 \\   -1/2 \rangle \rightarrow   -1 \rangle, \quad q_c = 1 \end{array} \right.$	$\lambda^*/4$	0 (2)	
		1/2	$\downarrow$	-1/2	-1					1 (2)	
	$\pm 1/2'$	-1/2	$\uparrow$			3/2	$3/2 - \lambda^*/4$ (4)			1 (2)	
		1/2	$\downarrow$							2 (2)	
0	0	0	$\uparrow$			0	0 (1)			0 (1)	
1/2	0	1	$\downarrow$			1	$1 - \lambda^*/2$ (1)	$ \varepsilon_a  \rightarrow  0 , \quad 1/2 \rightarrow 1$ $q_c = 1$	$0$	1 (1)	
0'	0	$\uparrow$		$\lambda^*/2 - 1/2$	0	1	1 (1)			1 (1)	
0	0'	$\uparrow$				1	1 (1)	$ -1/2\rangle \rightarrow   -1 \rangle, \quad 1/2 \rightarrow 1$		2 (1)	
1/2	$\pm 1$	0	$\uparrow$	$\lambda^*/2 - 1/2$	0	1	1 (2)	1	—	0	
1	$\pm 1/2$	1/2	$\uparrow$	$\lambda^* - 3/2$	0	1/2	$1/2 + \lambda^*/4$ (2)	$1/2 + \lambda^*/4$	—	$1/2 - \lambda^*/4$ (1)	
3/2	0	1	$\uparrow$	$(\lambda^* - 1)3/2$	1	1	$1 + \lambda^*/2$ (1)	$1/2 + \lambda^*/2$	$1/2 \rightarrow 1$	$1/2 - \lambda^*/2$ (2)	

TABLE III. Construction of the 1CK model's finite-size spectrum for  $h_i = h_e = 0$  and  $P_0 = 1$ , corresponding to Fig. 7. The table shows all states with  $S_T \geq 0$  that have a strong-coupling Fermi liquid fixed-point energy  $\mathcal{E}_{\text{FL}}$  that is  $\leq 1$ , as well as some higher-lying states. (The states with  $S_T < 0$  double the degeneracies of those with  $S_T > 0$  listed here, as explained below.) All energies are given in units of  $\Delta_L$ , e.g.  $\mathcal{E}_G \equiv E_G/\Delta_L$ , with degeneracies in brackets. States in the same sector  $\mathcal{S}_{\text{phys}}(S_T, \mathcal{N}_c)$  are grouped together between a pair of horizontal lines (and have the same  $\varepsilon_d$ ,  $\mathcal{N}_{\tilde{E}}$ ,  $\mathcal{E}_G$  and  $\delta\mathcal{E}_G^d$ ). (i) The construction of the *phase-shifted spectrum* for  $\lambda_{\perp} = 0$  is shown to the left of the braces: in each sector, we list the lowest-lying free eigenstates of  $H'(\lambda_{\perp} = 0)$ ; each is labeled by the further quantum numbers  $(\mathcal{N}_s, S_z)$ , satisfies the free gluing condition (D2) and spin-conservation condition (D3), and has energy  $\mathcal{E}_{\text{free}}$  or  $\mathcal{E}_{\text{phase}}$  for  $\lambda_z = 0$  or  $\lambda_z = \lambda_z^* = 2 - \sqrt{2}$ , respectively. ( $\mathcal{N}_y = 0'$  and the braces here have the same meaning as in Table I.) (ii) The construction of the *crossover spectrum* for  $\lambda_{\perp} \neq 0$  at  $\lambda_z = \lambda_z^*$  is shown to the right of the braces: in each sector, we list the lowest-lying physical eigenstates  $|\tilde{E}\rangle$  of the full  $H'(\lambda_{\perp} \neq 0)$  in that sector; each such  $|\tilde{E}\rangle$  is characterized by the excitation energies  $\mathcal{E}_{\text{ex}} = \varepsilon, |\varepsilon|$  or  $q_y$  of the excitations  $\tilde{c}_{\varepsilon > 0}^{\dagger}, \tilde{c}_{\varepsilon \leq 0}$  or  $b_{qy}^{\dagger}$  which it contains relative to the reference state  $|\tilde{0}\rangle_{\mathcal{S}_{\text{ext}}}$  in  $\mathcal{S}_{\text{ext}}(S_T, \mathcal{N}_c)$ , and satisfies the generalized spin-conservation condition (D44). (For  $\varepsilon \leq 0$ ,  $|\varepsilon|$  denotes the hole excitation  $\tilde{c}_{\varepsilon}|\tilde{0}\rangle_{\mathcal{S}_{\text{ext}}}$ .) As  $\Gamma/\Delta_L$  increases from 0 to  $\infty$ , the excitation energies evolve from  $\mathcal{E}_{\text{ex}}(0) \rightarrow \mathcal{E}_{\text{ex}}(\infty)$ ; correspondingly, the energy of each eigenstate  $|\tilde{E}\rangle$  evolves from  $\mathcal{E}_{\text{phase}} = \mathcal{E}_G + \sum \mathcal{E}_{\text{ex}}(0)$  to  $\mathcal{E}_{\text{FL}} = \mathcal{E}_G + \sum \mathcal{E}_{\text{ex}}(\infty) + \delta\mathcal{E}_G^d - \frac{1-\lambda^*}{4}$  (the latter constant corresponds to subtracting  $\mathcal{E}_{\text{min}}$ , the sum goes over all excitations listed), as shown in Fig. 7. By spin reversal symmetry, each  $S_T > 0$  state shown here has a degenerate partner with total spin  $-S_T$ , obtained, for  $\Gamma = 0$ , by setting  $(\mathcal{N}_s, S_z) \rightarrow (-\mathcal{N}_s, -S_z)$ , or, for  $\Gamma \neq 0$ , by setting  $(\varepsilon_d, \mathcal{N}_{\tilde{E}}) \rightarrow (-\varepsilon_d, -\mathcal{N}_{\tilde{E}})$  and interchanging particle- and hole-excitations,  $|\varepsilon| \leftrightarrow \varepsilon$  [cf. (D26)]. For all  $S_T \neq 0$  levels, the degeneracies in Fig. 7 are thus twice those listed here.